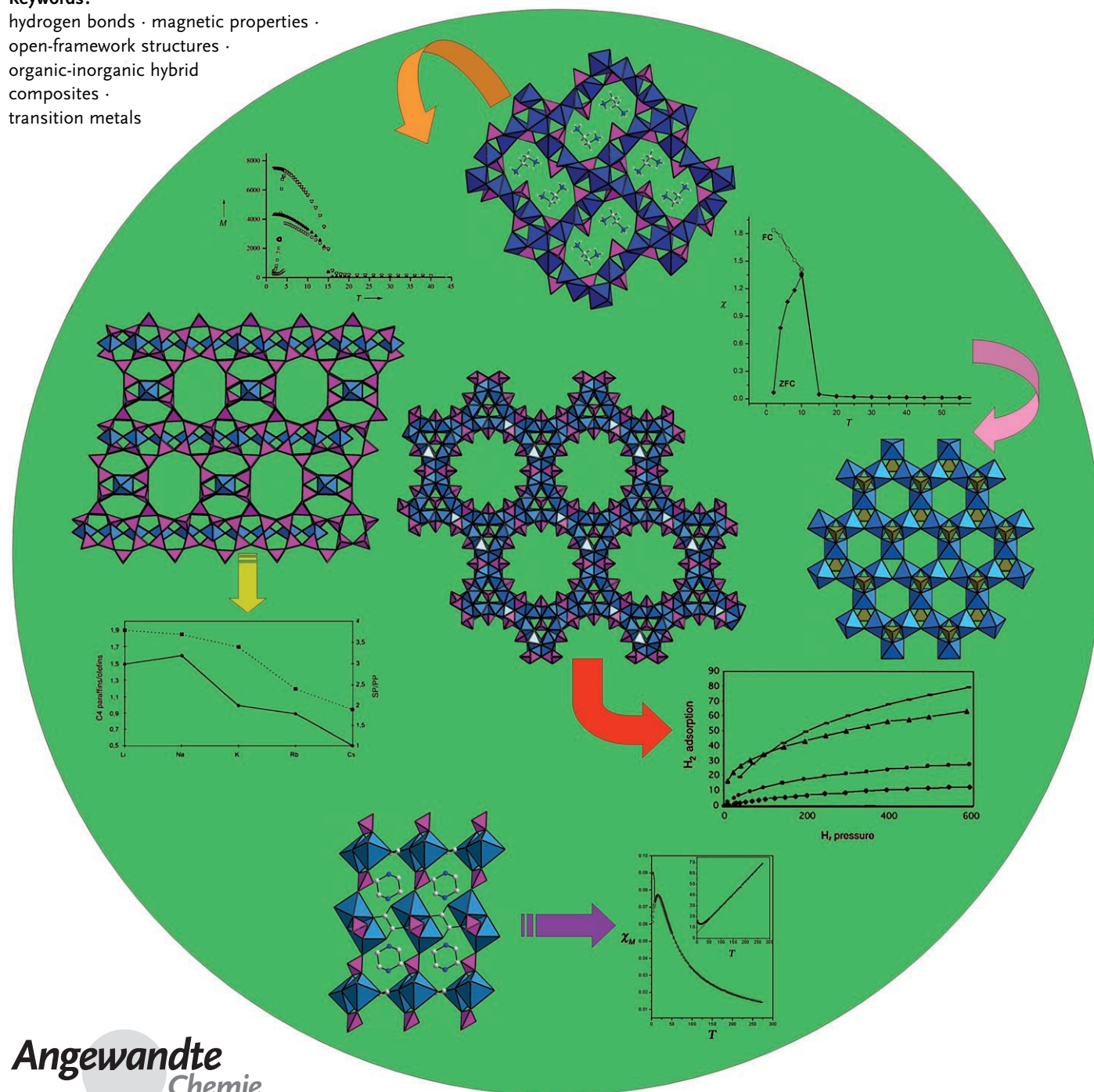


# Open-Framework Structures of Transition-Metal Compounds

Srinivasan Natarajan\* and Sukhendu Mandal

## Keywords:

hydrogen bonds · magnetic properties · open-framework structures · organic-inorganic hybrid composites · transition metals



*Inorganic framework solids are no longer limited to just the silicates and phosphates. Recent research has revealed that carboxylates, arsenates, sulfates, selenates, selenites, germanates, phosphites can also form such structures. One of the emerging areas combines the rich coordination chemistry of the central metal ions of many of these structures with the flexibility and functionality of the organic linkers to give rise to organic–inorganic hybrid compounds. The compounds of the transition-metals appear to provide many variations arising from their coordination preferences, ligand geometry, and the valence state. In addition, the combination of the magnetic nature of the transition metal center with the channel structure of open frameworks suggests interesting potential applications. In this Review the synthesis, structures and properties of the various transition-metal open-framework compounds are discussed.*

## 1. Introduction

Research in the area of framework solids exhibiting open structures continues to be exciting because of their many potential applications.<sup>[1–12]</sup> Open-framework solids having large channels and cavities have been exploited for catalysis and related studies. It is becoming equally important to discover new solids with fascinating structures offering new properties and applications.

Most of the earlier work in this area concentrated on aluminosilicate zeolites<sup>[1]</sup> until Flanigen and co-workers in the early 1980s discovered the aluminophosphate structures.<sup>[13]</sup> The formation of aluminophosphates with zeolitic and related structures has given rise to a flurry of activity resulting in many structures with different dimensionality.<sup>[14]</sup> The search for compounds exhibiting 1D, 2D, and 3-dimensionally extended structures has brought other elements into focus and presently compounds that exhibit open structures are known for most of the elements of the periodic table. The structures are, in general, formed by tetrahedra and/or octahedra linked through their vertices. The introduction of other anions, such as oxy-fluoride,<sup>[15,16]</sup> phosphite,<sup>[17,18]</sup> and sulfide,<sup>[19]</sup> added new possibilities and zest for research in this area. The combination of rigid polyhedral primary building units of the central metal ion along with flexible organic linkers has also attracted the attention of synthetic chemists.<sup>[20–24]</sup> The variety and diversity in such structures have been reviewed recently.<sup>[6]</sup> In addition to the simple metal carboxylates, it was shown that the inorganic networks of phosphates and related compounds can be linked by rigid and flexible organic linkers giving rise to new types of hybrid frameworks.<sup>[25]</sup>

Herein, we present a concise view of the structures and properties of the various families of compounds containing transition metals. The Review is divided into sections dealing with the one-, two- and three-dimensionally extended network structures of a family of compounds. To describe the structures we have used the concept of secondary building

## From the Contents

<b>1. Introduction</b>	4799
<b>2. Synthesis</b>	4800
<b>3. Secondary Building Units (SBUs)</b>	4801
<b>4. Silicates</b>	4803
<b>5. Germanates</b>	4804
<b>6. Phosphates</b>	4804
<b>7. Phosphites</b>	4809
<b>8. Phosphonates</b>	4811
<b>9. Arsenates</b>	4812
<b>10. Borates</b>	4813
<b>11. Sulfates, Selenites</b>	4814
<b>12. Hybrid Compounds (Mixed Oxo Anions)</b>	4816
<b>13. Organic–Inorganic Hybrid Compounds</b>	4817
<b>14. Magnetic Behavior in Transition-Metal-Based Framework Structures</b>	4820
<b>15. Concluding Remarks</b>	4822

units (SBUs), originally proposed by Férey et al.<sup>[26]</sup> In Section 3 we describe the structures of all the known SBUs. In some cases, we explain the complex structures in terms of simpler models and outline strategies for the preparation of newer ones. Finally, we have included a separate section dealing with the magnetic behavior in these compounds and also incorporated some of the theoretical models used to describe the magnetic phenomena. We have also provided a comprehensive list of references. In writing this, we were particularly guided by the Review of three-dimensional metal phosphates and related structures by Cheetham et al.,<sup>[2]</sup> and open-framework carboxylates by Rao et al.<sup>[6]</sup>

[\*] Prof. Dr. S. Natarajan, S. Mandal  
Framework Solids laboratory  
Solid State and Structural Chemistry Unit  
Indian Institute of Science, Bangalore–560012 (India)  
Fax: (+91) 80-2361-1310  
E-mail: snatarajan@sscu.iisc.ernet.in

Supporting information for this article is available on the WWW under <http://www.angewandte.org> or from the author.

## 2. Synthesis

Aluminosilicate zeolites are generally prepared by employing hydrothermal methods in basic media at temperatures between 80 and 200 °C. After the pioneering work of Barrer<sup>[27a]</sup> and Milton<sup>[27b]</sup> on synthetic zeolites, the syntheses were carried out in the presence of organic cations (alkyl ammonium ions). Later research showed that different frameworks are formed by the same amine, and the same framework can be formed by different amines.<sup>[28]</sup> Observations of this nature prompted many investigators to study the role of the amines in the formation of these structures. The various aspects of the synthesis of open-framework compounds have been reviewed by Davis and Lobo<sup>[28b]</sup> and Morris and Weigel.<sup>[29]</sup> The mechanism of the formation of a zeolitic structure is still poorly understood, although considerable progress has been made towards a better understanding.

One of the important issues with respect to the synthesis is the role of the amine molecules. The amine molecules appear to play three distinct roles: 1) templating, 2) structure directing, and 3) space filling. Templating refers to the formation of a unique structure that reflects the geometrical and electronic nature of the template. Unfortunately, such specificity between the organic guest and the framework host are very rare.<sup>[30]</sup> Structure direction describes the process whereby a specific organic amine preferentially leads to the formation of a specific zeolite structure. There are quite a few examples of such occurrences including works by Zones and co-workers using heterocyclic organic amines.<sup>[31]</sup> Space filling is a process in which the organic amines exclude solvent molecules; it enhances the interactions between the organic components and the framework leading to increased thermodynamic stability.

Based on these approaches, the formation of an open-framework solid can be outlined (Figure 1): The reaction involves the reactive species (hydrated metal ions and phosphate) arranging themselves around the organic amines (in this case tetramethylammonium cations) forming a cooperatively arranged complex, which is the nucleation center for the growing structure. Simple van der Waals interactions between the reactive species and the  $\text{NMe}_4^+$  ions can provide the necessary enthalpic driving force for the formation, while the release of the ordered solvent back into the bulk provides the entropic driving force. Other aspects

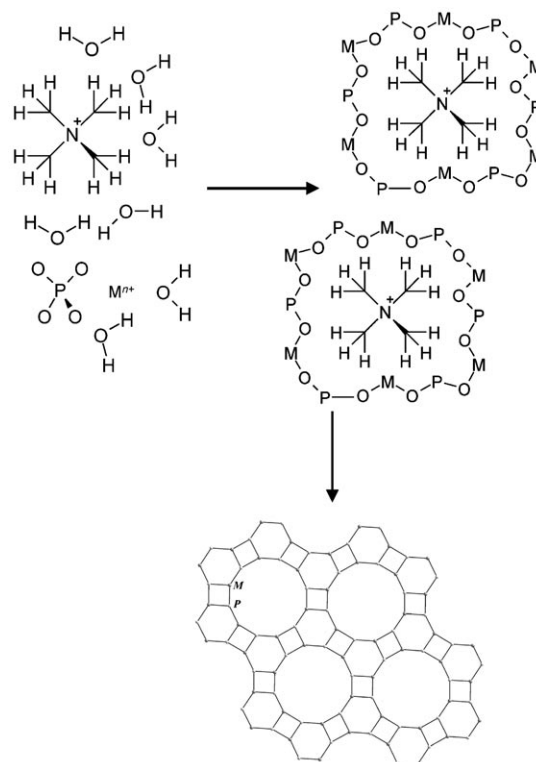


**Figure 1.** Schematic illustration of the formation of an open-framework transition-metal phosphate. The water molecules in the hydration sphere of the template are partially or fully replaced by metallophosphate species. The organic–inorganic interactions form the basis of the geometric relationship between the template and the metallophosphate pores once nucleation and crystal growth have occurred. M and P describe metal and phosphorous centers respectively.

related to crystallization concern solution-mediated transport and the solid–hydrogel transformation. The solution-mediated transport involves the dissolution of the reactants in the solvent and subsequent transport of the dissolved species by diffusion to the nucleating site, where the phase growth occurs. The solid–hydrogel transformation is a reorganization of a solid phase from an amorphous precursor state to one with long-range order.



Srinivasan Natarajan gained his Ph.D. from the Indian Institute of Technology (1990) and carried out postdoctoral research at the Royal Institution of Great Britain and the University of California, Santa Barbara. He was at the Jawaharlal Nehru Center for Advanced Scientific Research until 2004 and then at the Solid State and Structural Chemistry Unit, Indian Institute of Science, where he is an Associate Professor. He is co-author of more than 200 journal articles and book chapters. He is the recipient of the B.M. Birla prize and the Ramanna Fellowship for chemistry. His research interests are in solid state and materials chemistry, especially functional inorganic solids with open structures.



Sukhendu Mandal received his B.Sc. degree from the Narendrapur Ramakrishna Mission Residential College, Kolkata in 1999 and his M.Sc. from Kalyani University in 2001. He is pursuing his Ph.D. studies at the Indian Institute of Science, Bangalore. His work pertains to open-framework materials.

### Role of the Solvent

The properties of the solvent are important for the success or the failure of an attempted synthesis. From Figure 1, the interaction between the solvent and the reacting species appears to be important. One of the essential criteria is that the structure-directing agent (organic amines) interacts with the solvent, but not too strongly, so that the amine molecules remain in isolation and the solvent molecules can facilitate the interactions between the framework particles (silicate/phosphate etc.) and the amine molecules. It is the subtle balance between the solvent, the organic amine, and the framework species that is important in the successful synthesis of a framework structure.

In recent years, many non-aqueous solvents with much higher viscosity than water have been employed. In such solvents gel formation is considerably reduced and hence the interaction between the organic amine and the framework species can occur by diffusion processes. This can reduce the chance of secondary nucleation as well as preventing crystallization by precipitation. The use of non-aqueous routes for the preparation of framework structures has been employed extensively by Xu and co-workers,<sup>[32]</sup> Chippindale and co-workers,<sup>[33]</sup> and Cheetham and co-workers.<sup>[34]</sup>

### Fluoride Route

The discovery that fluoride ions, in aqueous or non-aqueous solution, can act as a mineralizer has had a profound effect on the synthesis of framework solids. The first use of fluoride ion, belongs to Kessler and co-workers,<sup>[35,36]</sup> who synthesized the gallophosphate, Cloverite, using this approach. Subsequent research by many researchers, especially Férey and co-workers,<sup>[26d]</sup> extended this route for the synthesis of many fluorophosphate frameworks. The use of HF-pyridine and HF-alkylamine solvents gave rise to extra-large single crystals of many important zeolitic structures.<sup>[34a,37]</sup> In some of these syntheses, a small quantity of water is used to reduce the viscosity of the solvent as well as to assist in the transport of the framework species. Recently the fluoride route has been used to great success in the synthesis of arsenate- and sulfate-based open-framework compounds.<sup>[38]</sup>

### Other Approaches

It has been shown that transition-metal coordination complexes can also be used as structure-directing agents. This type of complex is more advantageous than simple amine molecules owing to its range of unique conformations, including chiral ones which could import chirality to the framework. Such chiral materials would be of use in enantioselective heterogeneous catalysis or separation processes. Different types of tris(diamine) complexes of cobalt(III) and nickel(II) have been used for the formation of such structures.<sup>[39]</sup> Generally the cobalt complexes appear to be stable and are trapped within the pores. In some cases the

complexes decompose under the hydrothermal conditions giving rise to unusual products.<sup>[39c]</sup>

Very recently, it has been shown that ionic liquids can be used for the synthesis of framework compounds. Such preparations are popularly known as ionothermal synthesis, in many cases the ionic liquid also becomes the template provider. Ionic liquids are a class of organic solvents with high polarity and a preorganized solvent structure. Ionic liquids are classically defined as organic salts that are liquid at ambient temperatures (or <100°C). They have excellent solvating properties, little measurable vapor pressure, and high thermal stability.<sup>[40–43]</sup> The negligible vapor pressure of ionic liquids when heated means that the ionothermal synthesis takes at near ambient pressure.<sup>[41]</sup> This feature eliminates the safety concerns associated with high pressures and allows for the solvothermal synthesis of microporous materials in glass vessels.<sup>[41]</sup> The different chemistry of the ionothermal solvent system compared to that of the traditionally used hydrothermal and solvothermal systems produces conditions under which novel structure types appear to be accessible. This new synthesis methodology is currently receiving a growing amount of interest from synthetic chemists. The preparation of aluminophosphates,<sup>[41]</sup> cobalt aluminophosphates,<sup>[44]</sup> and organic–inorganic hybrid materials,<sup>[45]</sup> has been accomplished using this method. Many of these structures are new, demonstrating the potential of ionothermal synthesis in the development of novel materials.

## 3. Secondary Building Units (SBUs)

The open-framework structure is built-up using a variety of building units. The primary building unit is, generally, the individual polyhedra of the central ion. A building unit is defined as the minimum assembly of atoms, ions, or molecules, which on condensation, either with the same or different unit, gives rise to the final structure irrespective of the symmetry and/or the dimensionality. The concept of the secondary building unit (SBU) is not only to describe the framework structure, but also an aid to imagining new topologies. The description of framework structures based on SBUs appears to have distinct advantages, as a few SBUs are sufficient to describe a whole family of related structures. The concept of building units was employed initially to describe the complex framework structures of aluminosilicates.<sup>[46]</sup> The SBU concept was also employed to expand and predict a number of possible theoretical zeolitic topologies.<sup>[47]</sup> In general, the careful analysis of SBUs in well-established and known structures provides clues for the organization of such structures and also facilitates the search for new topologies.

The concept of SBUs is beginning to be applied to octahedral–tetrahedral systems. Férey identified and classified many SBUs, commonly observed in non-tetrahedral open-framework structures.<sup>[26]</sup> Transition metals, generally, have octahedral coordination environments and many of their compounds have octahedral–tetrahedral connectivity. Herein, we present a description of all the known SBUs,

from the simplest to the most complex ones, observed in such structures (Figure 2 and Supporting Information, Table S1).

The simplest of all the building units is generated by linking one transition-metal polyhedron and a tetrahedron (SBU-2). Since the transition metal centers can have different coordination numbers and geometries, the SBU-2 appears to have variety of coordination numbers and geometries (Figure 2a–c). Due to the simple structural nature, SBU-2 is commonly observed along with other building units. The SBU-2s generally act as linkers between other SBUs. There are no known examples of SBU-3s in any of the framework structures. SBU-4s are among the most common building units. SBU-4s are generally built-up from two metal polyhedra and two tetrahedra and show variations arising out of the mode of bonding between the polyhedral units (Figure 2d–g). The simplest form of SBU-4 (Figure 2d) is one where two octahedra and two tetrahedra share vertices. Similar building units have also been observed in aluminophosphates,<sup>[46]</sup> which are based on pure tetrahedral connectivity. Another SBU-4 (Figure 2g) has two octahedral units sharing a common edge and being connected at the top and

the bottom by two tetrahedral units. Compounds whose structures are exclusively built up from SBU-4 units have been reported and are discussed in Section 9).

An SBU-5 consists of two octahedra and three tetrahedra connected through the vertices (Figure 2h). In SBU-5s, the SBU-4 shown in Figure 2d has a tetrahedral unit capping the four-ring. SBU-5s have been identified recently and are observed in only a few structures (see Section 9). SBU-6 units, like the SBU-4s, are common (Figure 2i–k). These are formed by three polyhedral (octahedral or pentahedral) and three tetrahedral units which can be connected in different ways and in different arrangements. Compounds, whose structures are exclusively built up from SBU-6s, are known (see Section 6). In addition, SBU-6s can also be connected with other building units, especially SBU-2s forming complex network structures. SBU-7s are formed by the association of three metal polyhedra and four tetrahedral units (Figure 2l,m). Similar to other odd numbered building units, this SBU is also not common and is only observed in a few structures (see Sections 6 and 13). SBU-8, on the other hand is more common. SBU-8s also show variations arising from the

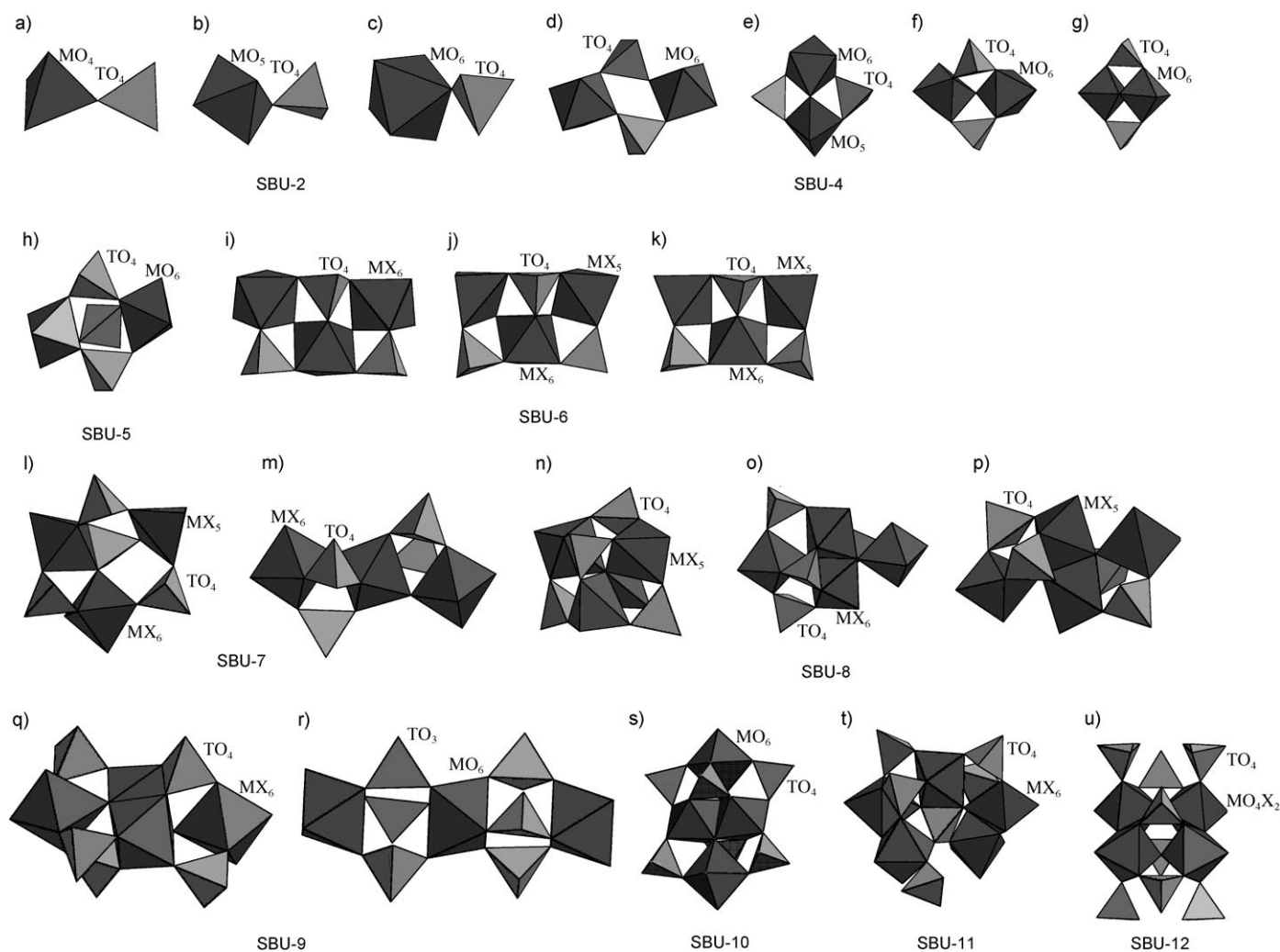


**Figure 2.** The various SBUs encountered in the transition-metal framework structures. M metal, O oxygen, X halogen or any anion, N tetrahedral center. See text for details.

different connectivity between four metal polyhedral and four tetrahedral units (Figure 2n–p). SBU-8s have been observed both in synthetic and naturally occurring mineral phosphates, especially those of iron (see Section 6). An addition of another tetrahedral unit to an SBU-8 gives rise to an SBU-9, (Figure 2q). An alternative SBU-9 has also been identified, in it three  $\text{MO}_6$  and six tetrahedra/pseudo tetrahedra connect through the vertices (Figure 2r; see Section 7). SBU-10 (Figure 2) contains four octahedral and six tetrahedral units (see Section 6), SBU-11 (Figure 2t) contains five octahedral and six tetrahedral units (see Section 6), and SBU-12 (Figure 2u) contains four octahedral and eight tetrahedral units (see Section 6). These SBUs have each only been observed in one compound. It may be noted that as the size of the SBU increases the number of structures formed using them decreases. We have listed typical examples for each of the SBUs described in this Section in the Supporting Information, Table S1.

In the following sections we present and describe the diversity in the structures based on octahedra–tetrahedra connectivity. We describe the zero-dimensional structures wherever known, followed by one-, two-, and three-dimensional structures. Any special properties associated with the compounds are also described.

#### 4. Silicates

Porous silicates that contain transition metals in octahedral or distorted octahedral framework sites have attracted interest for their ion-exchange and catalytic properties. Only two- and three-dimensional silicate structures are known. Most silicate structures are formed in the presence of alkali or alkaline-earth metals, and very few in the presence of organic amines. Recently, Rocha and co-workers reviewed the silicate structures and their important properties.<sup>[48]</sup>

Two-dimensional transition-metal silicates have been prepared in the presence of alkali-metal cations.<sup>[49,50]</sup> The layered titanosilicate AM-1,<sup>[49b]</sup> also called JDF-L1,<sup>[49a]</sup> has the composition  $[\text{Na}_4][\text{Ti}_2\text{Si}_8\text{O}_{22}] \cdot 4\text{H}_2\text{O}$  and contains  $\text{TiO}_5$  square pyramids linked to  $\text{SiO}_4$  tetrahedra to form two-dimensional sheets,  $[\text{TiO}_4(\text{SiO}_3)_4]$ . The interlamellar space is occupied by the  $\text{Na}^+$  ion. The compound adsorbs water reversibly in relatively large amounts and the water adsorption is found to show a type I isotherm. The interlamellar  $\text{Na}^+$  ions can be replaced by protonated amines. After treatment of the  $\text{Na}^+$  from of this compound with a mixture of dilute acid and hydrogen peroxide it can selectively oxidize phenol to quinone.<sup>[49a]</sup> Three novel layered sodium zirconosilicates,  $[\text{Na}_2][\text{Zr}_5\text{Si}_2\text{O}_{15}] \cdot 3\text{H}_2\text{O}$ ,  $[\text{Na}_2][\text{Zr}_5\text{Si}_2\text{O}_{15}] \cdot 4\text{H}_2\text{O}$ , and  $[\text{Na}_2][\text{Zr}_5\text{Si}_3\text{O}_9] \cdot 3\text{H}_2\text{O}$ , have been prepared by mild hydrothermal conditions.<sup>[50]</sup> The zirconium octahedra and  $\text{SiO}_4$  tetrahedra are connected to form the layered structure. The  $\text{Na}^+$  ions, situated in between the layers, can be ion-exchanged by, for example,  $\text{Li}^+$ ,  $\text{K}^+$ ,  $\text{Cs}^+$ ,  $\text{Ca}^{2+}$ ,  $\text{Ba}^{2+}$  and  $\text{Sr}^{2+}$  ions.

Most of the synthetic and natural silicate structures are three-dimensional in nature.<sup>[51–55]</sup> The silicate compounds have been prepared by the use of high-temperature solid-state reactions with inorganic cations as well as low-temperature

hydrothermal routes in the presence of amines as structure-directing agents. The best known three-dimensional synthetic transition-metal silicate is ETS-10,  $[\text{Na},\text{K}]_2\text{[TiSi}_5\text{O}_{13}] \cdot x\text{H}_2\text{O}$ .<sup>[51a–c]</sup> The structure contains  $\text{TiO}_6$  octahedra and  $\text{SiO}_4$  tetrahedra, and the  $\text{TiO}_6$  octahedra share *trans* vertices forming Ti–O–Ti infinite chains. The chains are connected by  $\text{SiO}_4$  tetrahedra to form  $[\text{TiSi}_4\text{O}_{13}]$  columns, which pack into layers. The layers are interconnected by other  $\text{SiO}_4$  tetrahedra forming the three-dimensional structure with twisting 12-ring channels (Figure 3). The  $\text{Na}^+$  ions occupy the channels.

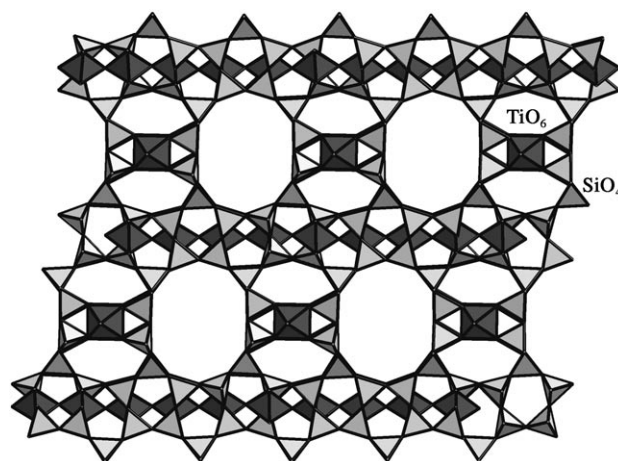


**Figure 3.** Polyhedral structure of ETS-10, projection down the [100] zone axis.

Owing to its high surface area, high ion-exchange capability, and the absence of an acidic function, ETS-10 was found to be a suitable support for metals. ETS-10 in which the  $\text{Na}^+$  was exchanged for  $\text{Co}^{2+}$  has been used as a catalyst for the Fischer–Tropsch reaction, addition of Ru was found to improve the reducibility of the cobalt.<sup>[51d,e]</sup> The reforming reaction of hexane to benzene has been studied over platinum-supported ETS-10.<sup>[51f,g]</sup> Rocha et al. ion-exchanged ETS-10 with both  $\text{Eu}^{3+}$  and  $\text{Er}^{3+}$  and showed that the  $\text{Eu}^{3+}$ -doped ETS-10 is optically active.<sup>[51h,i]</sup>  $\text{H}_2$ ,  $\text{N}_2$ ,  $\text{CO}$ , and  $\text{NO}$  have been adsorbed at liquid-nitrogen temperature in ETS-10.<sup>[51j]</sup> The ETS-10 structure has also been formed with vanadium instead of titanium.<sup>[52a]</sup> The other well-known titanosilicate ETS-4,  $[\text{Na}_9][\text{Ti}_5\text{Si}_{12}\text{O}_{38}(\text{OH})]$ ,<sup>[51k,l]</sup> is the synthetic analogue of the mineral Zorite,  $[\text{Na}_6](\text{Ti},\text{Nb})_5(\text{Si}_6\text{O}_{17})_2(\text{O},\text{OH})_5 \cdot 11\text{H}_2\text{O}$ .<sup>[51m]</sup> Some three-dimensional titanosilicates have found applications as ion-exchangers, especially for  $\text{Cs}^+$  and  $\text{Sr}^{2+}$  ions.<sup>[51n]</sup>

Most of the three-dimensional zirconosilicates are naturally occurring. A high-temperature hydrothermal reaction ( $350^\circ\text{C}$ – $500^\circ\text{C}$ ) yielded the mineral catapleiite,  $[\text{Na}_2][\text{ZrSi}_3\text{O}_9] \cdot 2\text{H}_2\text{O}$ , and elpidite,  $[\text{Na}_2][\text{ZrSi}_6\text{O}_{15}] \cdot 3\text{H}_2\text{O}$ .<sup>[54a]</sup> In elpidite, the double chains of  $\text{SiO}_4$  tetrahedra are connected by  $\text{ZrO}_6$  octahedra to form the three-dimensional structure.

Niobosilicates prepared in the presence of organic amines, have been reported.  $[\text{C}_4\text{N}_2\text{H}_{11}][\text{Nb}_3\text{SiO}_{10}]$  has been prepared in this way, it has  $\text{Nb}_2\text{O}_{10}$  dimers connected by  $\text{SiO}_4$  units to

form a chain.<sup>[55a]</sup> The  $\text{NbO}_6$  octahedra and the  $\text{SiO}_4$  tetrahedra are linked by shared vertices to form another chain. These chains in turn link with the dimer-containing chains to form the three-dimensional structure. Ion-exchange studies reveal that the piperazinium cations could be successfully exchanged for  $\text{Na}^+$  and  $\text{K}^+$  ions.<sup>[55a]</sup>

## 5. Germanates

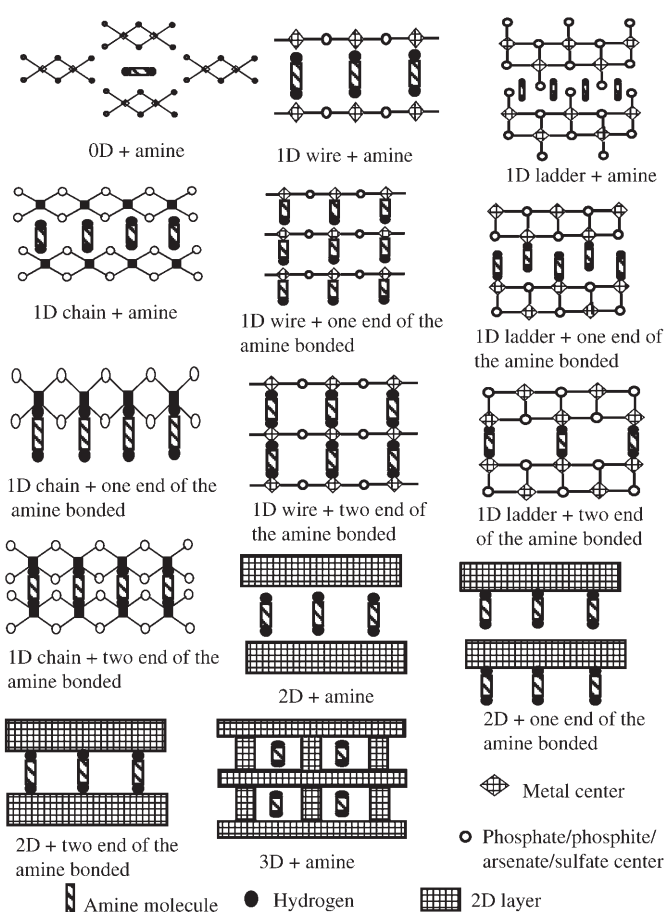
Open-framework structures based on transition-metal germanates have not been studied extensively when compared with the huge effort that has been expended on silicates and phosphates. Few amine-templated transition-metal germanates have been prepared and characterized.<sup>[56]</sup>

Similar to the silicates, niobogermanates have been prepared in the presence of amines. The structure of  $[\text{C}_6\text{N}_2\text{H}_{18}][\text{Ge}_{2.2}\text{Nb}_{0.8}\text{O}_{6.8}\text{F}_{1.2}]$  consists of  $\text{GeO}_4$  tetrahedra connected through the vertices to form one-dimensional chains. These chains are linked by  $\text{NbO}_5\text{F}$  octahedra to form the three-dimensional structure with intersecting 10- and eight-ring channels.<sup>[56a]</sup> The organic cations are located at the centers of the 10-ring windows. The niobogermanate  $[\text{C}_4\text{N}_2\text{H}_{11}][\text{Nb}_3\text{GeO}_{10}]$ <sup>[56b]</sup> is isotopic with  $[\text{C}_4\text{N}_2\text{H}_{11}][\text{Nb}_3\text{SiO}_{10}]$ .<sup>[55a]</sup> The structure of  $[\text{K}]_3[\text{Nb}_5\text{GeO}_{16}] \cdot 2\text{H}_2\text{O}$ <sup>[56c]</sup> is comparable to the that of  $[\text{C}_4\text{N}_2\text{H}_{11}][\text{Nb}_3\text{GeO}_{10}]$ .<sup>[56b]</sup>

The three-dimensional structure of the zirconogermanate  $[\text{C}_4\text{N}_2\text{H}_{14}][\text{Ge}_2\text{ZrO}_6\text{F}_2] \cdot \text{H}_2\text{O}$ <sup>[56d]</sup> has chains of vertex-sharing  $\text{GeO}_4$  tetrahedra linked by  $\text{ZrO}_4\text{F}_2$  octahedra, to give open channels running parallel to the crystallographic *a* and *b* axis. Two vertex-sharing  $\text{ZrGe}_2$  triangles form a planar  $\text{ZrGe}_4$  SBU, resembling a “bow tie”. The “bow tie” units are further linked by sharing the Ge vertices to make a 4-connected net in which two three-rings meet at every Ge vertex. If the Zr atoms are removed from the center of the bow ties, then  $\text{Ge}_4$  squares are formed and the whole net converges into the gismondine structure.<sup>[46]</sup>

## 6. Phosphates

In the field of open-framework metallophosphates, the aluminophosphates were the first to be considered because of their close structural relationship and isoelectronic nature with  $[\text{SiO}_4]^{4-}$ , which forms the basis for most of the aluminosilicate zeolite structures. The microporous aluminophosphate compounds,  $\text{ALPO}_4\text{-}n$  (*n* refers to a structural type), were discovered at the beginning of the 1980s by Flanigen et al.<sup>[13]</sup> There have been considerable attempts to prepare other phosphates, especially those containing transition metals, because these would offer good scope owing to their different valence states and/or coordination numbers. In the family of phosphates, the low-dimensional structures are stabilized by extensive hydrogen-bond interactions involving the hydrogen atoms of the amine molecules and the framework oxygen atoms. In Scheme 1, we show the variety of structures that can be imagined, from a simple monomeric unit to complex three-dimensional structures, to result from careful manipulation of the experimental parameters. Though



**Scheme 1.** The various possible one-, two-, and three-dimensional structures that can be prepared starting with zero-dimensional octahedral and tetrahedral building units in the presence of amine molecules.

a large variety of structures appears to be possible, only a few of them have been realized to date. Large number of vanadium and molybdenum cluster compounds, such as the Anderson ion, the Keggin ion, the Wells–Dawson ion, has been reported. However the discussion of these types of compounds would be beyond the scope of the present Review.

The first molecular cobaltophosphate,  $[\text{C}_6\text{N}_4\text{H}_{21}][\text{Co}(\text{H}_2\text{PO}_4)(\text{HPO}_4)_2]$ , contains  $\text{CoO}_4$  and  $\text{H}_2\text{PO}_4$  tetrahedra connected through the vertex forming a simple four-membered unit.<sup>[57]</sup> Two  $\text{HPO}_4$  units hang from the cobalt center and participate in extensive hydrogen-bonding interactions giving rise to a supramolecular, organized channel structure (Figure 4). In the family of zincophosphates, the molecular compounds have been shown to transform into higher dimensional structures under appropriate conditions (Scheme 1).<sup>[58]</sup>

The one-dimensional structures are, generally, formed by  $\text{MO}_4$  or  $\text{MO}_6$  polyhedral units connected to  $\text{PO}_4$  tetrahedra forming chain or ladder structures. In Figure 5, specific examples of the commonly observed 1D structures are shown and in the Supporting Information, Table S2 more details of these compounds and of others not shown here are presented. As can be seen, the structures show considerable variation in the connectivity between the primary building

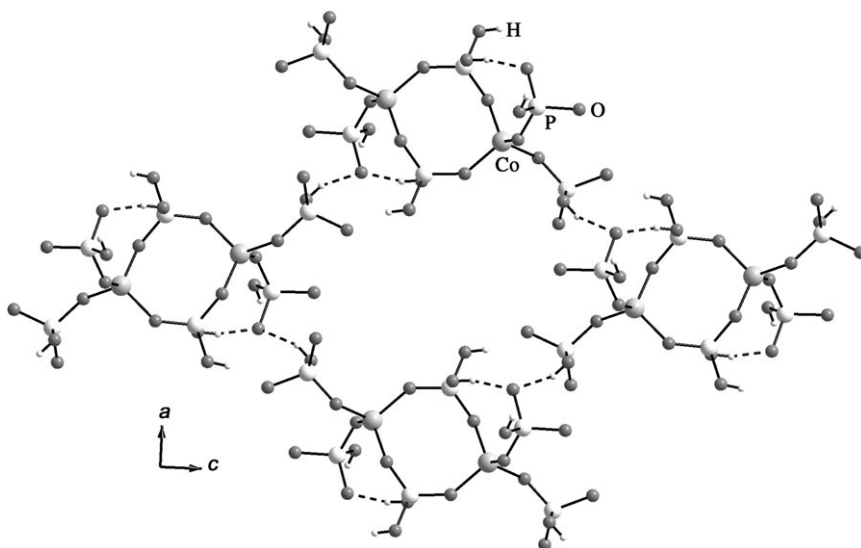


**Figure 4.** Ball-and-stick view of the molecular cobaltophosphate  $[\text{C}_6\text{N}_4\text{H}_{21}][\text{Co}(\text{H}_2\text{PO}_4)(\text{HPO}_4)_2]$ , showing the hydrogen-bond interactions.

units. Antiferromagnetic behavior has been identified for most of the compounds.

The simplest one-dimensional structure contains chains of corner-shared of four-rings (Figure 5a,b). This structure is exhibited by only a few transition metals (V,<sup>[59a]</sup> Co,<sup>[59b,c]</sup> Cu,<sup>[59d]</sup> and Nb<sup>[59e]</sup>). A truly tetrahedrally coordinate transition metal center forming the 1D chain structure does not have any terminal bonds, however, the higher coordination numbers (5, 6) of the transition-metal elements leads to the presence of terminal linkages in the form of a bond to either a ligand or a water molecule.<sup>[59a]</sup> This type of terminal bond appears to be more common when the four-rings share the edges, forming the 1D ladder structure (Figure 5c).<sup>[60]</sup>

The most common one-dimensional structure observed repeatedly in transition-metal phosphates resembles the structure of the naturally occurring mineral tancoite,  $[\text{LiNa}_2\text{H}][\text{Al}(\text{PO}_4)_2(\text{OH})]$ .<sup>[61]</sup> The general formula for the tancoite chain is  $[\text{M}(\text{TO}_4)_n\text{L}]_n$  (M and T are cations of different coordination, usually octahedral and tetrahedral, L is an anionic ligand, e.g.,  $\text{O}^{2-}$ ,  $\text{OH}^-$ , or  $\text{F}^-$ ; Figure 5d). Many compounds of transition-metal elements form this type of structure, especially titanium,<sup>[62a]</sup> vanadium,<sup>[62b,c]</sup> and iron.<sup>[62d–g]</sup> Apart from the simple one-dimensional structures, there are other one-dimensional structures possessing small metal-oxygen cluster units are also known.<sup>[63]</sup> In  $[\text{C}_4\text{H}_{12}\text{N}_2]_{1.5}[\text{Fe}_2(\text{OH})(\text{H}_2\text{PO}_4)(\text{HPO}_4)_2(\text{PO}_4)] \cdot 0.5\text{H}_2\text{O}$ , a tetramolecular iron–oxygen cluster is connected to  $\text{PO}_4$  tetrahedra forming a new SBU-10 (Figure 2s).<sup>[63a]</sup> The SBU-10 units are connected to give the 1D structure with terminal  $\text{H}/\text{H}_2\text{PO}_4$  units (Figure 5h).

In a cobaltophosphate,  $[\text{C}_4\text{N}_2\text{H}_{12}]_{1.5}[\text{Co}_2(\text{HPO}_4)_2(\text{PO}_4)(\text{H}_2\text{O})]$  two chains of vertex-shared polyhedra are fused through a three-coordinate oxygen center (Figure 5e).<sup>[64a]</sup> A three-legged ladder-like structure has been observed in  $[\text{H}_3\text{N}(\text{CH}_2)_3\text{NH}_2(\text{CH}_2)_2\text{NH}_2(\text{CH}_2)_3\text{NH}_3][\text{Fe}_3\text{F}_6(\text{HPO}_4)_2(\text{PO}_4)] \cdot 3\text{H}_2\text{O}$  (Figure 5f).<sup>[64b]</sup> Both the structures could be

intermediates between the one- and the two-dimensional structures.

Compared to the one-dimensional structures, there appears to be considerable variety and diversity in the two-dimensional structures.<sup>[65–72]</sup> The use of fluoride ions in the synthesis has given rise to many interesting layered structures, especially those containing scandium,<sup>[65]</sup> iron,<sup>[69]</sup> zirconium,<sup>[71]</sup> and niobium.<sup>[72]</sup> In most of the compounds, the one-dimensional structures are connected to either the  $\text{MO}_6$  octahedra or the  $\text{PO}_4$  tetrahedra giving rise to the two-dimensional structure. It would be a difficult task to describe the structures of all the known two-dimensional solids and only the interesting structures along with their properties are described herein.

In the layered scandophosphate  $[(\text{H}_3\text{NC}_4\text{H}_8\text{NH}_3)_2(\text{H}_3\text{O})][\text{Sc}_5\text{F}_4(\text{HPO}_4)_8]$ , four  $\text{ScO}_4\text{F}_2$  units are connected forming a tetramer (Figure 6a), which are linked by phosphates and isolated  $\text{ScO}_6$  octahedra giving rise to a layered structure with doubly protonated 1,4-diaminobutane molecules occupying the inter-layer spaces (Figure 6b).<sup>[65]</sup> This structure can thus be described as SBU-12s (Figure 2u) connected by  $\text{ScO}_6$  octahedral units to form a layer. In  $[\text{C}_6\text{H}_{11}\text{NH}_3][\text{ScF}(\text{HPO}_4)(\text{H}_2\text{PO}_4)]$ ,  $\text{ScO}_4\text{F}_2$  octahedral units are joined through fluorine atoms forming a one-dimensional chain structure, which are connected by the phosphate tetrahedra to form the layer.<sup>[65]</sup>

In some of the layered titanophosphates the amine molecules are bound to the titanium centers and project in the interlamellar region.<sup>[66a]</sup> The titanophosphate,  $[\text{C}_6\text{N}_2\text{H}_{16}]_{0.5}[\text{Ti}_2(\text{H}_2\text{PO}_4)(\text{HPO}_4)(\text{PO}_4)_2]$ ,<sup>[66d]</sup> has a close structural relationship to the  $\gamma$ -TiP structure, there are minor differences in the alignment of the terminal P–O groups, which are located alternately above and below the plane of the layers. One-dimensional tancoite-type chains connected through the  $\text{TiO}_4(\text{OH})_2$  octahedra were observed in  $[\text{H}_3\text{N}(\text{CH}_2)_3\text{NH}_3]_2[\text{Ti}_3\text{O}_2(\text{OH})_2(\text{HPO}_4)_2(\text{PO}_4)_2] \cdot 2\text{H}_2\text{O}$ .<sup>[66c]</sup>

Vanadophosphates with two-dimensional structures exhibit a wide variety and diversity.<sup>[67]</sup> The vanadophosphate  $[\text{CN}_3\text{H}_6]_2[(\text{VO}_2)_3(\text{PO}_4)(\text{HPO}_4)]$  has an infinite V–O–V network resembling the Kagomé lattice.<sup>[67a]</sup> Both octahedral as well as tetrahedral coordination has been observed for vanadium in  $[\text{V}_4\text{O}_7(\text{HPO}_4)_2(2,2'\text{-bipy})_2]$  (bipy = bipyridine).<sup>[67d]</sup> Infinite Mn–O–Mn chains connected by phosphate units have been observed in  $[\text{C}_2\text{H}_{10}\text{N}_2][\text{Mn}_2(\text{HPO}_4)_3] \cdot \text{H}_2\text{O}$ , with magnetic parameters  $C_m = 4.28 \text{ cm}^3 \text{ K mol}^{-1}$  and  $\theta = -28.1 \text{ K}$ .<sup>[68a]</sup> Most of the known two-dimensional manganese phosphates are antiferromagnetic with the Mn ions present in the +2 oxidation state.<sup>[68]</sup>

Of the many layered ferrophosphates,<sup>[69]</sup> the mixed-valent compound  $[\text{C}_6\text{N}_4\text{H}_{21}][\text{Fe}^{\text{III}}_{3-x}\text{Fe}^{\text{II}}_x\text{F}_2(\text{PO}_4)(\text{HPO}_4)_2]$  ( $x \approx 1.5$ ) is particularly interesting.<sup>[69f]</sup> In its structure, the  $\text{Fe}^{\text{II}}$  ions form the SBU-4s, which are connected together forming the infinite Fe–O/F–Fe chains. The  $\text{Fe}^{\text{III}}$  octahedra connect these chains

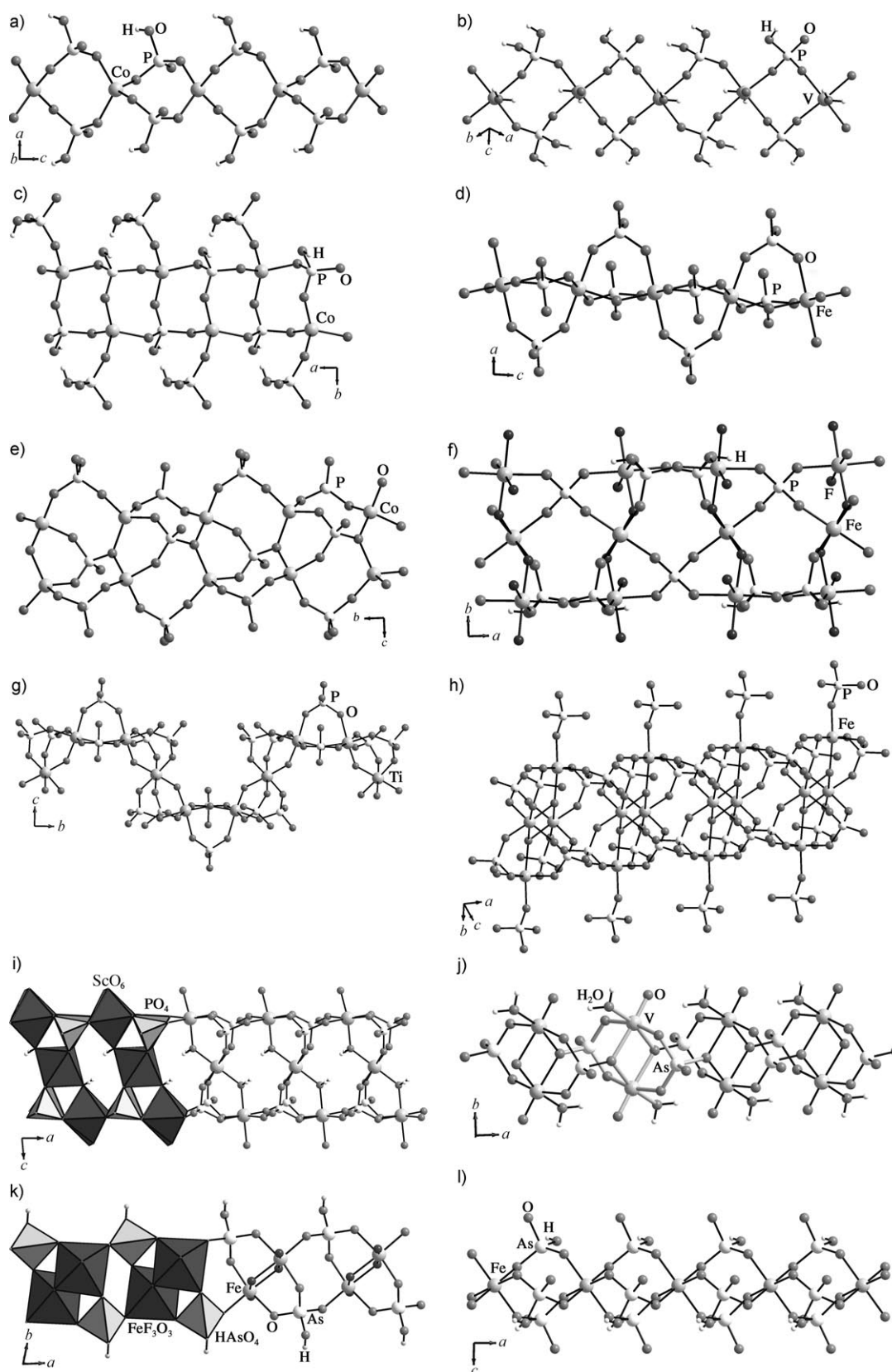


**Figure 5.** The one-dimensional structures observed in transition-metal compounds: a)  $[\text{C}_6\text{N}_2\text{H}_{16}][\text{Co}(\text{HPO}_4)_2]$ , b)  $[\text{CN}_3\text{H}_6][\text{VO}(\text{H}_2\text{O})(\text{HPO}_4)(\text{H}_2\text{PO}_4)] \cdot \text{H}_2\text{O}$ , c)  $[\text{H}_3\text{N}(\text{CH}_2)_3\text{NH}_3][\text{Co}(\text{HPO}_4)_2]$ , d)  $[\text{C}_3\text{N}_2\text{H}_{12}][\text{FeF}(\text{HPO}_4)_2] \cdot (\text{H}_2\text{O})_x$  ( $x \approx 0.20$ ), e)  $[\text{C}_4\text{N}_2\text{H}_{12}]_{1.5}[\text{Co}_2(\text{HPO}_4)_2(\text{PO}_4)(\text{H}_2\text{O})]$ , f)  $[\text{C}_8\text{N}_4\text{H}_{26}][\text{Fe}_3\text{F}_6(\text{HPO}_4)_2(\text{PO}_4)] \cdot 3\text{H}_2\text{O}$ , g)  $[\text{C}_2\text{N}_2\text{H}_{10}]_5[\text{Ti}_3\text{P}_6\text{O}_{27}] \cdot 2\text{H}_2\text{O}$ , h)  $[\text{C}_4\text{N}_2\text{H}_{12}]_{1.5}[\text{Fe}_2(\text{OH})(\text{H}_2\text{PO}_4)(\text{HPO}_4)_2(\text{PO}_4)] \cdot 0.5\text{H}_2\text{O}$ , i)  $[\text{H}_3\text{NC}_2\text{H}_4\text{NH}_3]_3[\text{Sc}_3(\text{OH})_2(\text{PO}_4)_2(\text{NC}_2\text{H}_4\text{NH}_3)_3] \cdot 2\text{H}_2\text{O}$ , j)  $[\text{C}_2\text{N}_2\text{H}_{10}][\text{V}(\text{HAsO}_4)_2(\text{H}_2\text{AsO}_4)] \cdot \text{H}_2\text{O}$ , k)  $[\text{H}_3\text{N}(\text{CH}_2)_2\text{NH}(\text{CH}_2)_2\text{NH}_3][\text{Fe}_2\text{F}_4(\text{HAsO}_4)_2]$ , l)  $[\text{C}_2\text{H}_{10}\text{N}_2][\text{Fe}(\text{HAsO}_4)_2(\text{H}_2\text{AsO}_4)] \cdot \text{H}_2\text{O}$ .

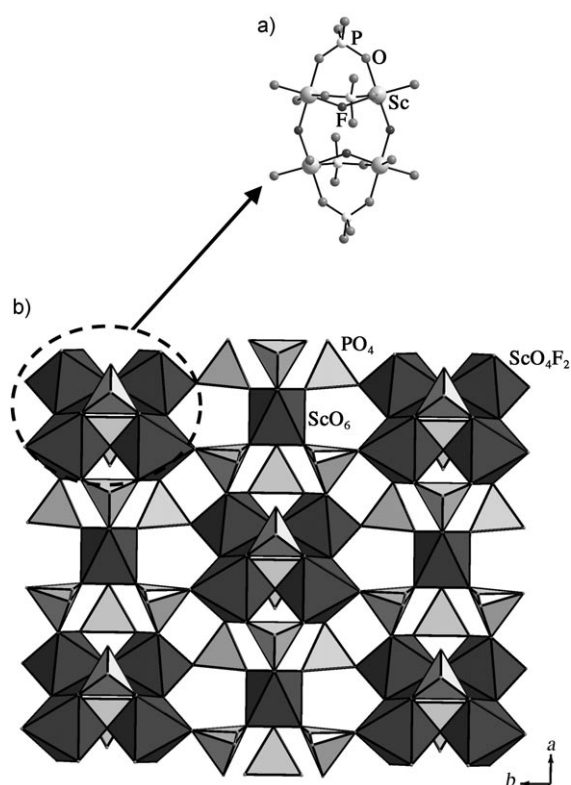


**Figure 6.** a) The basic building unit, b) view of the layer structure in  $[(\text{H}_3\text{NC}_4\text{H}_8\text{NH}_3)_2(\text{H}_3\text{O})][\text{Sc}_5\text{F}_4(\text{HPO}_4)_8]$ , along the  $c$ -axis.

forming the layer. The magnetic susceptibility studies indicate antiferromagnetic interactions with  $\theta = -128$  K. The compound shows a low Curie temperature ( $T_c = 25$  K) and exhibits a hysteresis loop at 4.5 K ( $H_c = 2300$  Oe and  $M_r = 2.3 \mu_B \text{ mol}^{-1}$ ). In  $[\text{H}_3\text{N}(\text{CH}_2)_3\text{NH}_3][\text{Fe}_2\text{O}(\text{PO}_4)_2]$  SBU-8s are connected to form the layers.<sup>[69b]</sup> The first examples of layered cobaltophosphates are from Haushalter et al.<sup>[70a]</sup> In  $[\text{H}_3\text{N}(\text{CH}_2)_3\text{NH}_3][\text{Co}(\text{PO}_4)] \cdot 0.5 \text{H}_2\text{O}$  and  $[\text{H}_3\text{N}(\text{CH}_2)_4\text{NH}_3][\text{Co}(\text{PO}_4)]$ ,  $\text{CoO}_4$  tetrahedra are connected together to form Co-O-Co 1D chains which are connected by  $\text{PO}_4$  units to form the layers.<sup>[70a]</sup> Magnetic susceptibility studies indicate predominant antiferromagnetic behavior. In  $[\text{C}_4\text{N}_2\text{H}_{12}]_{1.5}[\text{Co}_2(\text{HPO}_4)_2(\text{PO}_4)_2 \cdot \text{H}_2\text{O}]$  one-dimensional zigzag ladders are connected together forming the layer.<sup>[64a]</sup>

The classical layered zirconophosphates have the  $\alpha$ -ZrP structure.  $[\text{C}_2\text{N}_2\text{H}_{10}]_{0.5}[\text{Zr}(\text{PO}_4)(\text{HPO}_4)]$ <sup>[71]</sup> is topologically related to  $\gamma$ -ZrP ( $[\text{Zr}(\text{PO}_4)(\text{H}_2\text{PO}_4)] \cdot 2 \text{H}_2\text{O}$ ). In  $[\text{C}_5\text{N}_2\text{H}_7][\text{NbOF}(\text{PO}_4)]$ ,  $\text{NbO}_5\text{F}$  octahedra are connected by  $\text{PO}_4$  tetrahedra to form the  $\text{NbOPO}_4$  layers, the terminal F atoms project on both sides of the layer.<sup>[72]</sup>

The three-dimensional structures are the dominant phosphate structural class.<sup>[73, 74, 76, 77, 80–86]</sup> The variety and diversity of these structures have been reviewed by Cheetham et al in 1999.<sup>[2]</sup> Herein, we describe some of the important structures that have been discovered since that review. The three-dimensional structures have been described using SBUs. The presentation will follow the sequence in the periodic table.

The organic-amine-templated scandophosphates have been prepared recently.<sup>[73]</sup> In  $[\text{C}_2\text{N}_2\text{H}_{10}]_{0.5}[\text{Sc}(\text{HPO}_4)_2]$ , strictly

alternating  $\text{ScO}_6$  and  $\text{HPO}_4$  polyhedral units are connected together forming the three-dimensional structure.<sup>[73a]</sup> The mixed-valent  $[\text{C}_2\text{N}_2\text{H}_9][\text{Ti}^{\text{III}}\text{Ti}^{\text{IV}}(\text{HPO}_4)_4] \cdot \text{H}_2\text{O}$  contains one-dimensional chains formed by linking  $(\text{Ti}^{\text{III}}/\text{Ti}^{\text{IV}})\text{O}_6$  octahedra and  $\text{HPO}_4$  tetrahedra.<sup>[74b]</sup> These chains are connected by other  $\text{HPO}_4$  tetrahedra to form the layers, which are connected to each other forming the three-dimensional structure. The magnetic studies show a simple Curie behavior with an effective magnetic moment of  $1.23 \mu_B$ , consistent with one unpaired electron per formula unit. A related structure with mixed-valent titanium,  $[\text{H}_3\text{NCH}_2\text{CH}_2\text{CH}_2\text{NH}_3]_{0.5}[\text{Ti}^{\text{III}}\text{Ti}^{\text{IV}}(\text{PO}_4)(\text{HPO}_4)_2(\text{H}_2\text{O})]$ , has also been reported.<sup>[74a]</sup> The magnetic studies, however, indicate a paramagnetic behavior.

Vanadium-based compounds have been investigated with interest because vanadyl pyrophosphate,  $(\text{VO})_2\text{P}_2\text{O}_7$ , has been shown to be selective for the oxidation of butane to maleic anhydride.<sup>[75]</sup> There have been many reports of vanadophosphates with three-dimensional structures.<sup>[76]</sup> Since vanadium forms clusters quite easily, V-O-V linkages are found in many vanadium phosphates. In  $[\text{C}_2\text{N}_2\text{H}_{10}][(\text{VO})(\text{VO}_2)\{\text{V}(\text{OH})_2\}(\text{PO}_{3.5})_4] \cdot \text{H}_2\text{O}$ ,  $[\text{V}_3\text{O}_{16}]$  trimers are connected to four phosphates to form an SBU-7 ( $\text{V}_3\text{P}_4\text{O}_{18}$ ; Figure 2m).<sup>[76a]</sup> The SBU-7s are connected together forming the three-dimensional structure. In  $[\text{H}_2\text{N}(\text{CH}_2\text{CH}_2)_2\text{NH}_2][(\text{VO})_4(\text{H}_2\text{O})_4(\text{HPO}_4)_2(\text{PO}_4)_2]$ , tancoite chains are connected by  $\text{VO}_3(\text{OH})_2$  units to form layers, which in turn are connected by  $\text{VO}_5(\text{OH})$  units to give the three-dimensional structure.<sup>[76b]</sup> The magnetic studies indicate antiferromagnetic behavior with  $C_m = 1.58 \text{ cm}^3 \text{ K mol}^{-1}$  and  $\theta = -19$  K. In  $[\text{H}_2\text{N}(\text{C}_2\text{H}_4)_2\text{NH}_2]_{0.5}[(\text{VO})_4\text{V}(\text{HPO}_4)_2(\text{PO}_4)_2\text{F}_2(\text{H}_2\text{O})_4] \cdot 2 \text{H}_2\text{O}$ ,  $\text{V}_2\text{FO}_8$  dimers are connected by the phosphate tetrahedra to form the layers, which are cross-linked by  $\text{VO}_6$  octahedra.<sup>[76c]</sup> In  $[\text{NH}_4][\text{V}(\text{PO}_4)\text{F}]$ , ferromagnetic interactions with  $C_m = 0.865 \text{ cm}^3 \text{ K mol}^{-1}$  and  $\theta = +2.7$  K have been detected.<sup>[76e]</sup>

The manganophosphate,  $[\text{NH}_4][\text{Mn}_n(\text{PO}_4)_3]$ , has  $\text{MnO}_n$  ( $n = 5$  or  $6$ ) polyhedral and  $\text{PO}_4$  tetrahedral units, connected to form the three-dimensional structure.<sup>[77a]</sup> The magnetic studies show antiferromagnetic behavior ( $T_N \approx 17$  K,  $C_m = 4.09 \text{ cm}^3 \text{ K mol}^{-1}$ ,  $\theta = -33.5$  K). The difficulty in preparing three-dimensional manganophosphates prompted many researchers to study mixed-metal phosphates involving Mn. This research gave rise to a variety of compounds with three-dimensional structures.<sup>[77b–e]</sup>

Ferrophosphates are among the most important family of compounds known in the mineral kingdom, and have been reviewed by Moore and Shen.<sup>[78a]</sup> The most famous ferrophosphate mineral is cacoenite,  $[\text{AlFe}_{24}(\text{OH})_{12}(\text{PO}_4)_{17}(\text{H}_2\text{O})_{24}] \cdot 51 \text{H}_2\text{O}$ ,<sup>[78b]</sup> which contains a 24-ring with  $14.2 \text{ \AA}$  diameter channel structure. Some of the dense ferrophosphates have been used for the selective oxidative dehydrogenation of isobutyric acid into methacrylic acid. The combination of hydrothermal methods along with the use of the fluoride route paved the way for the discovery of many three-dimensional ferrophosphates. Major contribution in this area has been made by Férey in France (ULM phases)<sup>[26d]</sup> and Lii in Taiwan.<sup>[79]</sup>

The ferrophosphate  $[\text{H}_3\text{NCH}_2\text{CH}_2\text{NH}_3]_2[\text{Fe}_4\text{O}(\text{PO}_4)_4] \cdot \text{H}_2\text{O}$  consists of cubane-like building units, formed by four trigonal-bipyramidal iron centers, each connected

through four-coordinate oxygen atoms ( $\mu^4$ ) residing in the center of the cube.<sup>[80a]</sup> The phosphate groups occupy the remaining four vertices of the cube, forming the SBU-8 building unit (see Figure 2n). The eight vertices of the “Fe<sub>4</sub>P<sub>4</sub>” oxo clusters are connected through Fe-O-P bonds to form the three-dimensional structure (Figure 7). Mössba-

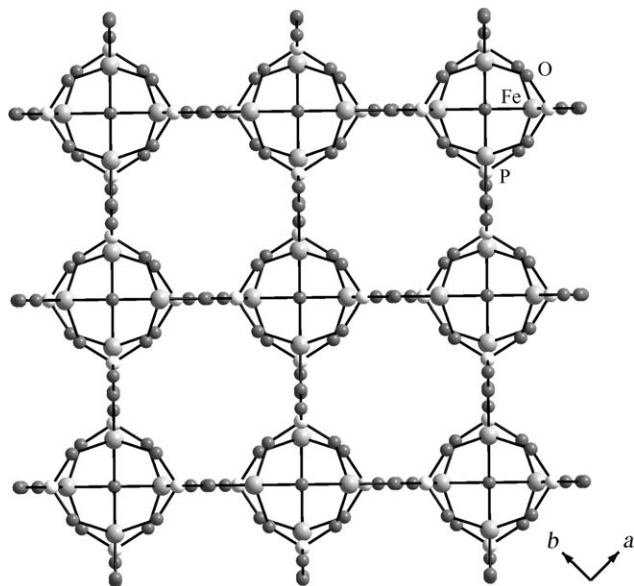


**Figure 7.** Structure of  $[\text{H}_3\text{NCH}_2\text{CH}_2\text{NH}_3]_2[\text{Fe}_4\text{O}(\text{PO}_4)_4] \cdot \text{H}_2\text{O}$  in the *ab* plane.

uer and alternating current (ac) magnetic susceptibility measurements indicate the presence of Fe<sup>2+</sup> and Fe<sup>3+</sup> species and show long-range magnetic ordering at approximately 12 K. The ferrophosphate  $[(\text{C}_4\text{N}_3\text{H}_{16})(\text{C}_4\text{N}_3\text{H}_{15})][\text{Fe}_5\text{F}_4(\text{H}_2\text{PO}_4)(\text{HPO}_4)_3(\text{PO}_4)_3] \cdot \text{H}_2\text{O}$  contains Fe-O/F-Fe infinite 1D chains, which are connected by the phosphate tetrahedra to give rise to a layered structure.<sup>[80b]</sup> The layers are pillared by further PO<sub>4</sub> tetrahedra forming the 3D structure with extra

large 24-ring channels in which the amine and H<sub>2</sub>O molecules reside (Figure 8a). The 3D structure can also be considered to be built-up by SBU-11s (five FeO<sub>6-*x*</sub>F<sub>*x*</sub> (*x* = 0–2) and six PO<sub>4</sub> tetrahedra; see Figure 2t). The compound exhibits a spin-crossover behavior (Figure 8b).

It is well established that cobalt(II) centers exhibit tetrahedral coordination and it is this preference that prompted researchers to investigate the formation of cobalt-containing framework compounds. The initial efforts were on substitution in aluminophosphates structures, AlPO-*n*.<sup>[81]</sup> Stucky and co-workers employed the electronic similarity between the bivalent phosphates with the aluminosilicates and prepared a large number of cobaltophosphates.<sup>[82]</sup> The isolation of first amine-templated cobaltophosphates<sup>[83a]</sup> opened the way to other similar compounds.<sup>[83]</sup> Of these species,  $[\text{H}_3\text{NC}_2\text{H}_4\text{NH}_3]_2[\text{Co}_7(\text{PO}_4)_6]$  is particularly interesting owing to the presence of three different coordination environments for cobalt (CoO<sub>4</sub>, CoO<sub>5</sub>, and CoO<sub>6</sub>; Figure 9a).<sup>[83d,e]</sup> The magnetic and differential scanning calorimetry (DSC) studies showed a possible structural transition at *T* ≈ 200 K, which was confirmed by single-crystal structure analysis. A slight change in the Co–O separations gave rise to infinite Co–O–Co two-dimensional layers. The magnetic studies showed possible ferrimagnetic behavior (Figure 9b). The *M* versus *H* studies at 2 K indicate a possible transition from one magnetic state to another (inset, Figure 9b). Zeolite analogues of cobaltophosphates are also known. Thus,  $[\text{C}_2\text{N}_2\text{H}_{10}]_2[\text{Co}_4(\text{PO}_4)_4] \cdot \text{H}_2\text{O}$ <sup>[83b]</sup> with a merlinoite structure<sup>[46]</sup> and  $[\text{H}_3\text{NCH}_2\text{CH}_2\text{NH}_3]_{0.5}[\text{CoPO}_4]$ <sup>[83c]</sup> with a gismondine<sup>[46]</sup> structure have been isolated and characterized.

Among the nanoporous materials, the family of aluminophosphates and the titanosilicates have yielded molecular sieves with interesting catalytic properties. The comparatively poor thermal stability of the nanoporous transition-metal phosphates (V, Fe, Co, etc.) rendered them unsuitable for applications that required a porous nature of the solid. Recently, nanoporous nickelophosphates (VSB-1, VBS-5) have been reported by Cheetham, Férey and co-workers with large pore diameter along with a reasonable thermal stabil-

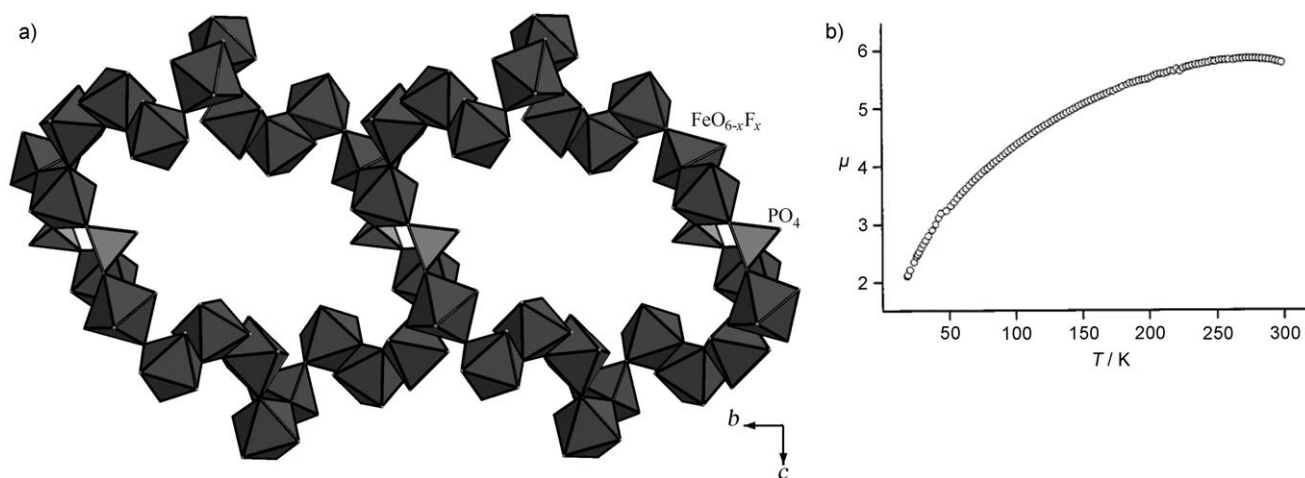


**Figure 8.** a) Skeletal structure of  $[(\text{C}_4\text{N}_3\text{H}_{16})(\text{C}_4\text{N}_3\text{H}_{15})][\text{Fe}_5\text{F}_4(\text{H}_2\text{PO}_4)(\text{HPO}_4)_3(\text{PO}_4)_3] \cdot \text{H}_2\text{O}$ , showing the one-dimensional Fe-O/F-Fe chains and their connectivity with the PO<sub>4</sub> units. b) The temperature variation of the magnetic moment  $\mu$  for each iron center in units of  $\mu_B$ .

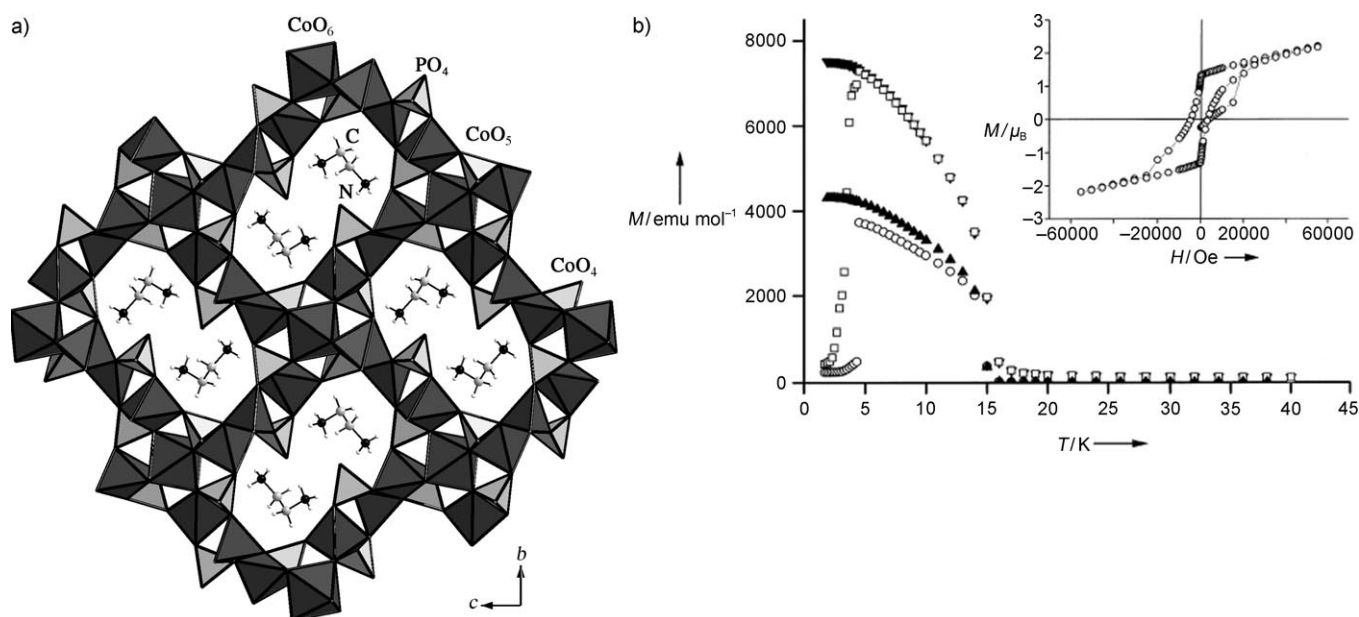


**Figure 9.**  $[\text{H}_3\text{NC}_2\text{H}_4\text{NH}_3]_2[\text{Co}_7(\text{PO}_4)_6]$ : a) The polyhedral connectivity showing the channels along the  $a$  axis. b) Thermal variation of the magnetic susceptibility. The field-cooled (FC) data show a saturation behavior.  $\circ$  ZFC,  $\blacktriangle$  FC, 50 Oe;  $\square$  ZFC,  $\blacktriangledown$  FC, 1000 Oe. The inset shows the  $M$  vs  $H$  studies at 2 K.

ity.<sup>[84]</sup> Thus,  $[\text{NH}_4/\text{H}_3\text{O}][\text{Ni}_{18}(\text{HPO}_4)_{14}(\text{OH})_3\text{F}_9] \cdot 12\text{H}_2\text{O}$  (VSB-1), has a network of vertex- and edge-sharing  $\text{NiO}_6$  octahedra with the  $\text{PO}_4$  groups decorating the surface of the network, forming 24-ring one-dimensional channels with an effective width of 8.8 Å (Figure 10a).<sup>[84a]</sup> The compound shows canted antiferromagnetic ordering ( $T_N = 10.5$  K) with  $\theta = -71$  K. On calcining in air at 350°C, VSB-1 yields a BET surface area of 82 m<sup>2</sup> g<sup>-1</sup>, and appears to be stable in air up to 500°C. VSB-1 has low surface area compared to aluminosilicates but the density is twice that of the zeolites and the channel walls are also thick. The catalytic properties of VSB-1 appear to be promising with high selectivity (> 80%) for the dehydrocyclodimerization of 1,3-butadiene to ethylbenzene (Figure 10b).<sup>[84b]</sup> The lack of acidity in VSB-1 appears to be a virtue in this case as it suppresses the formation of oligomeric products.

The other nickelophosphate,  $[\text{Ni}_{20}(\text{OH})_{12}(\text{H}_2\text{O})_6(\text{HPO}_4)_4(\text{PO}_4)_8] \cdot 12\text{H}_2\text{O}$ , (VSB-5) possesses a much higher surface area (500 m<sup>2</sup> g<sup>-1</sup>).<sup>[84c]</sup> Like VSB-1, it is also stable in air up to 500°C, it exhibits good catalytic behavior for the partial hydrogenation of butadiene selectively into butenes.<sup>[84c]</sup> Its hydrogen absorption capacity is five-times higher than that of VSB-1, twice that of ZSM-5, and similar to that of the activated carbon (Figure 10c).<sup>[84d]</sup>

The use of the fluoride route has generated a few three-dimensional zirconophosphates.<sup>[85]</sup> The three-dimensional zirconophosphate  $[\text{C}_2\text{N}_2\text{H}_{10}]_{0.5}[\text{Zr}_2(\text{PO}_4)_2(\text{HPO}_4)\text{F}] \cdot \text{H}_2\text{O}$  has eight-ring channels formed by alternating  $\text{ZrO}_5\text{F}$  octahedra and  $\text{PO}_4$  tetrahedra.<sup>[85]</sup> The molybdophosphates with a Mo/P ratio < 1 appear to form a very large family with many of them being prepared in solid-state reactions at temperatures above 750°C. Haushalter et al. reported the successful synthesis of molybdophosphates with open-framework structures employing the hydrothermal method.<sup>[86]</sup> The compound

$[\text{Me}_4\text{N}]_{1.3}[\text{H}_3\text{O}]_{0.7}[\text{Mo}_4\text{O}_8(\text{PO}_4)_2] \cdot 2\text{H}_2\text{O}$  is built up from a tetramer ( $\text{Mo}_4\text{O}_8$ ) and  $\text{PO}_4$  tetrahedra connected together to form the three-dimensional structure which has large voids, these are occupied by the organic amine and the lattice water molecules.<sup>[86a]</sup> In  $[\text{NH}_4][\text{Mo}_2\text{P}_2\text{O}_{10}] \cdot \text{H}_2\text{O}$ , the  $\text{Mo}_4$  oxo units connected by  $\text{PO}_4$  groups form tunnels.<sup>[86b]</sup>

## 7. Phosphites

After the aluminosilicate zeolites, the aluminophosphates and other related phosphate-based compounds have been studied in most detail. Recently, it has been shown that the pseudotetrahedral phosphite group  $\text{HPO}_3^{2-}$  can be employed instead of the more traditional  $\text{PO}_4^{3-}$  group in open-framework structures. Thus, the phosphite structures are beginning to emerge as an important family. One of the features of the phosphite groups is that the three P–O bonds (unlike four in  $\text{PO}_4$  tetrahedra) can give rise to structures that are not generally observed in the four-connected phosphate-based compounds. There has been considerable research effort in this area, especially from the groups of Feng in China,<sup>[87]</sup> Harrison in the UK,<sup>[88]</sup> and Rojo in Spain.<sup>[89]</sup> Important structures of this family are presented below.

One of the challenging tasks in preparing transition-metal-based framework structures<sup>[89–91]</sup> is to obtain compounds based on  $\text{Cr}^{\text{III}}$ . The octahedrally coordinate  $\text{Cr}^{\text{III}}$  ion was expected to be very stable owing to its large ligand-field stabilization energy. However,  $\text{Cr}^{\text{III}}$  in solution is not stable and the formation of chromium(III)-based compounds exhibiting framework structures has always been difficult. The first chromium containing one-dimensional compound,  $[\text{C}_2\text{N}_2\text{H}_{10}][\text{Cr}^{\text{III}}(\text{HPO}_3\text{F})_3]$ , was isolated only a few years ago.<sup>[89,90]</sup>  $\text{CrF}_3\text{O}_3$  octahedra and  $\text{HPO}_3$  units are connected to form a

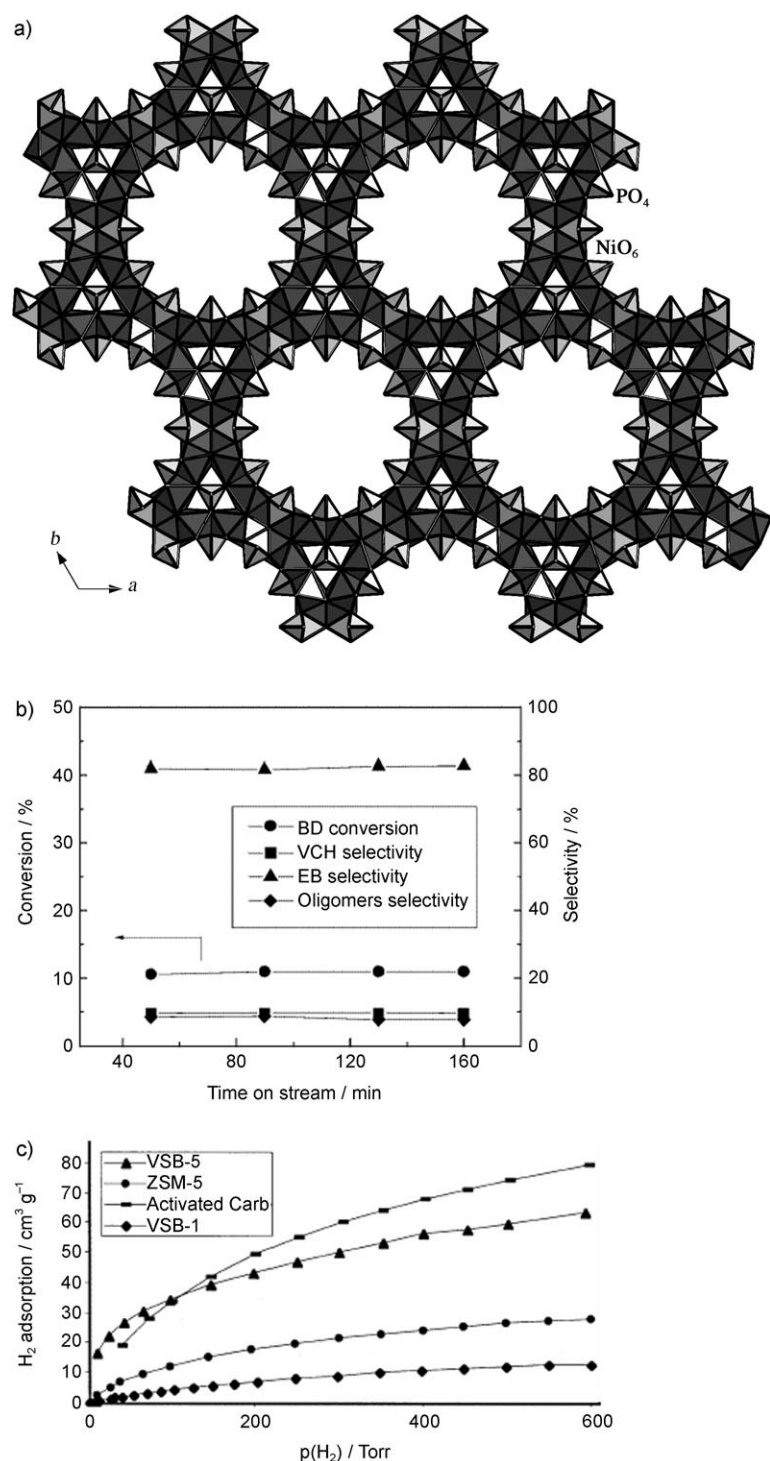


**Figure 10.** a) The structure of VSB-1 along the *c* axis. Water molecules and extra-framework cations are omitted for clarity. b) The Diels–Alder cyclodimerization of 1,3-butadiene over VSB-1. Reaction conditions:  $T = 400^{\circ}\text{C}$ , GHSV =  $7800\text{ cm}^3\text{ g}^{-1}\text{ h}^{-1}$  (GHSV: gas hourly space velocity), feed gas: 1,3-butadiene/helium (3/10). 1,3-butadiene (BD), 4-vinylcyclohexane (VCH), ethylbenzene (EB). c) Hydrogen uptake of VBS-1, VSB-5, and other porous compounds.

simple ladder structure with the Cr–F bonds being terminal. Similar structure was also isolated with vanadium,  $[\text{C}_2\text{N}_2\text{H}_{10}][\text{V}(\text{HPO}_3)_3\text{F}_3]$ ,<sup>[89]</sup> and iron,  $[\text{C}_2\text{N}_2\text{H}_{12}][\text{Fe}(\text{HPO}_3)_3\text{F}_3]$ .<sup>[91b]</sup> The magnetic studies indicate antiferromagnetic interactions in all

the compounds. A mixed-valent ferrophosphite,  $[\text{C}_4\text{N}_2\text{H}_{12}][\text{Fe}^{\text{II}}\text{Fe}^{\text{III}}(\text{HPO}_3)_2\text{F}_3]$ , contains  $\text{Fe}^{\text{II}}\text{O}_4\text{F}_2$ ,  $\text{Fe}^{\text{III}}\text{O}_3\text{F}_3$ , and  $\text{HPO}_3$  units connected to form the corner-shared chain structure, with antiferromagnetic interactions.<sup>[91c]</sup>

Unlike the phosphate structures, the number of, as well as the variety in layered phosphites is considerably less. It is likely that the phosphite structures are just beginning to emerge.<sup>[92–95]</sup> Of the layered structures,  $[\text{C}_2\text{N}_2\text{H}_{20}][\text{M}_3(\text{HPO}_3)_2]$  ( $\text{M} = \text{Mn}, \text{Fe}, \text{Co}$ ), is particularly interesting.<sup>[92b, 93b, 94a]</sup> The structure has trimeric  $\text{M}_3\text{O}_{12}$  units, formed by the face-shared  $\text{MO}_6$  octahedra, which are connected by the phosphite units. Magnetic studies show antiferromagnetic interactions with  $J = -17\text{ K}$  for Mn and  $\theta = -18.3\text{ K}$  and  $-44.8\text{ K}$  for Fe and Co, respectively. In  $[\text{C}_6\text{N}_2\text{H}_{16}][\text{M}(\text{HPO}_3)\text{F}]$  ( $\text{M} = \text{Fe}, \text{Co}$ ), infinite one-dimensional M–F–M chains have been observed, which order antiferromagnetically with  $\theta = -4.6\text{ K}$  and  $-13.59\text{ K}$  for Fe and Co, respectively.<sup>[93a]</sup> The mixed-valent vanadophosphite  $[\text{C}_6\text{N}_2\text{H}_{16}][\text{V}^{\text{III}}(\text{OH})_2(\text{V}^{\text{IV}}\text{O})_2(\text{HPO}_3)_4]\cdot\text{H}_2\text{O}$  consists of  $[\text{VO}^{\text{IV}}(\text{HPO}_3)_2]^{2-}$  chains connected by  $\text{VO}^{\text{III}}_4(\text{OH})_2$  octahedral units.<sup>[95c]</sup> Magnetic susceptibility studies indicate antiferromagnetic behavior with  $\theta = -4.05\text{ K}$ .

Of the many three-dimensional phosphite structures, those belonging to Zn are the major class.<sup>[18, 88]</sup> Only a few three-dimensional transition-metal phosphite structures have been prepared and characterized.<sup>[96, 97]</sup> Since the phosphite can form only three P–O–M linkages, it is easier for a four-coordinate zinc to form a three-dimensional structure than the usually six-coordinate transition-metal element.

The  $[\text{C}_2\text{N}_2\text{H}_{10}]_{0.5}[\text{M}(\text{HPO}_3)_2]$  ( $\text{M} = \text{V}^{\text{III}}, \text{Fe}^{\text{III}}$ ), compounds have structures built up from  $\text{MO}_6$  octahedra and  $\text{HPO}_3$  units.<sup>[96a]</sup> The ethylenediamine molecules occupy the eight-ring channels in the structure. Magnetic studies indicate antiferromagnetic interactions with  $\theta = -34.7\text{ K}$  and  $-88.4\text{ K}$  for  $\text{V}^{\text{III}}$  and  $\text{Fe}^{\text{III}}$ , respectively. In  $[\text{C}_5\text{N}_3\text{H}_{18}][\text{Fe}_3(\text{HPO}_3)_6]\cdot 3\text{H}_2\text{O}$ , SBU-9s (Figure 2r) formed by three  $\text{FeO}_6$  octahedra and six  $\text{HPO}_3$  units have been observed.<sup>[97b]</sup> The SBU-9s link together to give the three-dimensional structure (Figure 11a). Specific-heat and magnetic measurements show a  $\lambda$ -type transition at  $32\text{ K}$  (Figure 11b), along with an antiferromagnetic behavior and a reorientation of the spins below  $15\text{ K}$  because of incomplete cancellation of the spins. In  $[\text{C}_5\text{N}_2\text{H}_{14}][\text{VO}(\text{H}_2\text{O})_3(\text{HPO}_3)_4]\cdot\text{H}_2\text{O}$  two dimensional layers connected by one-dimensional ladders have been observed.<sup>[96b]</sup> Magnetic susceptibility studies indicate antiferromagnetic interactions with  $\theta = -2.24\text{ K}$ . Feng and co-workers have employed organic ligands for the construction of three-dimensional structures.<sup>[96c]</sup> Thus, in  $[(\text{V}^{\text{IV}}\text{O})_4(4,4'\text{-bpy})_2(\text{HPO}_3)_4]$ , the 4,4'-bpy (4,4'-bipyridine) ligands have been employed for connecting of vanadophosphite layers. Magnetic susceptibility studies show antiferromagnetic ordering with  $T_N = 12\text{ K}$ .

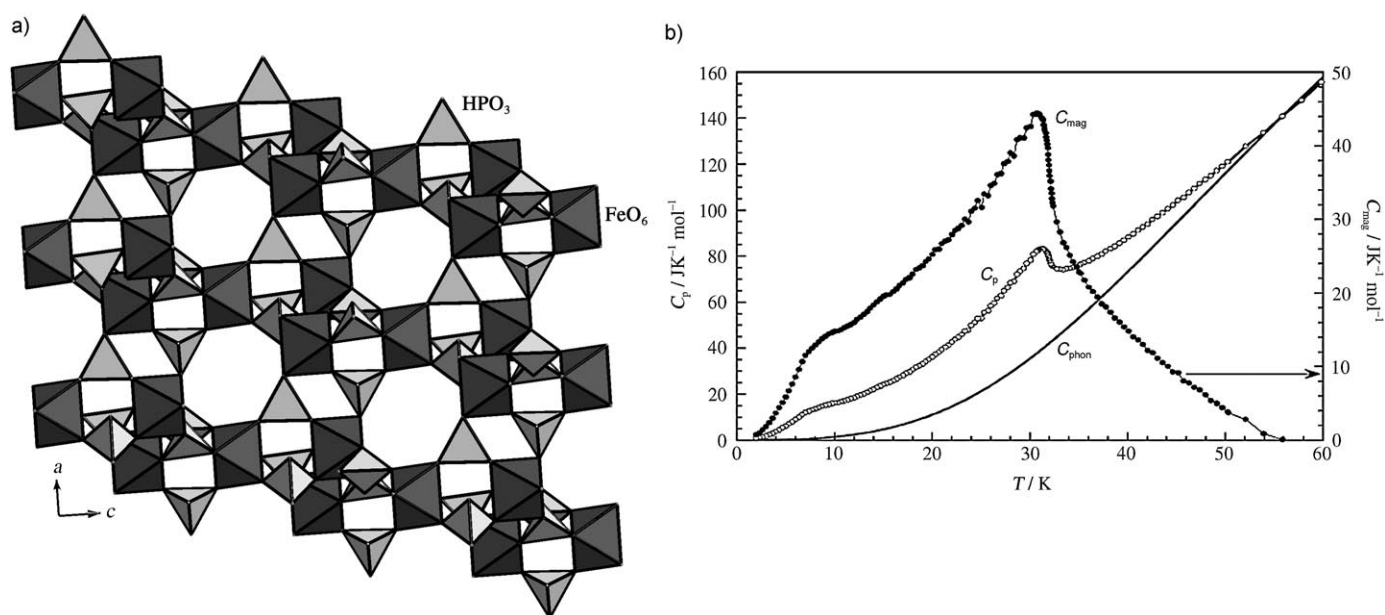


**Figure 11.** a) Polyhedral view of the structure of  $[\text{C}_5\text{N}_3\text{H}_{18}][\text{Fe}_3(\text{HPO}_3)_6] \cdot 3\text{H}_2\text{O}$  along the  $b$  axis, showing the connectivity between the SBU-9s. b) Thermal evolution of  $C_p$  (specific heat),  $C_{\text{phon}}$  (lattice contribution), and  $C_{\text{mag}}$  (magnetic contribution).

## 8. Phosphonates

The idea of using organophosphonates was to replace the phosphate anions in framework compounds. The phosphonate group,  $\text{RPO}_3^{2-}$ , with its lower charge and connectivity can form interesting networks, similar to the phosphite group discussed above. Alberti<sup>[98]</sup> employed monophosphonates to enlarge the interlayer spacing, this is because there is little interaction between the hydrophobic alkyl chains attached to the phosphonate group. Thus, the use of monophosphonates always resulted in lower-dimensional structures and in particular, layered ones. One of the advantages of the organophosphonate compounds is the flexibility provided by the organic tail (Supporting Information, Table S3).<sup>[99]</sup> There are only a few reports of zero-dimensional,<sup>[100]</sup> and one-dimensional<sup>[101]</sup> monophosphonates.

The use of methyl phosphonic acid has given rise to a variety of two-dimensional structures.<sup>[102]</sup> In  $[\text{ScF}(\text{H}_2\text{O})\text{PO}_3\text{CH}_3]$ ,<sup>[102a]</sup> one-dimensional Sc-F-Sc chains are observed while in  $[\text{Fe}(\text{PO}_3\text{CH}_3)] \cdot \text{H}_2\text{O}$ ,<sup>[102d]</sup> the layers are formed by the strictly alternating arrangement of  $\text{FeO}_6$  octahedra and  $\text{CH}_3\text{PO}_3$  units. Magnetic studies of the ferrophosphonates show antiferromagnetic interactions with  $C_m = 3.99 \text{ cm}^3 \text{ K mol}^{-1}$  and  $\theta = -59 \text{ K}$ . The only known three-dimensional monophosphonate,  $[\text{Cu}(\text{O}_3\text{PCH}_3)]$ , consists of zigzag one-dimensional chains of Cu-O-Cu, formed by  $\text{CuO}_5$  units, connected by the phosphonate units giving rise to 24-ring channel structure.<sup>[103]</sup> The methyl groups protrude into the channels and the magnetic studies show antiferromagnetic behavior with  $T_N = 15 \text{ K}$ .

Diphosphonate groups are more versatile for the formation of higher dimensional structures through pillaring of the layers and other similar structural arrangements. Earlier work

in this area was by Jacobson and co-workers,<sup>[104]</sup> Zubieta and co-workers,<sup>[105]</sup> and Férey and co-workers.<sup>[106]</sup> The use of the methylene diphosphonate anion in preparing vanadium compounds has given rise to zero-,<sup>[105b]</sup> one-,<sup>[105b]</sup> and two-dimensional structures.<sup>[105b]</sup> Magnetic studies indicate that the compounds start to show weak ferromagnetic interactions as the dimensionality increases. In the functionalized diphosphonate,  $[\text{Ni}\{\text{NH}_3\text{CH}(\text{PO}_3\text{H})_2\}_2] \cdot x\text{H}_2\text{O}$ ,  $\text{NiO}_6$  octahedra and phosphonate groups form a square-grid-like layered structure.<sup>[107]</sup> Magnetic studies indicate antiferromagnetic behavior with  $T_N = 19.6 \text{ K}$ .

Most of the diphosphonate structures are three-dimensional.<sup>[106a,d-f,108]</sup> In  $[\text{Ti}_3\text{O}_2(\text{H}_2\text{O})_2(\text{O}_3\text{PCH}_2\text{PO}_3)_2] \cdot (\text{H}_2\text{O})_2$ , trimeric  $\text{Ti}_3\text{O}_{16}(\text{H}_2\text{O})$  units are connected through the phosphonate units forming the three-dimensional structure.<sup>[106d]</sup> In  $[\text{Cu}_4\{\text{CH}_3\text{C}(\text{OH})(\text{PO}_3)_2\}_2(\text{C}_4\text{N}_2\text{H}_4)(\text{H}_2\text{O})_4]$ , the hydroxyethylidene diphosphonate anions  $[\text{hedp}]^{4-}$  join  $\text{CuO}_4$  square-planar units forming  $\{\text{Cu}_3(\text{hedp})_2\}$  trimers which are connected through further  $\text{CuO}_4$  units forming layers, that are pillared by pyrazine.<sup>[108a]</sup> The compound shows a metamagnetic behavior.

During the last decade or so, a new variant to the phosphonate was discovered, in the form of carboxylates. The clever combination of transition-metal coordination and bonding preferences and the flexibility of the organic backbone has given rise to a spectacular variety and diversity of structures. The resulting compounds, especially those prepared using a more rigid aromatic backbone, show properties such as adsorption and catalysis. The description of these compounds is beyond the scope of this Review primarily because of the bewildering number and variety. Additionally, this area has recently been reviewed by Rao and co-workers<sup>[6]</sup> and by Vaciana and et al.<sup>[10]</sup>

## 9. Arsenates

Arsenic belongs to the same group as phosphorus, which has prompted investigations into the study of arsenate-based open-framework compounds. The larger size of the  $\text{As}^{5+}$  ion (0.335 Å) compared to the  $\text{P}^{5+}$  ion (0.17 Å) could lead to the formation of novel structures.<sup>[109]</sup> The  $\text{p}K_{\text{a}}$  values of the acids  $\text{H}_3\text{PO}_4$  and  $\text{H}_3\text{AsO}_4$  (for  $\text{H}_3\text{PO}_4$ :  $\text{p}K_{\text{a}1}$ ,  $\text{p}K_{\text{a}2}$ , and  $\text{p}K_{\text{a}3}$  values are 2.12, 7.21, and 12.32, for  $\text{H}_3\text{AsO}_4$ : 2.3, 6.9, and 11.5) show that the latter is relatively weaker. One of the important issues with regard to investigations involving arsenic-containing compounds is the toxicity associated with arsenic. Extensive precautions are required for handling such compounds. Research during the last decade or so, has resulted in the isolation of many new frameworks of different compositions and dimensionality. The earlier contributions to this area is from Xu's group in China, who have prepared many alumino- and gallioarsenates.<sup>[110]</sup>

As with the phosphates, molecular arsenate structures have been prepared,<sup>[111]</sup> though their reactivity has not been explored. It is safe to presume that the isolation of such structures is important in our understanding of the formation of complex three-dimensional architectures. A vanadoarsenate,  $[\text{C}_6\text{N}_2\text{H}_{14}]_2[\text{V}_4\text{As}_6\text{O}_{30}\text{H}_6] \cdot 8\text{H}_2\text{O}$ , contains  $[\text{V}_4\text{As}_6\text{O}_{30}\text{H}_6]^{4-}$  molecular clusters formed by two  $\text{VO}_6$  octahedra and three  $\text{HAsO}_4$  tetrahedra.<sup>[111a]</sup> Extensive hydrogen-bond interactions appear to be responsible for the structural stability. A similar four-ring vanadoarsenate,  $[(\text{VO}_2)_2(\text{AsO}_4)(2,2'\text{-bpy})] \cdot \text{H}_3\text{O} \cdot \text{H}_2\text{O}$ , has been prepared using 2,2'-bipyridene ligands.<sup>[111b]</sup>

The use of the 1,10-phenanthroline ligand instead of 2,2'-bpy creates a 1D vanadoarsenate,  $[(\text{VO})_2(\text{phen})_2(\text{HAsO}_4)_2]$ .<sup>[112c]</sup> One-dimensional tautoite structure and ladder structures have been observed in  $[\text{C}_4\text{N}_2\text{H}_{12}][(\text{VO})_2(\text{HAsO}_4)_2(\text{H}_2\text{AsO}_4)_2]$ <sup>[112a]</sup> and  $[\text{H}_3\text{NCH}_2\text{CH}_2\text{NH}_3][\text{V}(\text{HAsO}_4)_2(\text{H}_2\text{AsO}_4)] \cdot \text{H}_2\text{O}$ ,<sup>[112b]</sup> respectively. SBU-4s have been linked to form one-dimensional structures in the vanadoarsenate  $[\text{H}_3\text{NC}_2\text{H}_4\text{NH}_3]_{0.5}[\text{VO}(\text{H}_2\text{O})(\text{AsO}_4)]$ <sup>[112b]</sup> and in the ferroarsenate  $[\text{NH}_3(\text{CH}_2)_2\text{NH}(\text{CH}_2)_2\text{NH}_3][\text{Fe}_2\text{F}_4(\text{HAsO}_4)_2]$ .<sup>[113a]</sup> Structures built exclusively based on a simple SBU unit have not been observed in one-dimensional phosphate structures, whereas the arsenates form such structures, possibly because of the larger As ion size. Similarly, SBU-5s (see Figure 2h), formed by three  $\text{AsO}_4$  tetrahedra and two  $\text{FeO}_6$  octahedra, form another one-dimensional structure in  $[\text{C}_2\text{N}_2\text{H}_{10}][\text{Fe}(\text{HAsO}_4)_2(\text{H}_2\text{AsO}_4)] \cdot \text{H}_2\text{O}$  (see Figure 5l).<sup>[113b,c]</sup> Similar to the phosphates, the one-dimensional arsenates also exhibit simple antiferromagnetic behavior.

SBU-4s forming extended two-dimensional structures have been observed in  $[\text{Ba}][\text{VO}_2(\text{AsO}_4)]$ ,  $[\text{Sr}][(\text{VO})_2(\text{AsO}_4)_2]$ ,<sup>[114a]</sup> and  $[\text{C}_{10}\text{N}_4\text{H}_{28}][\text{FeF}(\text{OH})(\text{HAsO}_4)_4]$ .<sup>[115c]</sup> The use of ligands such as 4,4'-bpy, 2,2'-bpy, and 1,10-phen, gives rise to interesting layered structures.<sup>[114b-d]</sup> The 2,2'-bpy and 1,10-phen ligands project above and below the plane of the layers in these structures and participate in  $\pi \cdots \pi$  interactions. The 4,4'-bpy ligand in  $[(\text{VO})_2(4,4'\text{-bpy})_{0.5}(4,4'\text{-Hbpy})(\text{AsO}_4)] \cdot \text{H}_2\text{O}$  on the other hand connects one-dimensional vanadyl arsenate chains to form the layers.<sup>[114b]</sup> In  $[\text{C}_4\text{N}_2\text{H}_{12}]_{1.5}$ -

$[\text{Fe}_3\text{F}_5(\text{HAsO}_4)_2(\text{AsO}_4)]$ , infinite Fe-X-Fe chains of corner-sharing  $\text{FeX}_6$  (X = O, F) octahedra are connected through the SBU-4s forming the layer structure.<sup>[115b]</sup>

Three-dimensional arsenate structures have been prepared by high-temperature solid-state reactions using alkali metals.<sup>[116]</sup> These compounds usually form tunnel structures. The number of three-dimensional arsenate compounds formed in the presence of organic amine cations is comparatively low.<sup>[117,118]</sup> The use of fluoride ions has facilitated the formation of three-dimensional ferroarsenate structures, the most important of which is the mixed-valent ferroarsenate  $[\text{C}_4\text{N}_2\text{H}_{12}][\text{Fe}^{\text{III}}_2\text{Fe}^{\text{II}}(\text{AsO}_4)_2(\text{HAsO}_4)_2]$  formed exclusively by SBU-4s.<sup>[118b]</sup> Four SBU-4s are connected forming an unusual cluster  $[\text{Fe}_6\text{As}_8\text{O}_{36}(\text{OH})_4]$  (Figure 12a); these clusters are connected together to form the three-dimensional structure with 1D channels (Figure 12b). In  $[\text{C}_2\text{N}_2\text{H}_{10}][\text{Fe}_2\text{F}_2(\text{AsO}_4)_2(\text{H}_2\text{O})]$ , two puckered layers are observed.<sup>[113c]</sup> While, the first layer is formed by SBU-4s, (Figure 13a)<sup>[115c]</sup> the second layer contains corner-sharing  $[\text{FeO}_4\text{F}(\text{OH}_2)]$  octahedra and  $\text{AsO}_4$

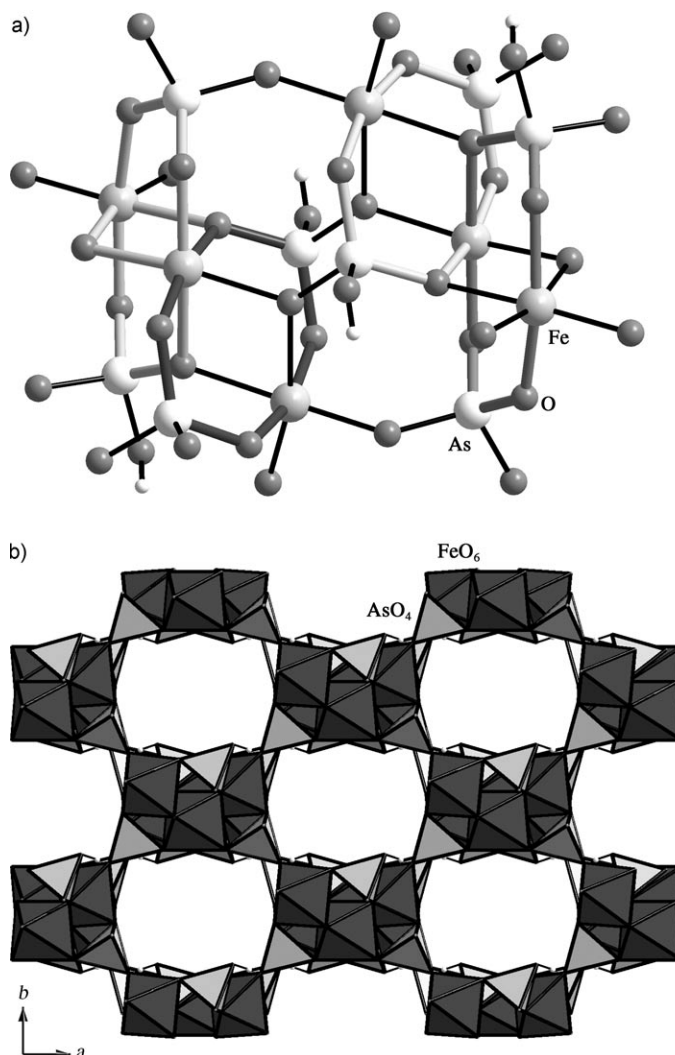


**Figure 12.** a) Structure of the  $[\text{Fe}_6\text{As}_8\text{O}_{36}(\text{OH})_4]$  cluster in  $[\text{C}_4\text{N}_2\text{H}_{12}][\text{Fe}_2^{\text{III}}\text{Fe}^{\text{II}}(\text{AsO}_4)_2(\text{HAsO}_4)_2]$ . b) The polyhedral view of the 3D structure formed by the connectivity between the  $[\text{Fe}_6\text{As}_8\text{O}_{36}(\text{OH})_4]$  units. The amine molecules are not shown.

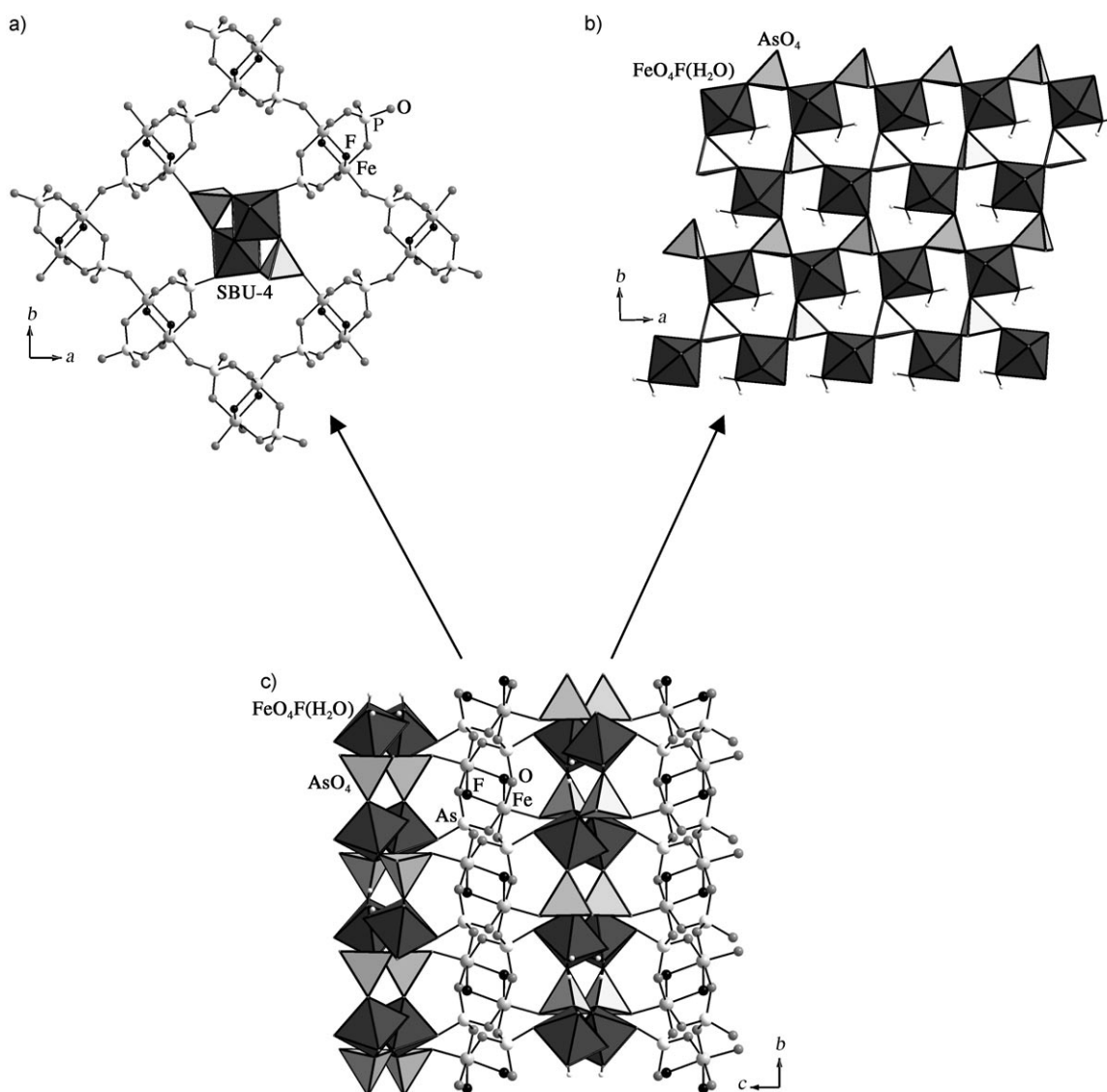


**Figure 13.** a) The SBU-4 layers in  $[\text{C}_2\text{N}_2\text{H}_{10}][\text{Fe}_2\text{F}_2(\text{AsO}_4)_2(\text{H}_2\text{O})]$ . b) A second layer formed by a strictly alternating arrangement of the Fe and As polyhedral units. c) The 3D structure formed by the connectivity between the two layers.

tetrahedra (Figure 13b). Both layers are linked to form the three-dimensional structure (Figure 13c). Infinite Fe-F-Fe chains have been observed in  $[\text{C}_6\text{N}_2\text{H}_{14}][\text{Fe}_3(\text{HAsO}_4)_2(\text{AsO}_4)\text{F}_4] \cdot 0.5\text{H}_2\text{O}$ .<sup>[118a]</sup> A mixed-valent vanadoarsenate,  $[\text{NH}_4]_3[(\text{V}^{\text{V}}\text{O})(\text{V}^{\text{IV}}_2\text{O}_3)(\text{AsO}_4)_2(\text{HAsO}_4)]$ , has a one-dimensional tancoite-like structure which is connected to give the three-dimensional structure by  $[\text{V}_2\text{O}_{10}]$  dimers and  $\text{AsO}_4$  tetrahedra.<sup>[117a]</sup> In all the arsenate compounds only antiferromagnetic interactions have been observed.

## 10. Borates

Although open-framework borosilicates and borophosphates have attracted the attention of synthetic chemists, there are few reports of exclusively borate compounds. A large number of borate minerals are known and considerable progress has been made in classifying and understanding their

structures. There are many synthetic borate compounds and a few amine-templated vanadoborates with large molecular-cluster structures have been reported.<sup>[119]</sup> In spite of the considerable synthetic efforts in preparing organically templated borates, this area is still in the early phases of development. Generally, in most of the compounds, borate clusters of different shape and sizes have been encountered.

Of the borate compounds, the vanadoborate clusters prepared using ethylenediamine are particularly interesting.<sup>[119a]</sup> The compound  $[\text{C}_2\text{N}_2\text{H}_9][\text{C}_2\text{N}_2\text{H}_{10}]_4[(\text{VO})_{12}\text{B}_{17}\text{O}_{38}(\text{OH})_8] \cdot \text{H}_2\text{O}$  contains  $\text{V}_{12}\text{B}_{17}$  clusters and a second compound,  $[\text{C}_2\text{N}_2\text{H}_{10}]_5[(\text{VO})_{12}\text{O}_6\text{B}_3\text{O}_6(\text{OH})_6] \cdot \text{H}_2\text{O}$ , contains  $\text{V}_{12}\text{B}_{18}$  clusters. In the first cluster V–O rings, formed by edge-shared  $\text{VO}_5$  square pyramids, partially interpenetrate to form the  $\text{V}_{12}$  rings. The gaps within the rings are occupied by  $\text{B}_8$  and  $\text{B}_9$  polyborate chains, resulting in the vanadoborate cluster. The interior cavity of the cluster is occupied by water molecules and the intercluster

space is filled by  $[\text{C}_2\text{N}_2\text{H}_{10}]^{2+}$  and water molecules. The second cluster consists of a puckered  $\text{B}_{18}\text{O}_{36}(\text{OH})_6$  ring sandwiched between two triangles of six alternating *cis* and *trans*, edge-sharing  $\text{VO}_5$  square pyramids. The vanadium atoms are in the +4 and +5 oxidation states. In  $[\text{Rb}]_4[(\text{VO})_6\{\text{B}_{10}\text{O}_{16}(\text{OH})_6\}_2] \cdot 0.5\text{H}_2\text{O}$ <sup>[119c]</sup> and  $[\text{H}_3\text{O}]_{12}[(\text{VO})_{12}\{\text{B}_{16}\text{O}_{32}(\text{OH})_4\}_2] \cdot 28\text{H}_2\text{O}$ ,<sup>[119d]</sup>  $[\text{V}_6\text{B}_{20}(\text{OH})_{12}]^{4-}$  and  $[(\text{VO})_{12}\{\text{B}_{16}\text{O}_{32}(\text{OH})_4\}_2]^{12-}$  cluster units have been observed, respectively.

In  $[\text{C}_2\text{N}_2\text{H}_{10}]_4[\text{C}_2\text{N}_2\text{H}_9]_2[\text{V}_6\text{B}_{22}\text{O}_{53}\text{H}_8] \cdot 5\text{H}_2\text{O}$ ,  $[\text{V}_6\text{B}_{20}\text{O}_5\text{H}_6]$  cluster units are linked together through diborate bridges. The cluster contains six  $\text{VO}_5$  units capped at the top and the bottom by the  $[\text{B}_{10}\text{O}_{16}\text{H}_3]$  polyborate units.<sup>[120]</sup>

There are no known examples of amine-templated three-dimensional borate structures. The three-dimensional structure of  $[\text{Na}]_3[\text{B}_6\text{O}_9(\text{VO}_4)]$  consists of sheets of hexaborate units linked by  $\text{VO}_4$  tetrahedra.<sup>[121a]</sup> The hexaborate sheets are formed by the linking of triangular  $\text{BO}_3$  and tetrahedral  $\text{BO}_4$  species. The sodium atoms occupy the channels. Recently, a number of transition-metal borates with open framework structures were reported.<sup>[121b,c]</sup> These include  $\text{M}[\text{CuB}_7\text{O}_{12}] \cdot n\text{H}_2\text{O}$  ( $\text{M} = \text{Na}, \text{K}$ ) which contains  $\text{CuO}_6$  octahedra, connected to  $\text{BO}_3$  and  $\text{BO}_4$  groups forming the three-dimensional structure with 14-ring channels.<sup>[121c]</sup> In  $[\text{Na}]_2[\text{Co}_2\text{B}_{12}\text{O}_{21}]$ ,  $\text{CoO}_6$  octahedra are connected to  $\text{BO}_3$  and  $\text{BO}_4$  units forming the three-dimensional structure with 12-ring channels, which are occupied by alkali-metal ions and water.<sup>[121b]</sup> The alkali-metal ions are ion-exchangable.

## 11. Sulfates, Selenites

### 11.1. Sulfates

Sulfate ions have stable tetrahedral structure and in principle can be employed to prepare extended network structures similar to silicates, phosphates, arsenates, etc. Using this analogy there has been considerable interest in recent years to study sulfate-based open-framework compounds. However, there are several possible problems to overcome: The S–O bonds have less charge (0.5) than the P–O bonds (0.75), which could create difficulties in forming extended network structures. In addition, the  $\text{SO}_4^{2-}$  ions may be similar to  $\text{C}_2\text{O}_4^{2-}$  ions and have similar reactivity. The S–O bonds are also less covalent and thus polysulfate units are less readily formed than polyborates, -phosphates, and -silicates. In spite of these issues, there are a few reports of open-framework sulfate structures with different dimensionalities. Most of the sulfate structures are prepared employing a large excess of fluoride ions to form an M–O/F–M network, which forms the basis for all the structures. The sulfate anions generally link the M–O/F–M network. The variety and diversity exhibited by this class of compounds has been reviewed recently by Rao et al.<sup>[38]</sup> Figure 14, shows representative examples of one-, two-, and three-dimensionally extended sulfate structures along with their magnetic properties. Most of the one-dimensional sulfate structures are related to known minerals. The two-dimensional structures predominately contain Kagomé layers, and there are only few reports of three-

dimensional structures. In the Supporting Information, Table S4 some representative sulfate structures are presented.

Similar to the phosphate structures, the one-dimensional sulfate structures form in any one of the well established structure types described earlier. Thus, the compounds with the general formula,  $[\text{C}_4\text{N}_2\text{H}_{12}][\text{M}(\text{F}_3(\text{SO}_4))]$ , ( $\text{M} = \text{V}, \text{Fe}$ ) (Figure 14a),<sup>[122,123]</sup> resemble the mineral butlerite,  $[\text{M}(\text{TO}_4)\phi_3]$  (where  $\phi$  is any unspecified anion ligand).<sup>[124]</sup> Magnetic susceptibility studies indicate weak antiferromagnetic behavior (Figure 14b). The structures of  $[\text{H}_3\text{N}(\text{CH}_2)_2\text{NH}_3][\text{V}(\text{OH})(\text{SO}_4)_2] \cdot \text{H}_2\text{O}$ ,<sup>[122a]</sup> and  $[\text{HN}(\text{CH}_2)_6\text{NH}][(\text{VO})_2(\text{OH})_2(\text{SO}_4)_2] \cdot \text{H}_2\text{O}$ <sup>[122a]</sup> resemble tancoite<sup>[61]</sup> and the kröhnkite  $[\text{Na}]_2[\text{Cu}(\text{SO}_4)_2] \cdot 2\text{H}_2\text{O}$ <sup>[125]</sup> structure, respectively. Though the Kagomé layers are the dominant class in the transition-metal sulfate structures, there have been reports of other layered structures.<sup>[123a,126,127]</sup> Thus,  $[\text{H}_3\text{N}(\text{CH}_2)_2\text{NH}_3][\text{Fe}_2\text{F}_2(\text{SO}_4)_2(\text{H}_2\text{O})_2]$  has infinite Fe–F–Fe chains connected by  $\text{SO}_4$  tetrahedra, and shows a magnetic transition at 22 K and a hysteresis at 10 K.<sup>[123a]</sup> In  $[\text{C}_4\text{N}_2\text{H}_{12}][\text{Ni}_3\text{F}_2(\text{SO}_4)_3(\text{H}_2\text{O})_2]$  trimeric  $\text{Ni}_3\text{F}_3\text{O}_{12}$  units connected to three sulfate tetrahedra form hexameric units, which in turn are connected to form the layers.<sup>[127]</sup> Magnetic susceptibility studies indicate a ferromagnetic behavior with hysteresis at 5 K.

Cobaltosulfate layers pillared by a variety of aliphatic linear diamines have been observed in  $[(\text{H}_2\text{N}(\text{CH}_2)_n\text{NH}_2)_{0.5}\{\text{Co}_4(\text{SO}_4)(\text{OH})_6\}] \cdot 3\text{H}_2\text{O}$  (where  $n = 2, 4, 6, 8$ ).<sup>[128]</sup> The channel size in the structures appears to correlate with the length of the amine employed. The compound with ethylenediamine ( $n = 2$ ) shows a metamagnetic behavior. In the three-dimensional nickelosulfate  $[\text{C}_4\text{N}_2\text{H}_{12}][\text{Ni}_2\text{F}_4(\text{SO}_4)_2\text{H}_2\text{O}]$  infinite Ni–F–Ni chains connected by  $\text{SO}_4$  units have been observed (Figure 14c).<sup>[127]</sup> The magnetic studies show very weak antiferromagnetic behavior with  $\theta = -10$  K (Figure 14d).

#### 11.1.1. Kagomé Layers in Transition-Metal Sulfates

Many two-dimensional sulfate frameworks form with the Kagomé lattice.<sup>[126,129–132]</sup> In all these compounds, the metal atoms are connected by F bridges forming the two-dimensional Kagomé nets. The sulfate anion influences the planarity of the resulting layers. In addition, M–F–M bridges also play an important role in the overall structure as well as the magnetic properties. Though most of the compounds show only short-range magnetic interactions there are a few examples wherein long-range ordering has been observed. Herein we discuss two special cases, one involving a mixed-valent iron compound,  $[\text{H}_2\text{dabco}][\text{H}_3\text{O}][\text{Fe}^{\text{III}}\text{Fe}^{\text{II}}_2\text{F}_6(\text{SO}_4)_2]$  (dabco: 1,4-Diazabicyclo[2.2.2]octane),<sup>[126]</sup> and the other with nickel,  $[\text{C}_6\text{N}_2\text{H}_8][\text{NH}_4]_2[\text{Ni}_3\text{F}_6(\text{SO}_4)_2]$ .<sup>[132]</sup>

In  $[\text{H}_2\text{dabco}][\text{H}_3\text{O}][\text{Fe}^{\text{III}}\text{Fe}^{\text{II}}_2\text{F}_6(\text{SO}_4)_2]$  a near perfect Kagomé structure is formed by  $\text{Fe}^{\text{III}}\text{F}_4\text{O}_2$  and  $\text{Fe}^{\text{II}}\text{F}_4\text{O}_2$  octahedral units.<sup>[126]</sup> The triangular Fe–F–Fe units are close enough to allow the  $\text{SO}_4$  units to act as a cap. Magnetic studies indicate a ferromagnetic as well as a spin-glass behavior at 12 K owing to extreme magnetic frustration.

In  $[\text{C}_6\text{N}_2\text{H}_8][\text{NH}_4]_2[\text{Ni}_3\text{F}_6(\text{SO}_4)_2]$ , Ni–F–Ni bonds form the Kagomé layer with the sulfate units capping the triangular unit similar to the ferrosulfate (Figure 14e).<sup>[132]</sup> Magnetic susceptibility studies show canted antiferromagnetic behavior

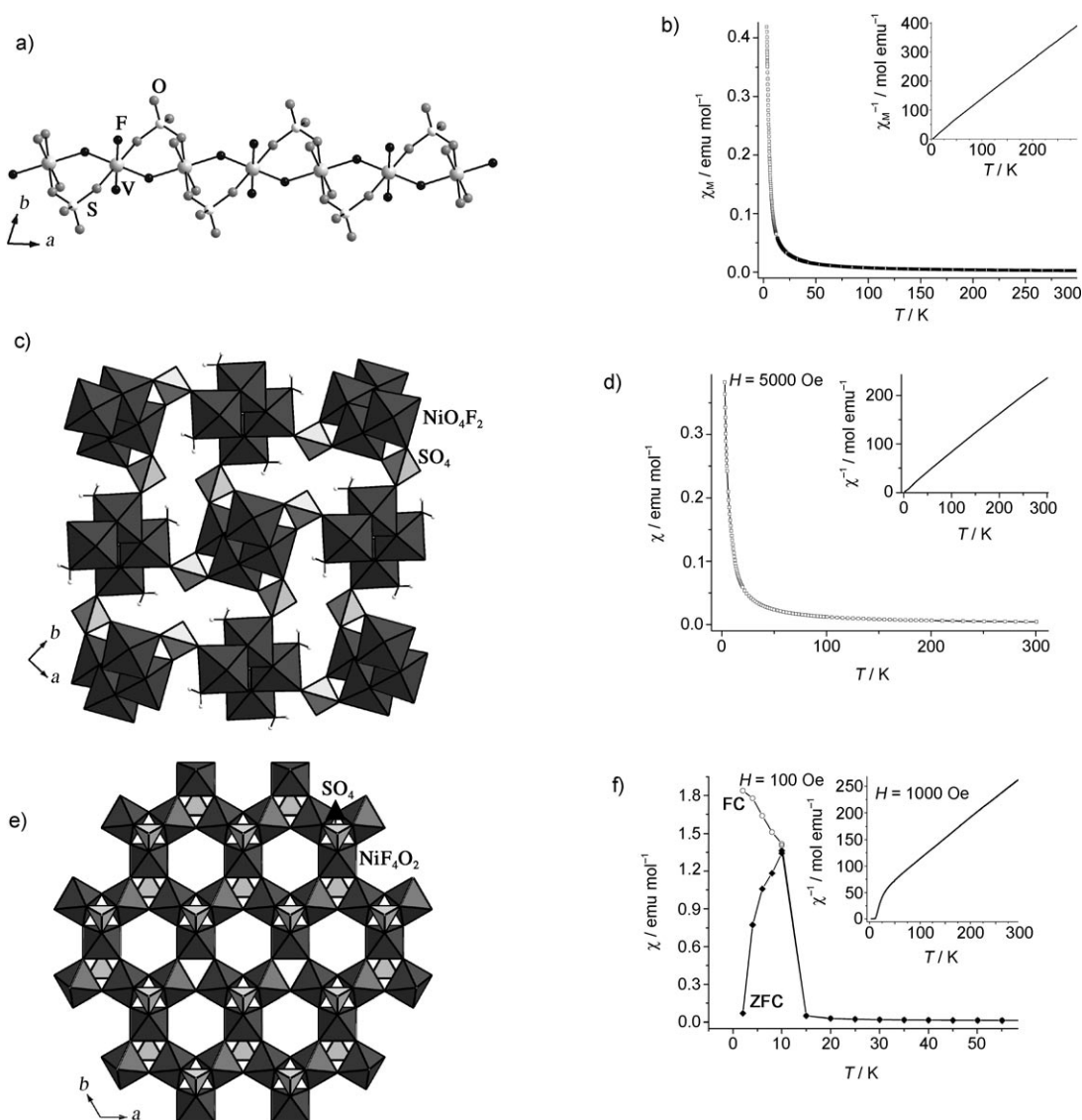


**Figure 14.** The one-dimensional structure (a) and magnetic properties (b) of  $[\text{C}_4\text{N}_2\text{H}_{12}][\text{VF}_3(\text{SO}_4)]$ . The inset shows the variation of the inverse susceptibility. The three-dimensional structure (c) and the temperature variation of the magnetic susceptibility (d) of  $[\text{C}_4\text{N}_2\text{H}_{12}][\text{Ni}_2\text{F}_4(\text{SO}_4)\text{H}_2\text{O}]$ . The two-dimensional structure of  $[\text{C}_6\text{N}_2\text{H}_8][\text{NH}_4][\text{Ni}_3\text{F}_6(\text{SO}_4)_2]$  showing the Kagomé lattice (e) and its magnetic behavior in FC and ZFC conditions (f). The insets show the temperature dependence of the inverse susceptibility.

with  $\theta = -60$  K and  $\mu_{\text{eff}} = 3.02 \mu_{\text{B}}$  (Figure 14 f). The in situ formation of diazacubane during the reaction is noteworthy.

## 11.2. Selenites

Selenite-based frameworks are of interest because of the possibility of investigating the role of the lone pair of electrons in directing the structure. The stereochemically active lone pair of electrons in  $\text{Se}^{4+}$  generally occupies one of the vertices of the Se coordination polyhedron. Synthesis of open-framework transition-metal selenites was found to be difficult, because of the low reduction potential of the  $\text{Se}^{\text{IV}}/\text{Se}^0$  couple, which leads to the likely formation of elemental selenium under hydrothermal conditions. Some representa-

tive selenite structures are listed in the Supporting Information, Table S5.

The molecular vanadoselenite  $[(1,10\text{-phen})_2(\text{V}_2\text{SeO}_7)]$  contains  $\text{VO}_4\text{N}_2$  octahedra and  $\text{SeO}_3$  trigonal pyramids linked to form the molecular structure with 1,10-phen ligands acting as terminal units.<sup>[133]</sup> The use of 2,2'-bpy results in a one-dimensional vanadoselenite,  $[(2,2'\text{-bpy})(\text{VSeO}_4)]$ .<sup>[133]</sup> The structure is formed by edge-shared  $\text{VO}_4\text{N}_2$  octahedra and  $\text{SeO}_3$  trigonal pyramidal units to give four-rings. The 2,2'-bpy units are terminal.

The layered vanadoselenite  $[\text{H}_3\text{NCH}_2\text{CH}_2\text{NH}_3][(\text{VO})(\text{SeO}_3)_2]$  contains  $\text{VO}_5$  square-pyramidal and  $\text{SeO}_3$  trigonal-pyramidal units linked to form a layer with eight-ring apertures.<sup>[134a]</sup> In  $[\text{C}_6\text{N}_2\text{H}_{14}]_{0.5}[(\text{VO})(\text{HSeO}_3)(\text{SeO}_3)]\cdot\text{H}_2\text{O}$ , the  $\text{VO}_6$  and  $\text{SeO}_3$  units are connected through the vertices to

form one-dimensional ladders, which are connected by  $\text{HSeO}_3$  units forming the layer.<sup>[134b]</sup> In the mixed-valent  $[\text{C}_2\text{N}_2\text{H}_{10}][(\text{V}^{\text{IV}}\text{O})_2(\text{V}^{\text{VO}}\text{O}_2(\text{SeO}_3)_3) \cdot 1.25\text{H}_2\text{O}]$ , four  $\text{VO}_6$  units share edges to form  $\text{V}_4\text{O}_{18}$  clusters, which are connected with  $\text{VO}_5$  and  $\text{SeO}_3$  units to form the layer with eight-ring apertures.<sup>[134b]</sup> The low reactivity of selenites prompted the formation of such structures by employing two transition metals to be studied. Thus, a bimetallic selenite,  $[\text{Cu}(\text{phen})_2(\text{V}_2\text{Se}_2\text{O}_{11})]$  containing a layer formed from linked  $[\text{V}_2\text{Se}_2\text{O}_{11}]^{2-}$  and  $[\text{Cu}(\text{phen})]^{2+}$  has been prepared.<sup>[134c]</sup> The phen ligands, which protrude into the interlamellar region, appear to have strong  $\pi \cdots \pi$  interactions.

The three-dimensional selenite structure  $[\text{A}][\text{Fe}_4\text{F}_6(\text{SeO}_3)_4]$  ( $\text{A}$  = different amines) contains an unusual building unit.<sup>[135a]</sup> Four  $\text{FeF}_3\text{O}_3$  octahedra are corner shared through Fe-F-Fe linkages to form a tetrahedral tetrameric  $\text{Fe}_4\text{F}_6\text{O}_{12}$  cluster (Figure 15a). The clusters are connected by the

ethylenediamine molecules have been observed.<sup>[135c]</sup> The mixed-metal selenite structures  $[\text{M}(4,4'\text{-bpy})(\text{H}_2\text{O})\text{V}_2\text{Se}_2\text{O}_{10}]$  ( $\text{M} = \text{Co}, \text{Ni}$ ) have  $[\text{V}_2\text{Se}_4\text{O}_{14}]^{4-}$  clusters, connected by  $\text{VO}_4\text{N}$  units and by  $\text{MO}_6$  octahedra to form the layers, which are cross-linked by the 4,4'-bpy units giving rise to the three-dimensional structure.<sup>[135d]</sup> In  $[\text{Fe}_3(\text{H}_2\text{O})(\text{SeO}_3)_3]$ , both the right-handed and the left-handed helical one-dimensional Fe-O-Fe chains have been observed.<sup>[135e]</sup> The chains are linked by  $\text{Fe}_2\text{O}_{10}$  dimers to form the layers, which are further connected by  $\text{FeO}_6$  octahedra to form the three-dimensional structure. Thus, the entire three-dimensional structure consists of Fe-O-Fe linkages with the selenite anions being employed to satisfy the coordination requirements of iron as well as to provide charge neutrality.

## 12. Hybrid Compounds (Mixed Oxo Anions)

In addition to the structures formed by the use of one type of anion, there has been considerable interest to study the formation of network structures employing mixed anions. Thus, a new family of hybrid structures have been discovered. Herein we present the important members of this family of compounds (see also the Supporting Information, Table S6).

### 12.1. Borophosphates

Metalloborophosphates, compounds with the two oxo anions borate and phosphate, are expected to give a large diversity and variety of structures and there has been much work in this area. Kniep and co-workers have contributed extensively to the preparation and understanding of the borophosphate phases.<sup>[136]</sup> The anionic partial structures of the borophosphates include oligomeric units, chains, ribbons, layers, and 3D open-framework structures. The borophosphates are divided into anhydrous and hydrated phases. The hydrated phases contain isolated planar  $\text{BO}_3$  groups (that is, planar  $\text{BO}_3$  groups that are not bonded to other  $\text{BO}_3$  groups) and  $\text{PO}_4$  tetrahedra with the  $\text{BO}_3$  groups sharing one common oxygen vertex with the  $\text{PO}_4$  tetrahedra. In the anhydrous chain structures, generally, all the vertices of the  $\text{BO}_4$  unit are linked with the neighboring tetrahedra. Hydrated borophosphate compounds which have a B/P ratio  $> 1$  the boron is found with both trigonal and tetrahedral coordination, whereas those with a B/P ratio of  $\leq 1$  do not have trigonal boron centers.

Herein we describe some of the well established building units observed in the borophosphate structures. In  $[\text{NH}_4]_4-[\text{Mn}_9\text{B}_2(\text{OH})_2(\text{HPO}_4)_4(\text{PO}_4)_6]$ , the manganophosphate layers are formed from  $\text{MnO}_5$ ,  $\text{MnO}_6$ ,  $\text{PO}_4$ , and  $\text{HPO}_4$  polyhedral units. The layers are pillared by the  $\text{BO}_4$  tetrahedral units to form the three-dimensional structure.<sup>[137]</sup> The magnetic studies indicate antiferromagnetic interactions with  $C_m = 4.404 \text{ cm}^3 \text{ K mol}^{-1}$  and  $\theta = -51.2 \text{ K}$ .

The simplest building unit,  $[\text{BPO}_6]^{4-}$ , is formed by the corner sharing of  $\text{BO}_4$  and  $\text{PO}_4$  tetrahedra. These units are connected together to form one-dimensional borophosphate chains. The 1D chains are interconnected by chains of edge-

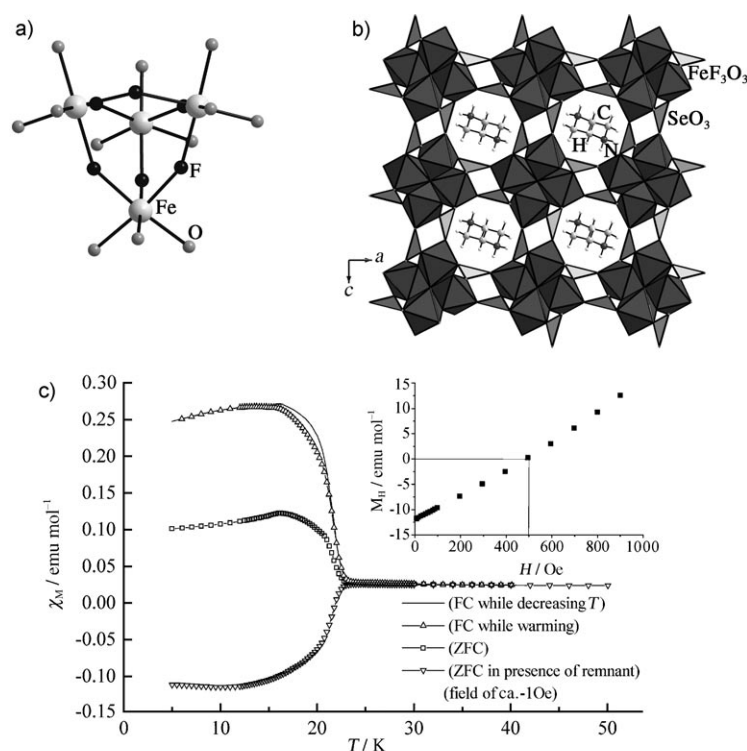


**Figure 15.** a) The tetrameric tetrahedral cluster  $\text{Fe}_4\text{F}_6\text{O}_{12}$  in  $[\text{C}_4\text{N}_2\text{H}_{12}]_{0.5}[\text{Fe}_2\text{F}_3(\text{SeO}_3)_2]$ . b) The 3D structure formed by the connectivity between the cluster units. c) The magnetic behavior in FC and ZFC conditions. Inset shows the  $M$  versus  $H$  curve at 5 K.

selenite groups to form the three-dimensional structure with eight-ring 1D channels (Figure 15b). The magnetic studies indicate a sharp transition at 20 K (Figure 15c). Two isotopic selenites,  $[\text{H}_2\text{N}(\text{CH}_2)_4\text{NH}_2]_{0.5}[\text{M}(\text{HSeO}_3)(\text{Se}_2\text{O}_5)]$  ( $\text{M} = \text{Co}, \text{Ni}$ ), contain layers cross-linked by the selenite unit.<sup>[135b]</sup>  $\text{MO}_6$  units are connected along with  $\text{Se}_2\text{O}_5$  and  $\text{HSeO}_3$  units to form the layers which are cross-linked by  $\text{SeO}_3$  units forming the three-dimensional structure, which resemble the non-interpenetrating diamondoid network. In  $[\text{H}_2\text{N}(\text{CH}_2)_2\text{NH}_2]_{0.5}[\text{CoSeO}_3]$  cobaltoselenite layers pillared by

sharing  $\text{MO}_6$  octahedra to form the three-dimensional structure. This type of structural arrangement has been observed in  $\text{M}^{\text{II}}[\text{BPO}_4(\text{OH})_2]$ ,  $\text{M} = \text{Mn}$ ,  $\text{Fe}$ , and  $\text{Co}$ .<sup>[138a]</sup> The magnetic studies of these compounds indicate antiferromagnetic interactions with  $T_N = 7.4$ ,  $3.6$ , and  $2.4$  K for  $\text{Mn}$ ,  $\text{Fe}$ , and  $\text{Co}$ , respectively. In  $[\text{Co}_5\text{BP}_3\text{O}_{14}]$ ,  $\text{BPO}_6$  units connected to form the layers have been observed;<sup>[138b]</sup> the layers are cross-linked by isolated  $\text{PO}_4$  tetrahedra and  $\text{MO}_6$  octahedra giving rise to the three-dimensional structure.

The borophosphate units  $[\text{BP}_2\text{O}_8]^{3-}$  generally form infinite loop-branched helical chains, and are connected by  $\text{MO}_4(\text{H}_2\text{O})_2$  octahedra ( $\text{M} = \text{Sc}$ <sup>[139a]</sup> and  $\text{Fe}$ <sup>[139b–e]</sup>) forming the three-dimensional structure. On heating, the scandium compound undergoes a reversible release of water from the structure.<sup>[139a]</sup>

The most commonly observed borophosphate unit is the  $[\text{BP}_2\text{O}_{10}]^{7-}$  unit. These units are connected with the metal-centered octahedra that make up many transition-metal borophosphate structures.<sup>[140]</sup> The structures of  $[\text{H}_3\text{NC}_2\text{H}_4\text{NH}_2\text{C}_2\text{H}_4\text{NH}_2\text{C}_2\text{H}_4\text{NH}_3]_4\text{H}[\text{M}(\text{VO})_{12}(\text{BP}_2\text{O}_{10})_6] \cdot n\text{H}_2\text{O}$  ( $\text{M} = \text{NH}_4^+$ ,  $\text{K}^+$ ) are formed by 12-rings of  $[(\text{VO})_{12}(\text{BP}_2\text{O}_{10})_6]^{18-}$  clusters.<sup>[140a]</sup> The cluster is formed by the linking of six  $\text{BP}_2\text{O}_{10}$  and six  $\text{V}_2\text{O}_{10}$  moieties, with the  $\text{NH}_4^+$  or  $\text{K}^+$  ions encapsulated inside the rings. The  $\text{BP}_2\text{O}_{10}$  and  $\text{V}_2\text{O}_{10}$  units are connected by sharing oxygen atoms to give a building unit of composition  $(\text{VO})_2\text{BP}_2\text{O}_{10}$ , which has been observed in  $[\text{C}_4\text{N}_2\text{H}_{12}]_6[(\text{VO})_2\text{BP}_2\text{O}_{10}]_4 \cdot n\text{H}_2\text{O}$  ( $n = 2, 6, 14$ ).<sup>[140b]</sup> Four  $(\text{VO})_2\text{BP}_2\text{O}_{10}$  units are connected in a cyclic fashion to form  $[(\text{VO})_2\text{BP}_2\text{O}_{10}]_4^{12-}$ . In  $[\text{H}_3\text{NCH}_2\text{CH}_2\text{NH}_3][(\text{VO})_5(\text{H}_2\text{O})(\text{BP}_2\text{O}_{10})_2] \cdot 1.5\text{H}_2\text{O}$ , the  $[\text{BP}_2\text{O}_{10}]^{7-}$  ions are linked through  $\text{VO}_6$  octahedra forming a two-dimensional layer.<sup>[140c]</sup> Unlike in the cluster compounds,<sup>[140a,b]</sup> in this case the  $\text{BP}_2\text{O}_{10}$  clusters are connected through  $\text{VO}_6$  octahedra to form the three-dimensional structure, with the ethylenediamine molecules occupying the one-dimensional channels.

$[\text{B}_2\text{P}_3\text{O}_{12}(\text{OH})]^{4-}$  building units have been observed various structures.<sup>[141]</sup> The structure of  $[\text{C}_4\text{N}_2\text{H}_{12}][\text{MB}_2\text{P}_3\text{O}_{12}(\text{OH})]$  ( $\text{M} = \text{Mn}$ ,  $\text{Co}$ ) contains loop-branched infinite chains of  $\text{B}_2\text{P}_3\text{O}_{12}(\text{OH})$ .<sup>[141a]</sup> The  $\text{Mn}$  or  $\text{Co}$  atoms, located between the borophosphate anionic chains, link the chains to form the three-dimensional structure. A series of manganoborophosphates with undulating chains of  $\{\text{B}_2\text{P}_3\text{O}_{12}(\text{OH})\}^{4-}$ ,  $[\text{H}_2\text{diamine}]^{2+}[\text{Mn}(\text{B}_2\text{P}_3\text{O}_{12}(\text{OH}))]^{2-}$ , has been prepared by varying the organic diamine.<sup>[141b]</sup> In the cobaltborophosphate  $[\text{C}_2\text{N}_2\text{H}_{10}][\text{CoB}_2\text{P}_3\text{O}_{12}(\text{OH})]$ , the  $\text{B}_2\text{P}_3\text{O}_{12}(\text{OH})$  units form the layers, which are connected by  $\text{CoO}_6$  octahedra forming the three-dimensional structure with 1D channels.<sup>[141d]</sup>

The rarely observed borophosphate building unit  $[\text{B}_2\text{P}_5\text{O}_{22}]^{13-}$  has the combination of two  $\text{BP}_2\text{O}_{10}$  and one  $\text{PO}_4$  tetrahedral unit. This unit, connected by dimeric  $\text{V}_2\text{O}_8$  units and  $\text{VO}_5$  square pyramids, has been observed in the layered compound  $[\text{C}_3\text{N}_2\text{H}_5]_{3.8}[\text{H}_3\text{O}]_{1.2}[(\text{VO})_4(\text{BO})_2(\text{PO}_4)_5] \cdot 0.3\text{H}_2\text{O}$  (Figure 16).<sup>[142]</sup> The magnetic susceptibility data indicate antiferromagnetic interactions with  $C_m = 0.367 \text{ cm}^3 \text{ K mol}^{-1}$  and  $\theta = -32.3 \text{ K}$ .

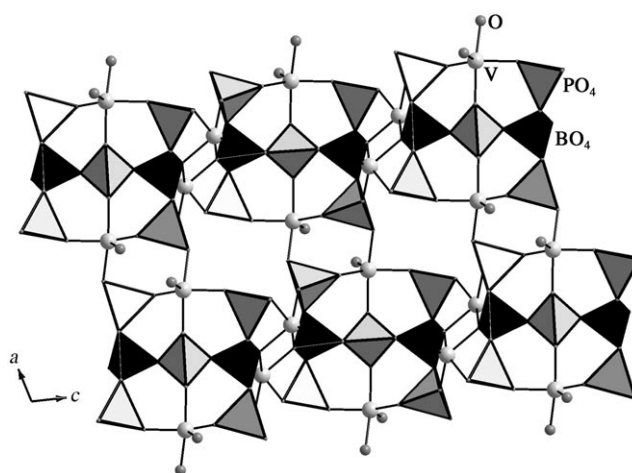


**Figure 16.** View of the layer structure in  $[\text{C}_3\text{N}_2\text{H}_5]_{3.8}[\text{H}_3\text{O}]_{1.2}[(\text{VO})_4(\text{BO})_2(\text{PO}_4)_5] \cdot 0.3\text{H}_2\text{O}$  along the  $b$  axis.

### 12.2. Phosphate–Phosphite and Phosphate–Arsenate Structures

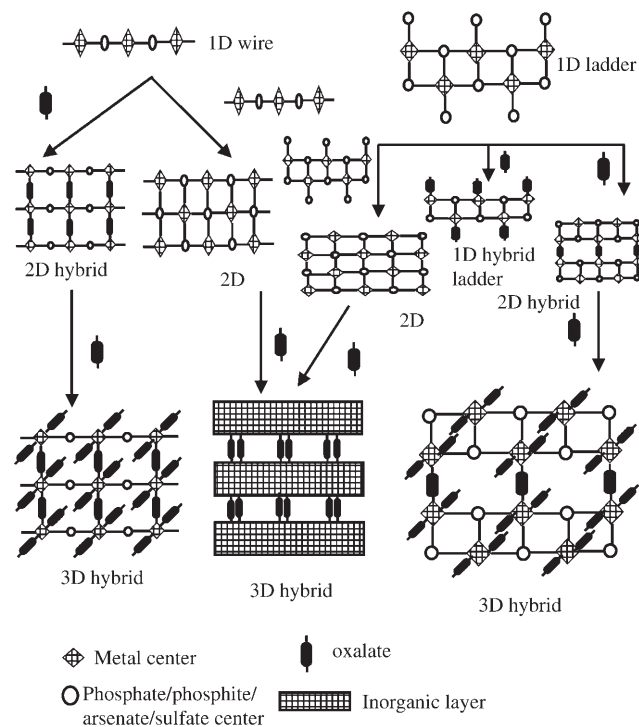
There have been some reports of compounds containing both phosphate and phosphite anions. The one-dimensional structure of the ferrophosphate phosphite  $[\text{Fe}(2,2'\text{-bpy})\text{-(HPO}_3\text{)}(\text{H}_2\text{PO}_4)]$ <sup>[143a]</sup> closely resembles the structure of the ferrophosphate  $[\text{Fe}(2,2'\text{-bpy})(\text{HPO}_4)(\text{H}_2\text{PO}_4)]$ .<sup>[60a,b]</sup> The ferrophosphate–phosphite was formed as a result of the partial oxidation of the  $\text{P}^{3+}$  ions during the reaction of iron with phosphorous acid and 2,2'-bpy. The magnetic studies show that the compound orders antiferromagnetically ( $T_N = 20 \text{ K}$ ) with  $C_m = 7.0 \text{ cm}^3 \text{ K mol}^{-1}$  and  $\theta = -69 \text{ K}$ . Deliberate and successful doping of the phosphite units in place of the phosphates has been encountered in  $[\text{C}_4\text{N}_2\text{H}_{12}][\text{Fe}_{0.86}^{\text{II}}\text{Fe}_{1.14}^{\text{III}}\text{-(HPO}_3\text{)}_{1.39}(\text{HPO}_4)_{0.47}(\text{PO}_4)_{0.14}\text{F}_3]$ <sup>[143b]</sup> and  $[\text{C}_2\text{N}_2\text{H}_{10}]_{0.5}[\text{Co}(\text{HPO}_3)_x(\text{PO}_4)_{1-x}\text{F}_x(\text{H}_2\text{O})_{0.25-x}] \cdot 0.25\text{H}_2\text{O}$  ( $x = 0.17$ ).<sup>[143c]</sup> Generally, the substitution of the phosphite does not alter the original phosphate structure and the magnetic properties of the hybrid compounds are also comparable to those of the parent compounds.

Similar to the phosphite substitution in place of phosphate, there have been some attempts to prepare arsenate-substituted phases. Thus,  $[\text{C}_6\text{N}_2\text{H}_{14}][\text{Fe}_3(\text{HAsO}_4)_{1.33}(\text{HPO}_4)_{0.67}(\text{AsO}_4)_{0.84}(\text{PO}_4)_{0.16}\text{F}_4] \cdot 0.5\text{H}_2\text{O}$ <sup>[144a]</sup> has the same structure as the arsenate compound  $[\text{C}_6\text{N}_2\text{H}_{14}][\text{Fe}_3(\text{HAsO}_4)_2(\text{AsO}_4)\text{F}_4] \cdot 0.5\text{H}_2\text{O}$ .<sup>[118a]</sup> Other similar compounds are  $[\text{C}_2\text{N}_2\text{H}_{10}][\text{Fe}_2(\text{AsO}_4)_{2-x}(\text{PO}_4)_x\text{F}_2(\text{H}_2\text{O})]$  ( $x = 0.46$ )<sup>[144b]</sup> and  $[\text{C}_4\text{N}_2\text{H}_{12}][\text{Fe}_3(\text{HAsO}_4)_{1.02}(\text{HPO}_4)_{0.98}(\text{AsO}_4)_{0.88}(\text{PO}_4)_{0.12}\text{F}_5]$ .<sup>[144c]</sup>

## 13. Organic–Inorganic Hybrid Compounds

The combination of organic and inorganic anions have great potential to form compounds with novel extended networks. Compounds based on oxalate anions along with phosphate, phosphite, and arsenate units have been prepared and characterized. In most of the compounds, the oxalate units act as “glue” connecting two inorganic moieties, such as two one-dimensional ladders or chains or two-dimensional layers, together. The oxalate units linking two one-dimen-

sional chains generally have “in-plane” connectivity and the linkage between two layers involves “out-of-plane” connectivity. The compounds, thus formed, have been classified as organic–inorganic hybrids. Many of these compounds were prepared in the presence of organic amines. The various ways to form such hybrid structures are presented in Scheme 2.



**Scheme 2.** Hybrid 1D, 2D, and 3D organic–inorganic hybrid systems formed from oxalate ligands and inorganic linkers.

### 13.1. Phosphate Oxalates

The report of low-dimensional hybrid structures is rare.<sup>[145–147]</sup> The only example is the one-dimensional vanadophosphate oxalate  $[\text{C}_4\text{N}_2\text{H}_{12}][\text{VO}(\text{C}_2\text{O}_4)(\text{HPO}_4)]$  that exhibits a ladder-like structure with the oxalate units bound to the metal center.<sup>[145a]</sup> The magnetic susceptibility data indicate antiferromagnetic behavior ( $T_N = 6$  K) with  $\theta = -2.2$  K.

Double six-ring (D6R) units formed by the connectivity of  $\text{VO}_6$  octahedra and  $\text{HPO}_4$  tetrahedra have been observed in  $[\text{C}_{10}\text{N}_4\text{H}_{28}][\text{V}_3(\text{C}_2\text{O}_4)_2(\text{HPO}_4)_3(\text{PO}_4)(\text{H}_2\text{O})] \cdot 6\text{H}_2\text{O}$ .<sup>[146a]</sup> The D6R units are connected through the oxalate and  $\text{PO}_4$  groups to form the layered structure. In  $[\text{NH}_4]_2[(\text{VO})_2(\text{HPO}_4)_2(\text{C}_2\text{O}_4)] \cdot 5\text{H}_2\text{O}$ , two one-dimensional ladders of  $[(\text{VO})_2(\text{HPO}_4)_2]$ , connected by the in-plane oxalates forming the layers have been observed.<sup>[146b]</sup> A classic oxalate honeycomb related structure has been observed in  $[\text{C}_6\text{N}_4\text{H}_{21}][\text{M}_2(\text{HPO}_4)(\text{C}_2\text{O}_4)_{2.5}] \cdot 3\text{H}_2\text{O}$  ( $\text{M} = \text{Mn}, \text{Fe}$ ).<sup>[147]</sup> The honeycomb structure is interrupted by the presence of two phosphate units that link two metal centers in exactly the same fashion as the oxalates.<sup>[6]</sup> Magnetic studies show

antiferromagnetic behavior with  $C_m = 4.45 \text{ cm}^3 \text{ K mol}^{-1}$ ,  $\theta = -21.2$  K for Mn ( $T_N = 12$  K).

The dual role of the oxalate units has been observed in many three-dimensional phosphate oxalates.<sup>[148–150]</sup> Thus in  $(\text{C}_4\text{N}_2\text{H}_{12})[\text{M}_4(\text{HPO}_4)_2(\text{C}_2\text{O}_4)_3]$  ( $\text{M} = \text{Fe}, \text{Co}$ ),<sup>[149a,150]</sup> one-dimensional zigzag ladders of the metallophosphates are connected by the in-plane oxalate to form the hybrid layers which are in turn connected by the out-of-plane oxalate forming the three-dimensional structure. Magnetic studies indicate antiferromagnetic ordering in both the compounds. A similar dual role of the oxalate has also been observed in the antiferromagnetic manganophosphate-oxalate  $[\text{CH}_3\text{NH}_2\text{CH}_3][\text{Mn}_2(\text{OH}_2)(\text{HPO}_4)(\text{C}_2\text{O}_4)_{1.5}]$ .<sup>[148d]</sup> Well-known inorganic layers based on tetrahedral connectivity (AlPOs and zinc phosphates) have been observed in many three-dimensional hybrid structures. Thus in  $[\text{NH}_3(\text{CH}_2)_2\text{NH}_3]_{1.5}[\text{Fe}_3(\text{PO}_4)(\text{HPO}_4)_3(\text{C}_2\text{O}_4)_{1.5}] \cdot x\text{H}_2\text{O}$  ( $x = 1.5\text{--}2.0$ ) the inorganic layers have the same structure as the 4.6.12 net (Figure 17a).<sup>[149b]</sup> The oxalate units pillar these layers satisfying the octahedral coordination for the transition metal and also giving rise to a porous solid with uniform one-dimensional pores (Figure 17b). The extra-framework water molecules form a hexameric unit and can be reversibly adsorbed (Figure 17c). Magnetic susceptibility studies indicate antiferromagnetic ordering with  $T_N = 31$  K.

### 13.2. Phosphite Oxalates

The close structural relationship between the phosphate and the phosphite units has already resulted in many closely related framework structures (see Section 7). Since it has been shown that hybrid structures can be prepared with phosphate units, the formation of hybrid structures with phosphites has also been investigated. This effort has led to the preparation of some phosphite oxalate compounds.<sup>[151–153]</sup> Not surprisingly, many of the phosphite oxalate structures have close resemblance to the phosphate oxalate ones.

The one-dimensional ferrophosphite oxalate,  $[\text{C}_6\text{N}_2\text{H}_{14}]_2[\text{Fe}_2\text{F}_2(\text{HPO}_3)_2(\text{C}_2\text{O}_4)_2] \cdot 2\text{H}_2\text{O}$ ,<sup>[151b]</sup> has the same structure as the vanadophosphate oxalate,  $[\text{C}_4\text{H}_{12}\text{N}_2][\text{VO}(\text{HPO}_4)(\text{C}_2\text{O}_4)]$ , structure.<sup>[145a]</sup> The two-dimensional ferrophosphite oxalate,  $[\text{C}_6\text{N}_4\text{H}_{21}]_2[\text{Fe}_4(\text{HPO}_3)_2(\text{C}_2\text{O}_4)_5] \cdot 5\text{H}_2\text{O}$  (Figure 18a),<sup>[151b]</sup> is closely related to  $[\text{C}_6\text{N}_4\text{H}_{21}][\text{Fe}_2(\text{HPO}_4)(\text{C}_2\text{O}_4)_{2.5}] \cdot 3\text{H}_2\text{O}$ ,<sup>[147]</sup> and has antiferromagnetic behavior ( $T_N = 22$  K,  $C_m = 3.55 \text{ cm}^3 \text{ K mol}^{-1}$  and  $\theta = -32$  K; Figure 18b).

The lower number of P–O bonds in the phosphite ( $\text{HPO}_3$ ; 3) compared to the phosphate ( $\text{PO}_4$ ; 4) can also impart some subtle differences in the hybrid structures. In the manganophosphite oxalate  $[\text{C}_4\text{N}_2\text{H}_{12}][\text{Mn}_2(\text{HPO}_3)_2(\text{C}_2\text{O}_4)]$  the SBU-4s are linked to form the  $[\text{Mn}(\text{HPO}_3)]$  layers, which are cross-linked by the oxalate units.<sup>[152]</sup> Magnetic studies indicate antiferromagnetic interactions with  $C_m = 0.1958 \text{ cm}^3 \text{ K mol}^{-1}$  and  $\theta = -24.55$  K. The differences between the zero-field corrected (ZFC) and field-corrected (FC) direct current (dc) susceptibilities below  $T = 7$  K indicate exchanges between the manganese centers made possible through the structure geometry.

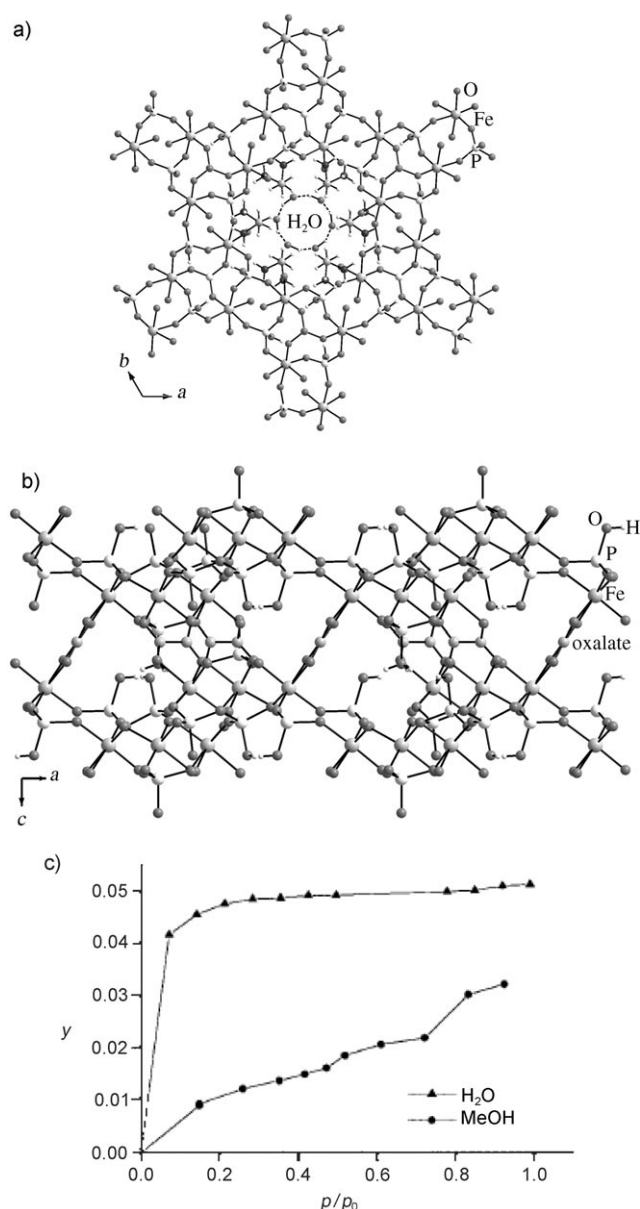


**Figure 17.** Structure of  $[H_3N(CH_2)_2NH_3]_{1.5}[Fe_3(PO_4)(HPO_4)_3(C_2O_4)_{1.5}] \cdot xH_2O$  ( $x = 1.5-2.0$ ) a) along [001] direction showing the 12-membered pore openings. The amine molecules sit at the edge of the ring and the water molecules form hexameric clusters at the center. b) View perpendicular to the inorganic layers, showing the connectivity between the layers by the oxalates. c) Room-temperature adsorption isotherm for  $H_2O$  and  $CH_3OH$  in the dehydrated sample;  $y$  is the weight adsorbed/total weight.

In  $[C_8N_4H_{26}][Fe_6(HPO_4)_8(C_2O_4)_3] \cdot 4H_2O$ , the oxalate units have unique functional role.<sup>[151b]</sup> The connectivity between  $FeO_6$  and  $HPO_3$  units forms SBU-7s, which are connected together forming the three-dimensional structure. The role of the oxalate units in this structure is mainly to satisfy the coordination requirement of iron and also to contribute to the charge neutrality of the framework, similar to the role of selenite in the ferroselenite  $[Fe_3(H_2O)(SeO_3)_3]$ .<sup>[135e]</sup> The magnetic studies indicate antiferromagnetic interaction with  $C_m = 4.79 \text{ cm}^3 \text{ K mol}^{-1}$  and  $\theta = -93 \text{ K}$ .

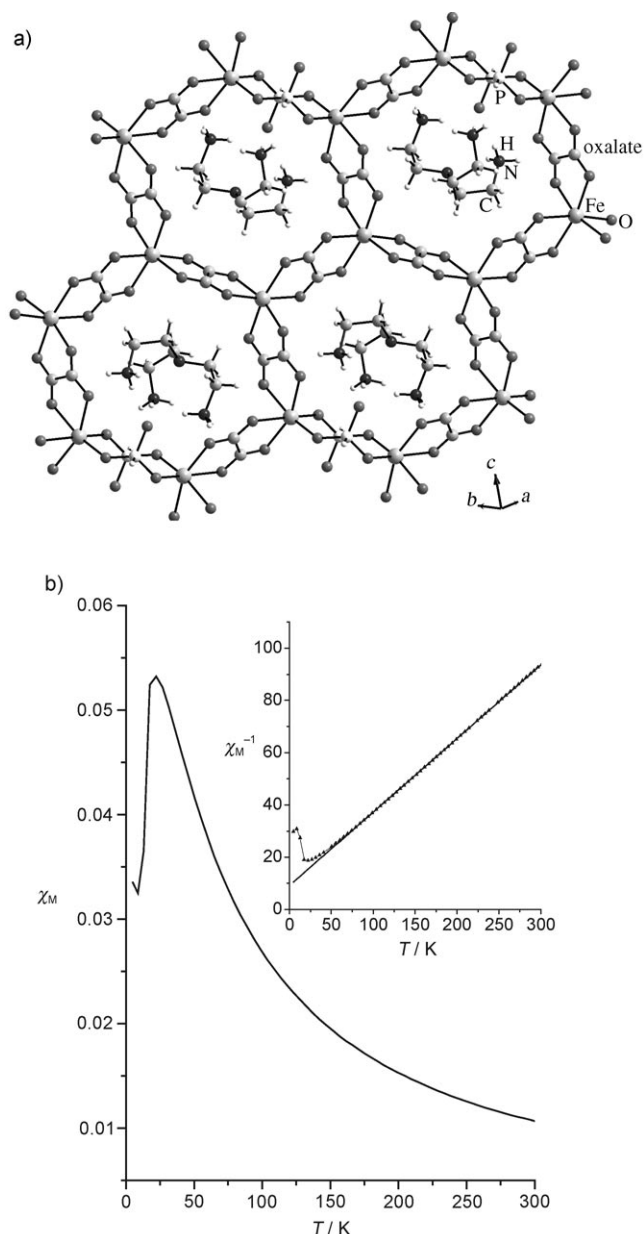


**Figure 18.** a) Structure of  $[C_6N_4H_{21}]_2[Fe_4(HPO_3)_2(C_2O_4)_5] \cdot 5H_2O$  in the  $bc$  plane showing the honeycomb-like structure. Note that the two phosphite groups replace one oxalate unit. b) Temperature variation of the magnetic susceptibility  $\chi_M$  [emu mol<sup>-1</sup>] and its inverse (inset).

### 13.3. Arsenate Oxalates

The one-dimensional structure of  $[C_4N_2H_{12}][Fe(OH)(C_2O_4)(HAsO_4)]$ <sup>[118b]</sup> is isotypic with that of the vanadophosphate oxalate  $[C_4N_2H_{12}][VO(C_2O_4)(HPO_4)]$ .<sup>[145a]</sup> There are no reported two-dimensional transition-metal arsenate oxalates. Two three-dimensional arsenate oxalate structures have been reported, and their structures are also similar to the phosphate oxalate structures. The structure of  $[C_4N_2H_{12}][Fe_4(HAsO_4)_6(C_2O_4)_2]$ <sup>[154]</sup> is isotypic with those of  $[C_5N_2H_{14}][Fe_2(HPO_4)_3(C_2O_4)]$ <sup>[149e]</sup> and  $[C_{10}N_4H_{28}][Fe_2(HPO_4)_3(C_2O_4)_2]$ <sup>[149g]</sup> and the structure of the second three-dimensional ferroarsenate oxalate,  $[NH_3(CH_2)CH(NH_3)CH_3]_3[Fe_6(AsO_4)_2]$

$(\text{HAsO}_4)_6(\text{C}_2\text{O}_4)_3$ ]<sup>[155]</sup> is isotypic with that of  $[\text{NH}_3-(\text{CH}_2)_2\text{NH}_3]_{1.5}[(\text{Fe}_3(\text{PO}_4)(\text{HPO}_4)_3(\text{C}_2\text{O}_4)_{1.5}) \cdot x\text{H}_2\text{O}]$  ( $x = 1.5-2.0$ ).<sup>[149b]</sup>

#### 14. Magnetic Behavior in Transition-Metal-Based Framework Structures

A main impetus to study transition-metal-based compounds is to investigate the interaction between the unpaired electrons. To understand the magnetic behavior in these compounds, many different approaches have been made. Herein, we present a concise account of the magnetic phenomena encountered in transition-metal-based open-framework compounds. We have provided some basic ideas coupled with some of the popular models regularly employed to explain the magnetic behavior.

Generally, the magnetic property of a solid depends on the number of unpaired electrons in the ground state. When the excited states are close to the ground state (i.e. the energy differences are only of the order of  $kT$ ), then it is likely that the excited states are also populated. In general, there are three scenarios to be distinguished: the excited states have 1) high energy than  $kT$ , 2) lower energy than  $kT$ , and 3) comparable energy to  $kT$ .<sup>[156a-d]</sup>

Case 1: When the excited state energies are larger than  $kT$ , the  $L$  (orbital) and  $S$  (spin) vectors interact strongly and precess rapidly about the direction of the resultant  $J$  vector. In this situation,  $J$  becomes dominant and  $L$  and  $S$  no longer dictate the macroscopic magnetic properties. Then Equation (1) is obeyed, where  $g$  is the Landé factor for the electron ( $= 1 + [J(J+1) + S(S+1) - L(L+1)]/2J(J+1)$ ) and  $\mu$  is the magnetic moment.

$$\mu = g[J(J+1)]^{1/2} \quad (1)$$

Case 2: When the excited states energies are small compared to  $kT$ , Then Equations (2) and (3) are obeyed, where  $\chi_M$  is the molar magnetic susceptibility,  $N$  is the Avogadro number,  $\mu_B$  is Bohr Magneton ( $= eh/4\pi mc$ ,  $e$  is the electron charge,  $h$  is the Planck constant,  $m$  is the mass of an electron,  $c$  is the velocity of light),  $\mu_L$  is the magnetic moment for the orbital contribution and  $\mu_S$  is the magnetic moment for the spin contribution.

$$\chi_M = N\mu_L^2/3kT + N\mu_S^2/3kT \\ = N/3kT(\mu_L^2 + \mu_S^2) = N\beta^2/3kT[L(L+1) + 4S(S+1)] \quad (2)$$

$$\mu_{L+S} = [L(L+1) + 4S(S+1)]^{1/2}\mu_B \quad (3)$$

Case 3: When the excited state energies are comparable to  $kT$ , then Equations (4) and (5) are obeyed, where  $E$  is the energy difference between the ground and excited state and  $k$  is the Boltzman constant.

$$\chi_M = N\mu_B^2/3kT \left\{ \sum g^2 J(J+1)(2J+1)e^{-E/(kT)} / \sum (2J+1)e^{-E/(kT)} \right\} \quad (4)$$

$$\mu = \left\{ \sum g^2 \mu_B^2 J(J+1)(2J+1)e^{-E/(kT)} / \sum (2J+1)e^{-E/(kT)} \right\}^{1/2} \quad (5)$$

Most of the reported compounds this Review show antiferromagnetic interactions, for these species the high temperature region of the magnetic susceptibility behavior can be fitted to the Curie–Weiss law [Eq. (6)] where  $C_m = [N\mu_B^2/(3k)]$  is the Curie constant and  $\theta$  is the Weiss constant.

$$\chi = C/(T-\theta) \quad (6)$$

For an antiferromagnet,  $\theta$  is negative, whereas for a ferromagnet, it is positive and for a paramagnet it is zero. The Curie equation relates the molar susceptibility and the magnetic moment of a substance. This relationship helps to determine the effective moment ( $\mu_{\text{eff}}$ ) of the substance, if the experimental molar susceptibility of the substance is known [Eq. (7)].

$$\mu_{\text{eff}} = [3k/(N\mu_B^2)]^{1/2}(\chi_M T)^{1/2} \quad (7)$$

The magnetic behavior of a solid depends on many factors including the site symmetry of the magnetic ion. In framework compounds, metal–metal bonds are rarely encountered and hence most of the exchanges between the transition-metal centers are by super-exchange or super–super-exchange interactions through the connecting ligand. Thus, the M–O/F–M angle becomes important in understanding the magnetism in framework solids. According to the postulations of Goodenough and Kanamori,<sup>[156a,157]</sup> for ideal ferromagnetic interactions, the M–O/F–M angle is  $90^\circ$  and for an antiferromagnetic interaction, it is  $180^\circ$ . This approach gives qualitative information about the strength of interactions between the magnetic centers. To quantify this interaction, different models have been employed. Below we present the important models.

##### 14.1. Heisenberg Model

The Heisenberg model<sup>[156]</sup> is useful for understanding the magnetic interactions in a linear chain system. An array of metal ions connected by ligands (such as, O, F) can be considered a linear chain. When the chains are isolated, the interaction is primarily one-dimensional, that is, interchain interactions can be neglected. The Hamiltonian for the interacting spins, then, is given by Equation (8), where  $S_i$  and  $S_j$  are the spin quantum numbers of  $i^{\text{th}}$  and  $j^{\text{th}}$  atom and  $J$  is the exchange coupling constant. The value and sign of  $J$  indicate the strength and nature of interactions between the magnetic ions ( $>0$ : ferromagnetic,  $<0$ : antiferromagnetic). This is a simple model to describe the magnetic behavior in transition-metal compounds.

$$\mathcal{H} = -J \sum S_i S_j \quad (8)$$

##### 14.2. Dimer Model

The dimer model<sup>[156c]</sup> is an extension of the Heisenberg model and generally applicable when two metal polyhedra share a vertex, edge, or face and form a dimer, which can be

linked to other dimers through a non-magnetic unit (phosphate, arsenate, etc.). From the Heisenberg Model, the energy per electron is  $J[S(S+1)]/2$  if the two electrons have a total spin = 0 and  $-JS^2/2$  if the two electrons have a total spin =  $2S$ .

The magnetic susceptibility can be expressed as Equation (9), where  $[\langle M^2 \rangle - \langle M \rangle^2]$  is the fluctuation in magnetization,  $M$ .

$$\chi = g^2 \mu_B^2 [\langle M^2 \rangle - \langle M \rangle^2] / kT \quad (9)$$

For an antiferromagnetic substance in the absence of a magnetic field, the average magnetization,  $\langle M \rangle$ , vanishes. Thus the magnetic susceptibility for the dimer can be written as Equation (10) with  $S = 0, 1, 2, 3, 4, 5, \dots$

$$\chi_{\text{Dimer}} = g^2 \mu_B^2 / kT [\sum S(S+1) \exp(E_S/kT)] / \sum \exp(E_S/kT) \quad (10)$$

This dimer susceptibility is fitted with the experimental  $\chi_M T$ , by varying the exchange constant  $J$  and the Landé factor  $g$ . The magnitude of  $J$  indicates the strength of the interactions between the spins.

### 14.3. Fisher's Model

When the value of the local spin  $S_i$  becomes large, this spin may be treated as a classical vector. An analytical expression for the magnetic susceptibility of an infinite chain of classical spins has been derived by Fisher<sup>[156]</sup> [Eq. (11)]. In this

$$\chi/N = [g^2 S(S+1) \mu_B^2 / 3kT] [(1+u)/(1-u)] \quad (11)$$

expression the classical spin has been scaled to a real quantum spin  $S$  where  $u$  is given by Equation 12.

$$u = \coth[2JS(S+1)/kT] - kT/[2JS(S+1)] \quad (12)$$

Of course, this classical approximation gets better the larger  $S_i$  is. In practice, this equation holds fairly well for  $S_i \geq 5/2$ . It has often been used for  $\text{Mn}^{\text{II}}$  and  $\text{Fe}^{\text{III}}$  chains.

### 14.4. Dzyaloshinsky–Moriya (DM) Interactions

When the dinuclear entity is not built from identical units, the antisymmetric interaction becomes relevant. This contributes to the zero-field splitting within the triplet state and, in addition, couples the  $S = 1$  and  $S = 0$  states. The antisymmetric interaction arises from the synergistic effect of local spin–orbit coupling and interactions between the magnetic centers. This effect vanishes when the dinuclear unit is centrosymmetric and when its molecular symmetry is at least  $C_{nv}$  ( $n \geq 2$ ) with the  $n$ -fold axis running through the interacting centers. Therefore, for most compounds, the antisymmetric interaction is actually zero.

The most general form for the spin Hamiltonian is given by Equation (13). This term was first proposed by Dzyaloshinsky<sup>[158]</sup> and then analyzed by Moriya.<sup>[159]</sup>

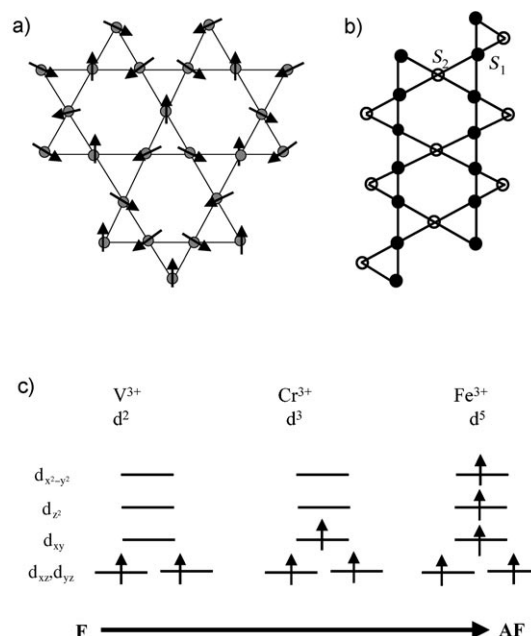
$$\mathcal{H}_{\text{DM}} = \sum \vec{D}_{ij} \cdot (\vec{S}_i \times \vec{S}_j) \quad (13)$$

Generally, DM interactions are weaker than the super exchange terms [Eq. (14)], but at low temperature, the coupling with other magnetic centers in all three dimensions can give rise to canted magnetic species with ferromagnetic polarization.<sup>[160]</sup>

$$\mathcal{H}_{\text{SE}} = \sum J_{ij} (\vec{S}_i \cdot \vec{S}_j) \quad (14)$$

### 14.5. Magnetism of Kagomé lattice

The Kagomé lattice is a very special case and important for the study and understanding of the magnetic frustration in transition-metal compounds. The frustration arises from the presence of triangular arrangement of the magnetic ions (Scheme 3a).<sup>[161]</sup> Most of the compounds belong to the



**Scheme 3.** a) The Kagomé lattice with the spin orientations in a possible ground-state configuration. b) Schematic representation of the Kagomé lattice with two types of spin. c) Correlation between the magnetic properties of the jarosite and the d-orbital occupancy of the  $M^{3+}$  ion in the tetragonal crystal field. F ferromagnetic, AF antiferromagnetic.

jarosite family ( $K_2[Fe^{3+}_6(SO_4)_4(OH)_{12}]$ ).<sup>[162]</sup> the classical example of a spin-frustrated magnetic structure. Magnetic properties of the Kagomé system depend upon the number of unpaired electrons in the magnetic ion.<sup>[165]</sup> As in the Kagomé structure one magnetic ion is shared by two adjacent triangles, two triangles with five spins can be considered as a basic unit. For a general understanding, we term the spins of the ions at the edges of the two triangles  $S_1$  and the spin of the magnetic ion at the shared corner  $S_2$ , so that there are four  $S_1$  spins and

one  $S_2$  spin in this five spin system (Scheme 3b). This system can be solved by assuming that the interaction of the site spins can be described by a nearest-neighbor Heisenberg exchange Hamiltonian. The cases with  $S_1 = S_2$  and  $S_1 \neq S_2$  can be considered separately within this simple exchange Hamiltonian.

For  $S_1 = S_2 = 1/2$ , the ground state is sixfold degenerate, with each doublet configuration of the shared ion giving rise to threefold degenerate states for each triangle. The ground-state magnetization is finite at each lattice point as a result of strong frustration. For  $S_1 = S_2 = 1$ , the ground state is threefold degenerate and is a singlet, and in each case, the edges as well as corner spins vanish separately.

Next we consider the cases with  $S_1 \neq S_2$ ; each can be either an integer or a half-odd-integer spin. 1)  $S_1 = 1/2$  and  $S_2 = 1$ , the ground state is a singlet and is threefold degenerate. The states are similar to the  $S_1 = S_2 = 1$  case, although with an antiferromagnetic coupling in each edge between the two spin  $1/2$  sites. 2)  $S_1 = 1/2$  and  $S_2 = 3/2$ , the ground state is a doublet with double degeneracy. The spin state of both edges together form a triplet, which couples with the  $S_2 = 1/2$  component of the  $S = 3/2$  spin. 3)  $S_1 = 1/2$  and  $S_2 = 2$ , the ground state is a singlet and nondegenerate. The magnetization at each site is zero. 4)  $S_1 = 1/2$  and  $S_2 = 5/2$ , the ground state is a doublet and has the same features as with case (2). 5) For  $S_1 = 1/2$  and  $S_2 = 3$ , the ground state has a finite magnetization and is a triplet. In the ground state, each of the edge sites with spin  $1/2$  forms a triplet and the corner spin site has a magnetization of two. This is a ferrimagnetic state, in which the frustration in the Kagomé structure is completely removed. By increasing the value of  $S_2$  further and keeping  $S_1 = 1/2$  fixed, same ferrimagnetic state is obtained with a ground-state spin  $S_G = S_2 - 4S_1$ . Thus, to observe a ferrimagnet-like behavior in a frustrated system, the spin quantum number of the corner-shared ion must be large compared to those of the edge ions.

Jarositic and analogous materials with  $\text{Fe}^{3+}$ ,  $\text{Co}^{2+}$ , and  $\text{Cr}^{3+}$  ions exhibit characteristics of frustrated low-temperature antiferromagnetism and occasional long-range antiferromagnetic order in the ground state.<sup>[131, 163, 164, 165c]</sup> Vanadium ( $\text{V}^{3+}$ ) jarosite and distorted iron ( $\text{Fe}^{2+}$ ) Kagomé compounds, however, exhibit ferromagnetic features.<sup>[130b, 164]</sup> This can be also explained using the classical crystal-field theory (Scheme 3c). The magnetic  $\text{M}^{3+}$  ions of jarosites and analogous materials reside in a tetragonally distorted crystal field. The axial elongation of the octahedron lifts the degeneracy of the  $t_{2g}$  and  $e_g$  orbital sets. The  $t_{2g}$  orbital splits into lower-energy, doubly degenerate ( $d_{xz}, d_{yz}$ ) orbitals and a nondegenerate ( $d_{xy}$ ) orbital. The  $e_g$  orbital splits into a lower-energy ( $d_z^2$ ) orbital and a higher-energy ( $d_{x^2-y^2}$ ) orbital.

For  $\text{V}^{3+}$  compound, two electrons occupy the  $d_{xz}, d_{yz}$  orbitals. The interaction of the  $d_{xz}, d_{yz}$  orbitals with the p orbital of the bridging  $\text{HO}^-$  (or  $\text{O}^{2-}$  or  $\text{F}^-$ ) ion leads to a ferromagnetic exchange interaction. The crystallographic data also indicate that the angle (M-O/F-M) is sufficient to decouple the  $d_{xz}$  or  $d_{yz}$  ( $\pi$ ) orbitals of neighboring  $\text{V}^{3+}$  centers to create a ferromagnetic ground state.<sup>[165c]</sup> But for  $\text{Cr}^{3+}$ , the nearest-neighbor magnetic coupling changes as the result of the presence of one more electron. Occupation of the  $d_{xy}$  orbital in the  $\text{Cr}^{3+}$  ion leads to an antiferromagnetic exchange

term through a  $d_{xy}(\sigma)\text{--p}(\text{O})\text{--}d_{xy}(\sigma)$  pathway that is stronger than the ferromagnetic contribution from the  $d_{xz}(\pi)\text{--p}(\text{O})\text{--}d_{xz}(\pi)$  coupling.<sup>[165c]</sup> In case of  $\text{Fe}^{3+}$ , two more electrons are available, these are in the  $d_z$  and  $d_{x^2-y^2}$  orbitals, increasing the antiferromagnetic exchange interaction by more than an order of magnitude. Even when the overlap between the  $d_z$  orbital and the p orbitals of the bridging ligand is small, it is the overlap of the  $d_{x^2-y^2}$  orbital with the bridging p orbital that gives rise to the large antiferromagnetic exchange interactions in  $\text{Fe}^{3+}$  compounds.<sup>[165c]</sup> This observation also agrees with the Goodenough and Kanamori rules and accounts for the high degree of spin frustration observed in the  $d^5$  ( $S = 5/2$ ) spin system.<sup>[156a]</sup>

A recent study based on the quantum many-body Heisenberg model shows that the magnitude of frustration depends strongly upon the spin quantum number of the magnetic ions of the lattice.<sup>[166]</sup> While the Kagomé systems with  $(n+1)/2$  spin would show strong frustration, the integer or mixed-valent systems can lift the small degeneracy of the spin excitations and develop a spin-gap thereby partly or fully removing the lattice-geometry-induced frustration. In fact, for a mixed-valent Kagomé system with a certain magnitude, the whole system behaves as a classical magnet with a ferrimagnetic ground state without any frustration. These theoretical findings are consistent with the experimental observations (see the Supporting Information, Table S7).<sup>[167]</sup>

## 15. Concluding Remarks

The discussion of the various structural types and dimensionalities illustrates the variety and diversity that exists in these compounds. It is likely that many more structures will be formed and one can safely assume that the landmark paper by Flanigen and co-workers in 1982<sup>[13]</sup> has been the turning point and a watershed for all the developments in this area. Although many transition-metal compounds of different dimensionalities have been isolated which demonstrate the structural hierarchy in these systems, it has not yet been shown whether the lower-dimensional structures can be transformed into higher-dimensional ones. Thus, there is much to be done in the design of the framework through subtle manipulations of the organic and inorganic components. Mechanistic insights would help to design better frameworks with controlled pore sizes. The transition-metal-based compounds continue to be at the center of attention of the synthetic chemists, as recent studies have clearly shown that these compounds are attractive candidates for hydrogen-storage materials.<sup>[168]</sup> Additionally, it should be possible to look for frameworks that display some of the many properties that are associated with the condensed transition-metal compounds, especially the oxides.<sup>[169]</sup>

When considering the many compounds that have been prepared during the last two decades or so, it appears that the limits are not the imagination and creativity of the researchers but by the lack of understanding of the subtler forces involved in the formation of such structures. The incorporation of phosphite,<sup>[17, 18]</sup> sulfite,<sup>[170]</sup> sulfate,<sup>[38]</sup> selenite,<sup>[133–135]</sup> selenate,<sup>[171]</sup> and other anions during the last few years clearly

shows that the open-framework structures can accommodate a large variety of anions. In the light of this, it should be possible to prepare compounds based on other anions, such as  $\text{VO}_4^{3-}$ ,  $\text{MoO}_4^{2-}$ ,  $\text{ReO}_4^-$ . A combination of these anionic ligands with transition metals would open up exciting possibilities for new properties and also expand the scope of research in this area. In addition to this, the combination of more than one type of anions forming the hybrid structures should also create interesting new possibilities. The combination of porous network structures with properties, such as ferromagnetism, metal-insulator transitions, and ferroelectricity would be exciting and may be achieved in the near future.

The scope for research in this area appears to be unlimited and, especially with regard to the three-dimensional frameworks, we can look forward to finding new topologies. New preparative techniques continue to appear, such as the use of ionic liquids,<sup>[40,41,44]</sup> the use of two different solvent systems (preferably immiscible ones),<sup>[172]</sup> the synthesis of new types of templates (organic chemists can contribute extensively to this), and the assembly of pre-formed molecular blocks (see Scheme 1).<sup>[58]</sup> In addition, the advancements made by the computational approaches towards the design and prediction of topologies will also be of considerable help.<sup>[168a,b,173]</sup> We can look forward to the excitement of discovering new materials which can exhibit applications that are more diverse than the traditional ones.

*The authors thank the Department of Science and Technology (DST), Government of India, for the award of research grants through their regular funding, and under the nano mission and nano initiatives. CSIR and DAE-BRNS are also thanked for the financial support. S.N. thanks DST for a Ramanna Fellowship. The authors are particularly thankful to Professors Diptiman Sen (IISc) and Swapan K. Pati (JNCASR) for their input towards the description of the magnetic behavior in these structures.*

Received: April 1, 2007

Revised: September 21, 2007

Published online: May 7, 2008

- [1] R. M. Barrer, *Hydrothermal Chemistry of Zeolites*, Academic Press, London, **1982**.
- [2] A. K. Cheetham, G. Férey, T. Loiseau, *Angew. Chem.* **1999**, *111*, 3466–3492; *Angew. Chem. Int. Ed.* **1999**, *38*, 3268–3292.
- [3] J. M. Thomas, *Angew. Chem.* **1999**, *111*, 3800–3843; *Angew. Chem. Int. Ed.* **1999**, *38*, 3588–3628.
- [4] F. Schüth, W. Schmidt, *Adv. Mater.* **2002**, *14*, 629–638.
- [5] *Supramolecular Organization and Materials Design* (Eds.: W. Jones, C. N. R. Rao), Cambridge University Press, Cambridge, **2002**.
- [6] C. N. R. Rao, S. Natarajan, R. Vidhyanathan, *Angew. Chem.* **2004**, *116*, 1490–1521; *Angew. Chem. Int. Ed.* **2004**, *43*, 1466–1496.
- [7] A. Müller, H. Reuter, S. Dillinger, *Angew. Chem.* **1995**, *107*, 2505–2539; *Angew. Chem. Int. Ed. Engl.* **1995**, *34*, 2328–2361.
- [8] P. J. Hagrman, D. Hagrman, J. Zubietta, *Angew. Chem.* **1999**, *111*, 2798–2848; *Angew. Chem. Int. Ed.* **1999**, *38*, 2638–2684.
- [9] S. R. Batten, R. Robson, *Angew. Chem.* **1998**, *110*, 1558–1595; *Angew. Chem. Int. Ed.* **1998**, *37*, 1460–1494.
- [10] D. Maspoeh, D. Ruiz-Molina, J. Vaciara, *Chem. Soc. Rev.* **2007**, *36*, 770–818.
- [11] A. Clearfield, *Curr. Opin. Solid State Mater. Sci.* **1996**, *1*, 268–278, and references therein.
- [12] M. Eddaoudi, D. B. Moler, H. Li, B. Chen, T. M. Reineke, M. O’Keeffe, O. M. Yaghi, *Acc. Chem. Res.* **2001**, *34*, 319–330, and references therein.
- [13] S. T. Wilson, B. M. Lok, C. A. Mesina, T. R. Cannan, E. D. Flanigen, *J. Am. Chem. Soc.* **1982**, *104*, 1146–1147.
- [14] J. Yu, R. Xu, *Chem. Soc. Rev.* **2006**, *35*, 593–604.
- [15] P. S. Halasyamani, S. M. Walker, D. O’Hare, *J. Am. Chem. Soc.* **1999**, *121*, 7415–7416.
- [16] P. M. Almond, C. E. Tally, A. C. Bean, S. M. Peper, T. E. Albrecht-Schmitt, *J. Solid State Chem.* **2000**, *154*, 635–641.
- [17] M. Shieh, K. J. Martin, P. J. Squattrito, A. Clearfield, *Inorg. Chem.* **1990**, *29*, 958–963.
- [18] J. A. Rodgers, W. T. A. Harrison, *Chem. Commun.* **2000**, 2385–2386.
- [19] P. Feng, X. Bu, N. Zheng, *Acc. Chem. Res.* **2005**, *38*, 293–303, and references therein.
- [20] J. M. Lehn, *Supramolecular Chemistry, Concepts and Perspectives*, VCH, Weinheim, **1995**.
- [21] B. Moulton, M. J. Zaworotko, *Chem. Rev.* **2001**, *101*, 1629–1658.
- [22] S. I. Noro, S. Kitagawa, M. Kondo, K. Seki, *Angew. Chem.* **2000**, *112*, 2161–2164; *Angew. Chem. Int. Ed.* **2000**, *39*, 2081–2084.
- [23] a) K. Biradha, Y. Hongo, M. Fujita, *Angew. Chem.* **2002**, *114*, 3545–3548; *Angew. Chem. Int. Ed.* **2002**, *41*, 3395–3398; b) E. J. Cussen, J. B. Claridge, M. J. Rosseinsky, C. J. Kepert, *J. Am. Chem. Soc.* **2002**, *124*, 9574–9581, and references therein; c) M. Eddaoudi, J. Kim, D. Vodak, A. Sudik, J. Wachter, M. O’Keeffe, O. M. Yaghi, *Proc. Natl. Acad. Sci. USA* **2002**, *99*, 4900–4904; d) N. W. Ockwig, O. Delgado-Friedrichs, M. O’Keeffe, O. M. Yaghi, *Acc. Chem. Res.* **2005**, *38*, 176–182; e) J. L. C. Rowsell, E. C. Spencer, J. Echart, J. A. K. Howard, O. M. Yaghi, *Science* **2005**, *309*, 1350–1354.
- [24] C. Mellot-Draznieks, S. Girard, G. Férey, J. C. Schön, Z. Cancarevic, M. Jansen, *Chem. Eur. J.* **2002**, *8*, 4102–4113, and references therein.
- [25] S. Natarajan, *Proc. Indian Acad. Sci. Chem. Sci.* **2000**, *112*, 249–272.
- [26] a) G. Férey, T. Loiseau, P. Lacorre, F. Taulelle, *J. Solid State Chem.* **1993**, *105*, 179–190; b) G. Férey, *J. Fluorine Chem.* **1995**, *72*, 187–193; c) G. Férey, *C. R. Acad. Sci. Ser. IIc* **1998**, *1*, 1–13; d) M. Riou-Cavellec, D. Riou, G. Férey, *Inorg. Chim. Acta* **1999**, *291*, 317–325; e) G. Férey, *J. Solid State Chem.* **2000**, *152*, 37–48; f) G. Férey, *Chem. Mater.* **2001**, *13*, 3084–3098.
- [27] a) R. M. Barrer, *J. Chem. Soc.* **1948**, 127–132; b) R. M. Milton, US-Pat. 2882434, **1959**.
- [28] a) S. L. Lawton, D. H. Olson, W. M. Meier, G. T. Kokotailo, *Nature* **1978**, *272*, 437–438; b) M. E. Davis, R. F. Lobo, *Chem. Mater.* **1992**, *4*, 756–768; c) A. Choudhury, S. Natarajan, C. N. R. Rao, *Inorg. Chem.* **2000**, *39*, 4295–4304.
- [29] R. E. Morris, S. J. Weigel, *Chem. Soc. Rev.* **1997**, *26*, 309–317.
- [30] S. L. Lawton, W. J. Rohrbaugh, *Science* **1990**, *247*, 1319–1322.
- [31] S. I. Zones, M. M. Olmstead, D. S. Santilli, *J. Am. Chem. Soc.* **1992**, *114*, 4195–4201.
- [32] a) J. Yu, R. Xu, J. Li, *Solid State Sci.* **2000**, *2*, 181–190; b) J. Yu, R. Xu, *Acc. Chem. Res.* **2003**, *36*, 481–490.
- [33] a) A. M. Chippindale, R. I. Walton, *J. Chem. Soc. Chem. Commun.* **1994**, 2453–2454; b) A. M. Chippindale, A. R. Cowley, *Zeolites* **1997**, *18*, 176–181.
- [34] a) S. J. Weigel, J.-C. Gabriel, G. Puebla, A. M. Bravo, N. J. Henson, L. M. Bull, A. K. Cheetham, *J. Am. Chem. Soc.* **1996**,

- 118, 2427–2435; b) A. Davidson, S. J. Weigel, L. M. Bull, A. K. Cheetham, *J. Phys. Chem. B* **1997**, *101*, 3065–3071.
- [35] J. L. Guth, H. Kessler, R. Wey, *Stud. Surf. Sci. Catal.* **1986**, *28*, 121–128.
- [36] M. Estermann, L. B. McCusker, C. Baerlocher, M. Merrouche, H. Kessler, *Nature* **1991**, *352*, 320–323.
- [37] a) A. Kuperman, S. Nadmi, S. Oliver, G. A. Ozin, J. M. Garces, M. M. Olken, *Nature* **1993**, *365*, 239–242; b) S. Nadmi, S. Oliver, A. Kuperman, A. Lough, G. A. Ozin, J. A. Garces, M. M. Olken, P. Rudolf, *Stud. Surf. Sci. Catal.* **1994**, *84*, 93–100.
- [38] C. N. R. Rao, J. N. Behera, M. Dan, *Chem. Soc. Rev.* **2006**, *35*, 375–378, and references therein.
- [39] a) K. Morgan, G. Gainsford, N. Milestone, *J. Chem. Soc. Chem. Commun.* **1995**, 425–426; b) D. A. Bruce, A. P. Wilkinson, M. G. White, J. A. Bertrand, *J. Chem. Soc. Chem. Commun.* **1995**, 2059–2060; c) S. Natarajan, J.-C. P. Gabriel, A. K. Cheetham, *Chem. Commun.* **1996**, 1415–1416; d) S. M. Stadler, A. P. Wilkinson, *Chem. Mater.* **1997**, *9*, 2168–2173.
- [40] a) T. Welton, *Chem. Rev.* **1999**, *99*, 2071–2084; b) E. R. Parnham, R. E. Morris, *Acc. Chem. Res.* **2007**, *40*, 1005–1013.
- [41] E. R. Cooper, C. D. Andrews, P. S. Wheatley, P. B. Webb, P. Wormald, R. E. Morris, *Nature* **2004**, *430*, 1012–1016.
- [42] P. Wasserscheid, T. Welton, *Ionic Liquids in Synthesis*, Wiley-VCH, Weinheim, **2003**, chap. 2; H. Weingärtner, *Angew. Chem.* **2008**, *120*, 664–682; *Angew. Chem. Int. Ed.* **2008**, *47*, 654–670.
- [43] A. P. Abbott, G. Chapper, D. L. Davies, R. K. Rasheed, V. Tambyrajah, *Chem. Commun.* **2003**, 70–71.
- [44] E. R. Parnham, R. E. Morris, *J. Am. Chem. Soc.* **2006**, *128*, 2204–2205.
- [45] C. Y. Sheu, S. F. Lee, K. H. Lii, *Inorg. Chem.* **2006**, *45*, 1891–1893.
- [46] a) International Zeolite Association, <http://www.iza-online.org>; b) W. M. Meier, D. H. Olson, C. Baerlocher, *Atlas of Zeolite Structure Types*, Elsevier, London, **1996**.
- [47] a) J. V. Smith, *Chem. Rev.* **1988**, *88*, 149–182; b) C. Mellot-Draznieks, S. Girard, G. Férey, *J. Am. Chem. Soc.* **2002**, *124*, 15326–15335.
- [48] a) J. Rocha, M. W. Anderson, *Eur. J. Inorg. Chem.* **2000**, 801–818; b) “Micro- and Mesoporous Mineral Phases”: J. Rocha, Z. Lin, *Rev. Mineral. Geochem.* **2005**, *57*, 173–201.
- [49] a) M. A. Roberts, G. Sankar, J. M. Thomas, R. H. Jones, H. Du, J. Chen, W. Pang, R. Xu, *Nature* **1996**, *381*, 401–404; b) Z. Lin, J. Rocha, P. Brandao, A. Ferreira, A. P. Esculcas, J. D. Pedrosa de Jesus, A. Philippou, M. W. Anderson, *J. Phys. Chem. B* **1997**, *101*, 7114–7120; c) M. S. Dadachov, J. Rocha, A. Ferreira, Z. Lin, M. W. Anderson, *Chem. Commun.* **1997**, 2371–2372.
- [50] A. I. Bortun, L. N. Bortun, A. Clearfield, *Chem. Mater.* **1997**, *9*, 1854–1864.
- [51] a) M. W. Anderson, O. Terasaki, T. Ohsuna, A. Philippou, S. P. Mackay, A. Ferreira, J. Rocha, S. Lidin, *Nature* **1994**, *367*, 347–351; b) S. M. Kuznicki, K. A. Thrush, F. M. Allen, S. M. Levine, M. M. Hamil, D. T. Hayhurst, M. Mansor, *Synth. Microporous Mater.* **1992**, *1*, 427–456; c) X. Wang, A. J. Jacobson, *Chem. Commun.* **1999**, 973–974; d) C. L. Bianchi, S. Vitali, V. Ragaini, *Stud. Surf. Sci. Catal.* **1998**, *119*, 167–172; e) C. L. Bianchi, R. Carli, S. Merlotti, V. Ragaini, *Catal. Lett.* **1996**, *41*, 79–82; f) A. Philippou, M. Naderi, N. Pervaiz, J. Rocha, M. W. Anderson, *J. Catal.* **1998**, *178*, 174–181; g) T. K. Das, A. J. Chandwadkar, S. Sivasanker, *Stud. Surf. Sci. Catal.* **1998**, *113*, 455–462; h) J. P. Rainho, L. D. Carlos, J. Rocha, *J. Lumin.* **2000**, *87–89*, 1083–1086; i) J. Rocha, L. D. Carlos, J. P. Rainho, Z. Lin, P. Ferreira, R. M. Almeida, *J. Mater. Chem.* **2000**, *10*, 1371–1375; j) A. Zecchina, C. O. Arean, G. T. Palomino, F. Geobaldo, C. Lamberti, G. Spoto, S. Bordiga, *Phys. Chem. Chem. Phys.* **1999**, *1*, 1649–1657; k) G. Cruciani, P. De Luca, A. Nastro, P. Pattison, *Microporous Mesoporous Mater.* **1998**, *21*, 143–153; l) S. Nair, H.-K. Jeong, A. Chandrasekaran, C. M. Braunbarth, M. Tsapatsis, S. M. Kuznicki, *Chem. Mater.* **2001**, *13*, 4247–4254; m) A. N. Merkov, I. V. Bussen, E. A. Goiko, E. A. Kul’chitskaya, Y. P. Meishikov, A. P. Nedorezova, *Zap. Vses. Mineral. O-va.* **1973**, *102*, 54–62; n) D. M. Poojary, R. A. Cahill, A. Clearfield, *Chem. Mater.* **1994**, *6*, 2364–2368; o) M. Nyman, F. Bonhomme, D. M. Teter, R. S. Maxwell, B. X. Gu, L. M. Wang, R. C. Ewing, T. M. Nenoff, *Chem. Mater.* **2000**, *12*, 3449–3458; p) M. Nyman, F. Bonhomme, R. S. Maxwell, T. M. Nenoff, *Chem. Mater.* **2001**, *13*, 4603–4611.
- [52] a) J. Rocha, P. Brandão, Z. Lin, M. W. Anderson, V. Alfredsson, O. Terasaki, *Angew. Chem.* **1997**, *109*, 134–136; *Angew. Chem. Int. Ed. Engl.* **1997**, *36*, 100–102; b) X. Wang, L. Liu, A. J. Jacobson, *Angew. Chem.* **2001**, *113*, 2232–2234; *Angew. Chem. Int. Ed.* **2001**, *40*, 2174–2176; c) J. Huang, X. Wang, L. Liu, A. J. Jacobson, *Solid State Sci.* **2002**, *4*, 1193–1198; d) X. Wang, L. Liu, A. J. Jacobson, *J. Am. Chem. Soc.* **2002**, *124*, 7812–7820.
- [53] a) X. Wang, L. Lui, A. J. Jacobson, *Angew. Chem.* **2003**, *115*, 2090–2093; *Angew. Chem. Int. Ed.* **2003**, *42*, 2044–2047; b) P. Brandão, F. A. A. Paz, J. Rocha, *Chem. Commun.* **2005**, 171–173.
- [54] a) G. Baussy, R. Caruba, A. Baumer, G. Turco, *Bull. Soc. Fr. Mineral. Cristallogr.* **1974**, *97*, 433–444; b) S. R. Jale, A. Ojo, F. R. Fitch, *Chem. Commun.* **1999**, 411–412; c) S. Ghose, C. Wan, G. Y. Chao, *Can. Mineral.* **1980**, *18*, 503–509.
- [55] a) R. J. Francis, A. J. Jacobson, *Angew. Chem.* **2001**, *113*, 2963–2965; *Angew. Chem. Int. Ed.* **2001**, *40*, 2879–2881; b) M. A. Salvadó, P. Pertierra, S. Garcia-Granda, S. A. Khainakov, J. R. Garcia, A. I. Bortun, A. Clearfield, *Inorg. Chem.* **2001**, *40*, 4368–4373; c) H.-M. Kao, K.-H. Lii, *Inorg. Chem.* **2002**, *41*, 5644–5646.
- [56] a) R. J. Francis, A. J. Jacobson, *Chem. Mater.* **2001**, *13*, 4676–4680; b) M. A. Monge, E. Gutiérrez-Puebla, C. Cascales, J. A. Campa, *Chem. Mater.* **2000**, *12*, 1926–1930; c) W. T. A. Harrison, T. E. Gier, G. D. Stucky, *J. Solid State Chem.* **1995**, *115*, 373–378; d) H. Li, M. Eddaoudi, J. Plévert, M. O’Keeffe, O. M. Yaghi, *J. Am. Chem. Soc.* **2000**, *122*, 12409–12410; e) P. Pertierra, M. A. Salvado, S. Garcia-Granda, C. Trabajo, J. R. Garcia, A. I. Bortun, A. Clearfield, *J. Solid State Chem.* **1999**, *148*, 41–49.
- [57] A. Dakhlaoui, S. Ammar, L. S. Smiri, *Mater. Res. Bull.* **2005**, *40*, 1270–1278.
- [58] C. N. R. Rao, S. Natarajan, A. Choudhury, S. Neeraj, A. A. Ayi, *Acc. Chem. Res.* **2001**, *34*, 80–87.
- [59] a) Z. Bircsak, A. K. Hall, W. T. A. Harrison, *J. Solid State Chem.* **1999**, *142*, 168–173; b) R. K. Chiang, *J. Solid State Chem.* **2000**, *153*, 180–184; c) A. Choudhury, S. Natarajan, C. N. R. Rao, *J. Chem. Soc. Dalton Trans.* **2000**, 2595–2598; d) S. Neeraj, T. Loiseau, C. N. R. Rao, A. K. Cheetham, *Solid State Sci.* **2004**, *6*, 1169–1173; e) G.-Z. Liu, S.-T. Zheng, G.-Y. Yang, *Inorg. Chem.* **2007**, *46*, 231–237.
- [60] a) H. Meng, S. Li, L. Liu, Y. Cui, G. Li, W. Pang, *Mater. Lett.* **2005**, *59*, 3861–3865; b) W.-J. Chang, Y.-C. Jiang, S.-L. Wang, K.-H. Lii, *J. Solid State Chem.* **2006**, *179*, 3059–3064; c) H. Meng, G. Li, Y. Liu, L. Liu, Y. Cui, W. Pang, *J. Solid State Chem.* **2004**, *177*, 4459–4464; d) A. R. Cowley, A. M. Chippindale, *J. Chem. Soc. Dalton Trans.* **1999**, 2147–2149.
- [61] a) R. A. Ramik, B. D. Sturman, P. J. Dunn, A. S. Poverennykh, *Can. Mineral.* **1980**, *18*, 185–190; b) F. C. Hawthorne, *Acta Crystallogr. Sect. B* **1994**, *50*, 481–510, and references therein.
- [62] a) Y. Guo, Z. Shi, J. Yu, J. Wang, Y. Liu, N. Bai, W. Pang, *Chem. Mater.* **2001**, *13*, 203–207; b) L. Liu, X. Wang, R. Bontchev, K. Ross, A. J. Jacobson, *J. Mater. Chem.* **1999**, *9*, 1585–1589; c) Y. Zhang, C. J. Warren, A. Clearfield, R. C. Haushalter, *Polyhedron* **1998**, *17*, 2575–2580; d) M. Cavellec, D. Riou, J.-M. Greneche, G. Férey, *Inorg. Chem.* **1997**, *36*, 2187–2190; e) S. Mahesh, M. A. Green, S. Natarajan, *J. Solid State Chem.* **2002**,

- 165, 334–344; f) S. Mandal, S. Natarajan, W. Klein, M. Panthöfer, M. Jansen, *J. Solid State Chem.* **2003**, *173*, 367–373; g) S. Mandal, M. A. Green, S. Natarajan, *J. Solid State Chem.* **2004**, *177*, 1117–1126.
- [63] a) V. Zima, K.-H. Lii, *J. Chem. Soc. Dalton Trans.* **1998**, 4109–4112; b) K. Abu-Shandi, H. Winkler, G. Gerdan, F. Emmerling, B. Wu, C. Janiak, *Dalton Trans.* **2003**, 2815–2823.
- [64] a) C. N. R. Rao, S. Natarajan, S. Neeraj, *J. Am. Chem. Soc.* **2000**, *122*, 2810–2817; b) S. Mandal, M. A. Green, S. Natarajan, S. K. Pati, *J. Phys. Chem. B* **2004**, *108*, 20351–20354.
- [65] S. R. Miller, A. M. Z. Slawin, P. Wormald, P. A. Wright, *J. Solid State Chem.* **2005**, *178*, 1738–1752.
- [66] a) Y. Zhao, G. Zhu, X. Jiao, W. Liu, W. Pang, *J. Mater. Chem.* **2000**, *10*, 463–467; b) C. Serre, F. Taulelle, G. Férey, *Solid State Sci.* **2001**, *3*, 623–632; c) C. Serre, F. Taulelle, G. Férey, *Chem. Mater.* **2002**, *14*, 998–1003; d) C. Chen, Y.-L. Yang, K.-L. Huang, Z.-H. Sun, W. Wang, Z. Yi, Y.-L. Liu, W.-Q. Pang, *Polyhedron* **2004**, *23*, 3033–3042.
- [67] a) Z. Bircsak, W. T. A. Harrison, *Inorg. Chem.* **1998**, *37*, 3204–3208; b) J. Do, R. P. Bontchev, A. J. Jacobson, *Inorg. Chem.* **2000**, *39*, 3230–3237; c) L.-I. Hung, S.-L. Wang, H.-M. Kao, K.-H. Lii, *Inorg. Chem.* **2002**, *41*, 3929–3934; d) Y. Lu, E. Wang, M. Yuan, G. Luan, Y. Li, H. Zhang, C. Hu, Y. Yao, Y. Qin, Y. Chen, *J. Chem. Soc. Dalton Trans.* **2002**, 3029–3031; e) C. Qin, L. Xu, Y. Wei, X. Wang, F. Li, *Inorg. Chem.* **2003**, *42*, 3107–3110.
- [68] a) J. Escobal, J. L. Pizarro, J. L. Mesa, L. Lezama, R. Olazcuaga, M. I. Arriortua, T. Rojo, *Chem. Mater.* **2000**, *12*, 376–382; b) K. O. Kongshaug, H. Fjillvag, K. P. Lillerud, *J. Solid State Chem.* **2001**, *156*, 32–36; c) Y. Song, P. Y. Zavalij, N. A. Chernova, M. S. Whittingham, *Chem. Mater.* **2003**, *15*, 4968–4973; d) S. G. Thoma, F. Bonhomme, R. T. Cygan, *Chem. Mater.* **2004**, *16*, 2068–2075.
- [69] a) J. R. D. DeBord, W. M. Reiff, R. C. Haushalter, J. Zubieta, *J. Solid State Chem.* **1996**, *125*, 186–191; b) K.-H. Lii, Y.-F. Huang, *Chem. Commun.* **1997**, 1311–1312; c) K.-H. Lii, Y.-F. Huang, *J. Chem. Soc. Dalton Trans.* **1997**, 2221–2225; d) M. Riou-Cavellec, J.-M. Greneche, D. Riou, G. Férey, *Chem. Mater.* **1998**, *10*, 2434–2439; e) A. R. Cowley, A. M. Chippindale, *J. Chem. Soc. Dalton Trans.* **2000**, 3425–3428; f) S. Mandal, S. Natarajan, J. M. Greneche, M. Riou-Cavellec, G. Férey, *Chem. Mater.* **2002**, *14*, 3751–3757.
- [70] a) J. R. D. DeBord, R. C. Haushalter, J. Zubieta, *J. Solid State Chem.* **1996**, *125*, 270–273; b) S. Ekambaram, S. C. Sevov, *J. Mater. Chem.* **2000**, *10*, 2522–2525; c) A. Choudhury, S. Natarajan, C. N. R. Rao, *J. Solid State Chem.* **2000**, *155*, 62–70.
- [71] M. Wloka, S. I. Trojanov, E. Kemnitz, *J. Solid State Chem.* **1998**, *135*, 293–301.
- [72] X. Wang, L. Liu, A. J. Jacobson, *J. Solid State Chem.* **2004**, *177*, 194–201.
- [73] a) D. Riou, F. Fayon, D. Massiot, *Chem. Mater.* **2002**, *14*, 2416–2420; b) H. Park, I. Bull, L. Peng, V. G. Young, Jr., C. P. Grey, J. B. Parise, *Chem. Mater.* **2004**, *16*, 5350–5356.
- [74] a) S. Ekambaram, S. C. Sevov, *Angew. Chem.* **1999**, *111*, 384–386; *Angew. Chem. Int. Ed.* **1999**, *38*, 372–375; b) S. Ekambaram, C. Serre, G. Férey, S. C. Sevov, *Chem. Mater.* **2000**, *12*, 444–449; c) Y. Fu, Y. Liu, Z. Shi, Y. Zou, W. Pang, *J. Solid State Chem.* **2001**, *162*, 96–102.
- [75] E. Bordes, P. Courtine, *J. Chem. Soc. Chem. Commun.* **1985**, 294–296.
- [76] a) L. Duan, M. Yuan, E. Wang, Y. Li, Y. Lu, C. Hu, *J. Mol. Struct.* **2003**, *654*, 95–101; b) V. Soghomonian, R. C. Haushalter, J. Zubieta, C. J. O'Connor, *Inorg. Chem.* **1996**, *35*, 2826–2830; c) G. Bonavia, R. C. Haushalter, J. Zubieta, *J. Solid State Chem.* **1996**, *126*, 292–299; d) N. Calin, C. Serre, S. C. Sevov, *J. Mater. Chem.* **2003**, *13*, 531–534; e) E. Alda, B. Bazan, J. L. Mesa, J. L. Pizarro, M. I. Arriortua, T. Rojo, *J. Solid State Chem.* **2003**, *173*, 101–108; f) Z. Shi, S. Feng, S. Gao, L. Zhang, G. Yang, J. Hua, *Angew. Chem.* **2000**, *112*, 2415–2417; *Angew. Chem. Int. Ed.* **2000**, *39*, 2325–2327; g) J.-X. Chen, C.-X. Wei, Z.-C. Zhang, Y.-B. Huang, T.-Y. Lan, Z.-S. Li, W.-J. Zhang, *Inorg. Chim. Acta* **2006**, *359*, 3396–3404.
- [77] a) S. Neeraj, M. L. Noy, A. K. Cheetham, *Solid State Sci.* **2002**, *4*, 397–404; b) F. Corà, G. Sankar, C. R. A. Catlow, J. M. Thomas, *Chem. Commun.* **2002**, 734–735; c) A. M. Chippindale, A. R. Cowley, *Microporous Mesoporous Mater.* **1998**, *21*, 271–279; d) K. F. Hsu, S. L. Wang, *Chem. Commun.* **2000**, 135–136; e) K. F. Hsu, S. L. Wang, *Inorg. Chem.* **2000**, *39*, 1773–1778.
- [78] a) P. B. Moore, *Am. Mineral.* **1970**, *55*, 135–169; b) P. B. Moore, J. Shen, *Nature* **1983**, *306*, 356–358.
- [79] K.-H. Lii, Y.-F. Huang, V. Zima, C.-Y. Huang, H.-M. Lin, Y.-C. Jiang, F.-L. Liao, S.-L. Wang, *Chem. Mater.* **1998**, *10*, 2599–2609.
- [80] a) J. R. D. DeBord, W. M. Reiff, C. J. Warren, R. C. Haushalter, J. Zubieta, *Chem. Mater.* **1997**, *9*, 1994–1998; b) A. Choudhury, S. Natarajan, C. N. R. Rao, *Chem. Commun.* **1999**, 1305–1306; c) K.-H. Lii, Y.-F. Huang, *Chem. Commun.* **1997**, 839–840; d) A. Choudhury, S. Natarajan, *J. Solid State Chem.* **2000**, *154*, 507–513; e) C. Y. Huang, S. L. Wang, K.-H. Lii, *J. Porous Mater.* **1998**, *5*, 147–152.
- [81] a) E. M. Flanigen, B. M. Lok, L. R. Patton, S. T. Wilson, *Pure Appl. Chem.* **1986**, *58*, 1351–1358; b) G. M. T. Cheetham, M. M. Harding, P. J. Rizkallah, V. Kaucic, N. Rajic, *Acta Crystallogr. Sect. C* **1991**, *47*, 1361–1364.
- [82] P. Feng, X. Bu, S. H. Tolbert, G. D. Stucky, *J. Am. Chem. Soc.* **1997**, *119*, 2497–2504, and references therein.
- [83] a) J. S. Chen, R. H. Jones, S. Natarajan, M. B. Hursthouse, J. M. Thomas, *Angew. Chem.* **1994**, *106*, 667–668; *Angew. Chem. Int. Ed. Engl.* **1994**, *33*, 639–640; b) S. Natarajan, S. Neeraj, A. Choudhury, C. N. R. Rao, *Inorg. Chem.* **2000**, *39*, 1426–1433; c) H.-M. Yuan, J.-S. Chen, G.-S. Zhu, J.-Y. Li, J.-H. Yu, G.-D. Yang, R.-R. Xu, *Inorg. Chem.* **2000**, *39*, 1476–1479; d) A. Choudhury, S. Neeraj, S. Natarajan, C. N. R. Rao, *Angew. Chem.* **2000**, *112*, 3221–3223; *Angew. Chem. Int. Ed.* **2000**, *39*, 3091–3093; e) R.-K. Chiang, *Inorg. Chem.* **2000**, *39*, 4985–4988; f) W. K. Chang, R. K. Chiang, Y. C. Jiang, S. L. Wang, S. F. Lee, K. H. Lii, *Inorg. Chem.* **2004**, *43*, 2564–2568; g) S. Natarajan, S. Neeraj, C. N. R. Rao, *Solid State Sci.* **2000**, *2*, 87–98; h) P. Feng, X. Bu, G. D. Stucky, *Nature* **1997**, *388*, 735–741; i) X. Bu, P. Feng, G. D. Stucky, *Science* **1997**, *278*, 2080–2085.
- [84] a) N. Guillou, Q. Gao, M. Nogués, R. E. Morris, M. Hervieu, G. Férey, A. K. Cheetham, *C. R. Acad. Sci. Ser. IIC* **1999**, 387–392; b) J.-S. Chang, S.-E. Park, Q. Gao, G. Férey, A. K. Cheetham, *Chem. Commun.* **2001**, 859–860; c) N. Guillou, Q. Gao, P. M. Foster, J.-S. Chang, M. Nogués, S.-E. Park, G. Férey, A. K. Cheetham, *Angew. Chem.* **2001**, *113*, 2913–2916; *Angew. Chem. Int. Ed.* **2001**, *40*, 2831–2834; d) P. M. Forster, J. Eckert, J.-S. Chang, S.-E. Park, G. Férey, A. K. Cheetham, *J. Am. Chem. Soc.* **2003**, *125*, 1309–1312.
- [85] E. Kemnitz, M. Wloka, S. Trojanov, A. Stiewe, *Angew. Chem.* **1996**, *108*, 2809–2811; *Angew. Chem. Int. Ed. Engl.* **1996**, *35*, 2677–2678.
- [86] a) R. C. Haushalter, K. G. Strohmaier, F. W. Lai, *Science* **1989**, *246*, 1289–1291; b) H. E. King, Jr., L. A. Mundi, K. G. Strohmaier, R. C. Haushalter, *J. Solid State Chem.* **1991**, *92*, 1–7.
- [87] Z. Shi, G. Li, D. Zhang, J. Hua, S. Feng, *Inorg. Chem.* **2003**, *42*, 2357–2361.
- [88] W. T. A. Harrison, M. L. F. Philips, T. M. Nenoff, *J. Chem. Soc. Dalton Trans.* **2001**, 2459–2461.
- [89] S. Fernández, J. L. Mesa, J. L. Pizarro, L. Lezama, M. I. Arriortua, T. Rojo, *Chem. Mater.* **2003**, *15*, 1204–1209.

- [90] S. Fernández, J. L. Mesa, J. L. Pizarro, L. Lezama, M. I. Arriortua, T. Rojo, *Angew. Chem.* **2002**, *114*, 3835–3837; *Angew. Chem. Int. Ed.* **2002**, *41*, 3683–3685.
- [91] a) S. Mandal, M. A. Green, S. Natarajan, *Curr. Sci.* **2005**, *89*, 1899–1903; b) S. Fernández-Armas, J. L. Mesa, J. L. Pizarro, J. M. Clemente-Juan, E. Coronado, M. I. Arriortua, T. Rojo, *Inorg. Chem.* **2006**, *45*, 3240–3248; c) S. Fernández-Armas, J. L. Mesa, J. L. Pizarro, M. I. Arriortua, T. Rojo, *Mater. Res. Bull.* **2007**, *42*, 544–552.
- [92] a) S. Fernández, J. L. Pizarro, J. L. Mesa, L. Lezama, M. I. Arriortua, R. Olazcuaga, T. Rojo, *Inorg. Chem.* **2001**, *40*, 3476–3483; b) S. Fernández, J. L. Mesa, J. L. Pizarro, L. Lezama, M. I. Arriortua, R. Olazcuaga, T. Rojo, *Chem. Mater.* **2000**, *12*, 2092–2098.
- [93] a) S. Fernández-Armas, J. L. Mesa, J. L. Pizarro, U.-C. Chung, M. I. Arriortua, T. Rojo, *J. Solid State Chem.* **2005**, *178*, 3604–3612; b) U.-C. Chung, J. L. Mesa, J. L. Pizarro, L. Lezama, J. S. Garitaonandia, J. P. Chapman, M. I. Arriortua, *J. Solid State Chem.* **2004**, *177*, 2705–2713.
- [94] a) S. Fernández, J. L. Pizarro, J. L. Mesa, L. Lezama, M. I. Arriortua, T. Rojo, *Int. J. Inorg. Mater.* **2001**, *3*, 331–336; b) S. Natarajan, S. Mandal, P. Mahata, V. K. Rao, P. Ramaswamy, A. Banerjee, A. K. Paul, K. V. Ramya, *J. Chem. Sci.* **2006**, *118*, 525–536.
- [95] a) G. Bonavia, J. DeBord, R. C. Haushalter, D. Rose, J. Zubieta, *Chem. Mater.* **1995**, *7*, 1995–1998; b) Z. Shi, D. Zhang, G. Li, L. Wang, X. Lu, J. Hua, S. Feng, *J. Solid State Chem.* **2003**, *172*, 464–470; c) W. Fu, G. Liang, Y. Sun, *Polyhedron* **2006**, *25*, 2571–2576.
- [96] a) S. Fernández, J. L. Mesa, J. L. Pizarro, L. Lezama, M. I. Arriortua, T. Rojo, *Chem. Mater.* **2002**, *14*, 2300–2307; b) R.-K. Chiang, N.-T. Chuang, *J. Solid State Chem.* **2005**, *178*, 3040–3045; c) Z. Shi, G. Li, D. Zhang, J. Hua, S. Feng, *Inorg. Chem.* **2003**, *42*, 2357–2361; d) S. Shi, L. Wang, H. Yuan, G. Li, J. Xu, G. Zhu, T. Song, S. Qiu, *J. Solid State Chem.* **2004**, *177*, 4183–4187.
- [97] a) Y. Fan, T. Song, G. Li, Z. Shi, G. Yu, J. Xu, S. Feng, *Inorg. Chem. Commun.* **2005**, *8*, 661–664; b) U.-C. Chung, J. L. Mesa, J. L. Pizarro, J. R. Fernández, J. S. Marcos, J. S. Garitaonandia, M. I. Arriortua, T. Rojo, *Inorg. Chem.* **2006**, *45*, 8965–8972.
- [98] G. Alberti, U. Constantino, S. Allulli, N. Tomassini, *J. Inorg. Nucl. Chem.* **1978**, *40*, 1113–1117.
- [99] a) A. Clearfield, *Chem. Mater.* **1998**, *10*, 2801–2810; b) A. Clearfield, *Prog. Inorg. Chem.* **1998**, *47*, 371–510; c) K. Maeda, *Microporous Mesoporous Mater.* **2004**, *73*, 47–55.
- [100] D.-K. Cao, J. Xiao, J.-W. Tong, Y.-Z. Li, L.-M. Zheng, *Inorg. Chem.* **2007**, *46*, 428–436.
- [101] G. Bonavia, R. C. Haushalter, C. J. O'Connor, C. Sangreorio, J. Zubieta, *Chem. Commun.* **1998**, 2187–2188.
- [102] a) S. R. Miller, E. Lear, J. Gonzalez, A. M. Z. Slawin, P. A. Wright, N. Guillou, G. Férey, *Dalton Trans.* **2005**, 3319–3325; b) Y.-S. Ma, Y.-F. Yang, S. Gao, Y.-Z. Li, L.-M. Zheng, *J. Solid State Chem.* **2006**, *179*, 3017–3023; c) J.-G. Mao, Z. Wang, A. Clearfield, *Inorg. Chem.* **2002**, *41*, 2334–2340; d) C. Bellitto, F. Federici, M. Colapietro, G. Portalone, D. Caschera, *Inorg. Chem.* **2002**, *41*, 709–714; e) C. Bellitto, E. M. Bauer, P. Leone, A. Meerschaut, C. Guillot-Deudon, G. Righini, *J. Solid State Chem.* **2006**, *179*, 579–589; f) E. M. Bauer, C. Bellitto, M. Colapietro, S. A. Ibrahim, M. R. Mahmoud, G. Portalone, G. Righini, *J. Solid State Chem.* **2006**, *179*, 389–397; g) L. A. Vermeulen, R. Z. Fateen, P. D. Robinson, *Inorg. Chem.* **2002**, *41*, 2310–2312.
- [103] J. Le Bideau, C. Payen, P. Palvadeau, B. Bujoli, *Inorg. Chem.* **1994**, *33*, 4885–4890.
- [104] a) J. W. Johnson, A. J. Jacobson, W. M. Butler, S. E. Rosenthal, J. F. Brody, J. T. Lewandowski, *J. Am. Chem. Soc.* **1989**, *111*, 381–383; b) G. Huan, J. W. Johnson, A. J. Jacobson, *J. Solid State Chem.* **1990**, *89*, 220–225; c) G. Huan, J. W. Johnson, A. J. Jacobson, E. W. Corcoran, Jr., *Chem. Mater.* **1990**, *2*, 91–93.
- [105] a) R. Laduca, D. Rose, J. R. D. DeBord, R. C. Haushalter, C. J. O'Connor, J. Zubieta, *J. Solid State Chem.* **1996**, *123*, 408–412, and references therein.; b) G. Bonavia, R. C. Haushalter, C. J. O'Connor, J. Zubieta, *Inorg. Chem.* **1996**, *35*, 5603–5612; c) G. H. Bonavia, R. C. Haushalter, S. Lu, C. J. O'Connor, J. Zubieta, *J. Solid State Chem.* **1997**, *132*, 144–150.
- [106] a) D. Riou, O. Roubeau, G. Férey, *Microporous Mesoporous Mater.* **1998**, *23*, 23–31; b) M. Riou-Cavellec, C. Serre, J. Robino, M. Nogues, J.-M. Greneche, G. Férey, *J. Solid State Chem.* **1999**, *147*, 122–131; c) C. Ninclaus, C. Serre, D. Riou, G. Férey, *C. R. Acad. Sci. Ser. IIC* **1998**, *1*, 551–556; d) C. Serre, G. Férey, *Inorg. Chem.* **1999**, *38*, 5370–5373; e) C. Serre, G. Férey, *Inorg. Chem.* **2001**, *40*, 5350–5353; f) D. Riou, C. Serre, J. Provost, G. Férey, *J. Solid State Chem.* **2000**, *155*, 238–242.
- [107] S.-S. Bao, T.-W. Wang, Y.-Z. Li, L.-M. Zheng, *J. Solid State Chem.* **2006**, *179*, 413–420.
- [108] a) P. Yin, L.-M. Zheng, S. Gao, X.-Q. Xin, *Chem. Commun.* **2001**, 2346–2347; b) S.-S. Bao, L.-M. Zheng, Y.-J. Liu, S. Feng, *Inorg. Chem.* **2003**, *42*, 5037–5039.
- [109] R. D. Shannon, *Acta Crystallogr. Sect. A* **1976**, *32*, 751–767.
- [110] a) G. Yang, L. Li, J. Chen, R. Xu, *J. Chem. Soc. Chem. Commun.* **1989**, 810–811; b) J. Chen, L. Li, G. Yang, R. Xu, *J. Chem. Soc. Chem. Commun.* **1989**, 1217–1218.
- [111] a) C. A. Bremner, W. T. A. Harrison, *Acta Crystallogr. Sect. E* **2002**, *58*, m319–m321; b) S. T. Zheng, J. Zhang, G.-Y. Yang, *Solid State Sci.* **2005**, *7*, 149–154.
- [112] a) R. C. Haushalter, Z. Wang, L. M. Meyer, S. S. Dhingra, M. E. Thomson, J. Zubieta, *Chem. Mater.* **1994**, *6*, 1463–1464; b) A.-H. Liu, S.-L. Wang, *Inorg. Chem.* **1998**, *37*, 3415–3418; c) Y. Hou, Y. Wei, E. Shen, D. Xiao, E. Wang, S. Wang, Y. Li, L. Xu, C. Hu, *Inorg. Chem. Commun.* **2004**, *7*, 128–130.
- [113] a) S. Chakrabarti, S. K. Pati, M. A. Green, S. Natarajan, *Eur. J. Inorg. Chem.* **2004**, 3846–3851; b) S. Bazan, J. L. Mesa, J. L. Pizarro, L. Lezama, M. I. Arriortua, T. Rojo, *Inorg. Chem.* **2000**, *39*, 6056–6060; c) S. Ekambaram, S. C. Sevov, *Inorg. Chem.* **2000**, *39*, 2405–2410.
- [114] a) F. Gagnard, C. Reisner, W. Trumel, *Inorg. Chem.* **1997**, *36*, 352–355; b) L.-H. Huang, H.-M. Kao, K.-H. Lii, *Inorg. Chem.* **2002**, *41*, 2936–2940; c) D. Xiao, Y. Lu, E. Wang, Y. Li, S. Wang, Y. Hou, G. De, *J. Solid State Chem.* **2003**, *175*, 146–151; d) Y. Hou, Y. Wei, D. Xiao, E. Shen, E. Wang, Y. Li, L. Xu, C. Hu, *Inorg. Chim. Acta* **2004**, *357*, 2477–2482.
- [115] a) Y.-C. Liao, S.-H. Luo, S.-L. Wang, H.-M. Kao, K.-H. Lii, *J. Solid State Chem.* **2000**, *155*, 37–41; b) S.-H. Luo, Y.-C. Jiang, S.-L. Wang, H.-M. Kao, K.-H. Lii, *Inorg. Chem.* **2001**, *40*, 5381–5384; c) S. Chakrabarti, S. K. Pati, M. A. Green, S. Natarajan, *Eur. J. Inorg. Chem.* **2003**, 3820–3825.
- [116] a) K. Schwendtner, U. Kolitsch, *Acta Crystallogr. Sect. C* **2004**, *60*, i84–i88; b) W. T. A. Harrison, M. L. F. Phillips, *Chem. Mater.* **1999**, *11*, 3555–3560; c) W. T. A. Harrison, M. L. F. Phillips, W. Clegg, S. J. Teat, *J. Solid State Chem.* **1998**, *139*, 299–303.
- [117] a) R. C. Haushalter, L. Mayer, S. S. Dhingra, M. E. Thomson, Z. Wang, J. Zubieta, *Inorg. Chim. Acta* **1994**, *218*, 59–63; b) S.-L. Wang, Y.-H. Lee, *Inorg. Chem.* **1994**, *33*, 3845–3847.
- [118] a) B. Bazan, J. L. Mesa, J. L. Pizarro, A. Goni, L. Lezama, M. I. Arriortua, T. Rojo, *Inorg. Chem.* **2001**, *40*, 5691–5694; b) S. Chakrabarti, S. Natarajan, *Angew. Chem.* **2002**, *114*, 1272–1274; *Angew. Chem. Int. Ed.* **2002**, *41*, 1224–1226; c) V. K. Rao, S. Natarajan, *Mater. Res. Bull.* **2006**, *41*, 973–980; d) B. Bazan, J. L. Mesa, J. L. Pizarro, A. Pena, M. I. Arriortua, T. Rojo, *Z. Anorg. Allg. Chem.* **2005**, *631*, 2026–2032; e) B. Bazan, J. L. Mesa, J. L. Pizarro, J. R. Fernández, J. S. Marcos, A. Roig, E. Molins, M. I. Arriortua, T. Rojo, *Chem. Mater.* **2004**, *16*, 5249–5259.

- [119] a) J. T. Rijssenbeek, D. J. Rose, R. C. Haushalter, J. Zubietta, *Angew. Chem.* **1997**, *109*, 1049–1052; *Angew. Chem. Int. Ed. Engl.* **1997**, *36*, 1008–1010; b) C. J. Warren, J. T. Rijssenbeek, D. J. Rose, R. C. Haushalter, J. Zubietta, *Polyhedron* **1998**, *17*, 2599–2605; c) C. J. Warren, D. J. Rose, R. C. Haushalter, J. Zubietta, *Inorg. Chem.* **1998**, *37*, 1140–1141; d) L. Zhang, Z. Shi, G. Yang, X. Chen, S. Feng, *J. Solid State Chem.* **1999**, *148*, 450–454.
- [120] I. D. Williams, M. Wu, H. H.-Y. Sung, X. X. Zhang, J. Yu, *Chem. Commun.* **1998**, 2463–2464.
- [121] a) M. Touboul, N. Penin, G. Nowogrocki, *J. Solid State Chem.* **2000**, *150*, 342–346; b) J. L. C. Rowsell, N. J. Taylor, L. F. Nazar, *J. Am. Chem. Soc.* **2002**, *124*, 6522–6523; c) T. Yang, G. Li, L. You, J. Ju, F. Liao, J. Lin, *Chem. Commun.* **2005**, 4225–4227.
- [122] a) G. Paul, A. Choudhury, R. Nagarajan, C. N. R. Rao, *Inorg. Chem.* **2003**, *42*, 2004–2013; b) J. N. Behera, C. N. R. Rao, *Chem. Asian J.* **2006**, *1*, 742–750.
- [123] a) G. Paul, A. Choudhury, C. N. R. Rao, *Chem. Mater.* **2003**, *15*, 1174–1180; b) Y. Fu, Z. Xu, J. Ren, H. Wu, R. Yuan, *Inorg. Chem.* **2006**, *45*, 8452–8458.
- [124] L. Fafani, A. Nunzi, P. F. Zanazzi, *Am. Mineral.* **1971**, *56*, 751–757.
- [125] F. C. Hawthorne, S. V. Krivovichev, P. C. Burns, *Rev. Mineral. Geochem.* **2000**, *40*, 1–112.
- [126] G. Paul, A. Choudhury, E. V. Sampathkumaran, C. N. R. Rao, *Angew. Chem.* **2002**, *114*, 4473–4476; *Angew. Chem. Int. Ed.* **2002**, *41*, 4297–4300.
- [127] J. N. Behera, K. V. Gopalkrishnan, C. N. R. Rao, *Inorg. Chem.* **2004**, *43*, 2636–2642.
- [128] a) A. Rujiwatra, C. J. Kepert, M. J. Rosseinsky, *Chem. Commun.* **1999**, 2307–2308; b) A. Rujiwatra, C. J. Kepert, J. B. Claridge, M. J. Rosseinsky, H. Kumagai, M. Kurmoo, *J. Am. Chem. Soc.* **2001**, *123*, 10584–10594; c) J. N. Behera, C. N. R. Rao, *Can. J. Chem.* **2005**, *83*, 668–673.
- [129] J. N. Behera, C. N. R. Rao, *Dalton Trans.* **2007**, 669–673.
- [130] a) G. Paul, A. Choudhury, C. N. R. Rao, *Chem. Commun.* **2002**, 1904–1905; b) C. N. R. Rao, E. V. Sampathkumaran, R. Nagarajan, G. Paul, J. N. Behera, A. Choudhury, *Chem. Mater.* **2004**, *16*, 1441–1446; c) J. N. Behera, C. N. R. Rao, *Inorg. Chem.* **2006**, *45*, 9475–9479.
- [131] J. N. Behera, G. Paul, A. Choudhury, C. N. R. Rao, *Chem. Commun.* **2004**, 456–457.
- [132] J. N. Behera, C. N. R. Rao, *J. Am. Chem. Soc.* **2006**, *128*, 9334–9335.
- [133] Z. Dai, Z. Shi, G. Li, D. Zhang, W. Fu, H. Jin, W. Xu, S. Feng, *Inorg. Chem.* **2003**, *42*, 7396–7402.
- [134] a) Z. Dai, Z. Shi, G. Li, X. Chen, X. Lu, Y. Xu, S. Feng, *J. Solid State Chem.* **2003**, *172*, 205–211; b) I. Pasha, A. Choudhury, C. N. R. Rao, *Inorg. Chem.* **2003**, *42*, 409–415; c) Z. Shi, D. Zhang, S. Feng, G. Li, Z. Dai, W. Fu, X. Chen, J. Hua, *J. Chem. Soc. Dalton Trans.* **2002**, 1873–1874.
- [135] a) A. Choudhury, D. K. Udayakumar, C. N. R. Rao, *Angew. Chem.* **2002**, *114*, 166–169; *Angew. Chem. Int. Ed.* **2002**, *41*, 158–161; b) D. Udayakumar, C. N. R. Rao, *J. Mater. Chem.* **2003**, *13*, 1635–1638; c) D. Xiao, H. An, E. Wang, C. Sun, L. Xu, *J. Coord. Chem.* **2006**, *59*, 395–402; d) Z. Dai, X. Chen, Z. Shi, D. Zhang, G. Li, S. Feng, *Inorg. Chem.* **2003**, *42*, 908–912; e) D. Xiao, Y. Hou, E. Wang, H. An, J. Lu, Y. Li, L. Xu, C. Hu, *J. Solid State Chem.* **2004**, *177*, 2699–2704; f) D. Xiao, H. An, E. Wang, L. Xu, *J. Mol. Struct.* **2005**, *740*, 249–253; g) A. Larranaga, J. L. Mesa, J. L. Pizarro, R. Olazcuaga, M. I. Arriortua, T. Rojo, *J. Chem. Soc. Dalton Trans.* **2002**, 3447–3453.
- [136] R. Kniep, G. Goetz, B. Eisenmann, C. Röhr, M. Asbrand, M. Kizilyalli, *Angew. Chem.* **1994**, *106*, 791–793; *Angew. Chem. Int. Ed. Engl.* **1994**, *33*, 749–751.
- [137] M. Yang, J. Yu, L. Shi, P. Chen, G. Li, Y. Chen, R. Xu, *Chem. Mater.* **2006**, *18*, 476–481.
- [138] a) Y.-X. Huang, B. Ewald, W. Schnelle, Y. Prots, R. Kniep, *Inorg. Chem.* **2006**, *45*, 7578–7580; b) R. P. Bontchev, S. C. Sevov, *Inorg. Chem.* **1996**, *35*, 6910–6911.
- [139] a) B. Ewald, Y. Prots, C. Kudla, D. Grüner, R. Cardoso-Gil, R. Kniep, *Chem. Mater.* **2006**, *18*, 673–679; b) R. Kniep, H. G. Will, I. Boy, C. Röhr, *Angew. Chem.* **1997**, *109*, 1052–1054; *Angew. Chem. Int. Ed. Engl.* **1997**, *36*, 1013–1014; c) Y.-X. Huang, G. Schäfer, W. Carrillo-Cabrera, R. Cardoso, W. Schnelle, J.-T. Zhao, R. Kniep, *Chem. Mater.* **2001**, *13*, 4348–4354; d) A. Yilmaz, X. Bu, M. Kizilyalli, G. D. Stucky, *Chem. Mater.* **2000**, *12*, 3243–3245; e) R. Kniep, I. Boy, H. Engelhardt, *Z. Anorg. Allg. Chem.* **1999**, *625*, 1512–1516.
- [140] a) Y. Zhao, Z. Shi, S. Ding, N. Bai, W. Liu, Y. Zou, G. Zhu, P. Zhang, Z. Mai, W. Pang, *Chem. Mater.* **2000**, *12*, 2550–2556; b) R. P. Bontchev, J. Do, A. J. Jacobson, *Angew. Chem.* **1999**, *111*, 2063–2066; *Angew. Chem. Int. Ed.* **1999**, *38*, 1937–1940; c) J. Do, L.-M. Zheng, R. P. Bontchev, A. J. Jacobson, *Solid State Sci.* **2000**, *2*, 343–351; d) C. J. Warren, R. C. Haushalter, D. J. Rose, J. Zubietta, *Inorg. Chem. Commun.* **1998**, *1*, 4–6; e) C. J. Warren, R. C. Haushalter, D. J. Rose, J. Zubietta, *Chem. Mater.* **1997**, *9*, 2694–2696.
- [141] a) M. Li, D. Xie, J. Chang, H. Shi, *Inorg. Chim. Acta* **2007**, *360*, 710–714; b) Y.-X. Huang, O. Hochrein, D. Zahn, Y. Prots, H. Borrmann, R. Kniep, *Chem. Eur. J.* **2007**, *13*, 1737–1745; c) R. P. Bontchev, A. J. Jacobson, *Mater. Res. Bull.* **2002**, *37*, 1997–2005; d) S. C. Sevov, *Angew. Chem.* **1996**, *108*, 2814–2816; *Angew. Chem. Int. Ed. Engl.* **1996**, *35*, 2630–2632; e) H. Engelhardt, W. Schnelle, R. Kniep, *Z. Anorg. Allg. Chem.* **2000**, *626*, 1380–1386.
- [142] R. P. Bontchev, J. Do, A. J. Jacobson, *Inorg. Chem.* **2000**, *39*, 3320–3324.
- [143] a) S. Mandal, S. K. Pati, M. A. Green, S. Natarajan, *Chem. Mater.* **2005**, *17*, 638–643; b) S. Fernández-Armas, J. L. Mesa, J. L. Pizarro, J. S. Garitaonandia, M. I. Arriortua, T. Rojo, *Angew. Chem.* **2004**, *116*, 995–998; *Angew. Chem. Int. Ed.* **2004**, *43*, 977–980; c) W.-K. Chang, C.-S. Wur, S.-L. Wang, R.-K. Chang, *Inorg. Chem.* **2006**, *45*, 6622–6627.
- [144] a) B. Bazán, J. L. Mesa, J. L. Pizarro, L. Lezama, J. S. Garitaonandia, M. I. Arriortua, T. Rojo, *Solid State Sci.* **2003**, *5*, 1291–1301; b) B. Bazán, J. L. Mesa, J. L. Pizarro, M. I. Arriortua, T. Rojo, *Mater. Res. Bull.* **2003**, *38*, 1193–1202; c) B. Bazán, J. L. Mesa, J. L. Pizarro, L. Lezama, A. Pena, M. I. Arriortua, T. Rojo, *J. Solid State Chem.* **2006**, *179*, 1459–1468.
- [145] a) Y.-M. Tsai, S.-L. Wang, C.-H. Huang, K.-H. Lii, *Inorg. Chem.* **1999**, *38*, 4183–4187; b) M.-Y. Lee, S.-L. Wang, *Chem. Mater.* **1999**, *11*, 3588–3594.
- [146] a) M.-F. Tang, K.-H. Lii, *J. Solid State Chem.* **2004**, *177*, 1912–1918; b) J. Do, R. P. Bontchev, A. J. Jacobson, *Inorg. Chem.* **2000**, *39*, 3230–3237; c) J. Do, R. P. Bontchev, A. J. Jacobson, *Chem. Mater.* **2001**, *13*, 2601–2607; d) F.-N. Shi, F. A. Almeida Paz, J. Rocha, J. Klinowski, T. Trindade, *Inorg. Chim. Acta* **2005**, *358*, 927–932.
- [147] Y.-C. Yiang, S.-L. Wang, S.-F. Lee, K.-H. Lii, *Inorg. Chem.* **2003**, *42*, 6154–6156.
- [148] a) Z. A. D. Lethbridge, A. D. Hiller, R. Cywinski, P. Lightfoot, *J. Chem. Soc. Dalton Trans.* **2000**, 1595–1599; b) Z. A. D. Lethbridge, S. K. Tiwary, A. Harrison, P. Lightfoot, *J. Chem. Soc. Dalton Trans.* **2001**, 1904–1910; c) M. T. Averbuch-Pouchot, A. Durit, *Acta Crystallogr. Sect. C* **1990**, *46*, 965–968; d) R. Yu, X. Xing, T. Saito, M. Azuma, M. Takano, D. Wang, Y. Chen, N. Kumada, N. Kinomura, *Solid State Sci.* **2005**, *7*, 221–226.
- [149] a) A. Choudhury, S. Natarajan, C. N. R. Rao, *J. Solid State Chem.* **1999**, *146*, 538–545; b) A. Choudhury, S. Natarajan, C. N. R. Rao, *Chem. Mater.* **1999**, *11*, 2316–2318; c) N. Rajic, D.

- Stojakovic, D. Hanzel, N. Z. Loger, V. Kaucic, *Microporous Mesoporous Mater.* **2002**, 55, 313–319; d) A. Choudhury, S. Natarajan, C. N. R. Rao, *Chem. Eur. J.* **2000**, 6, 1168–1175; e) H.-M. Lin, K.-H. Lii, Y.-C. Jiang, S. L. Wang, *Chem. Mater.* **1999**, 11, 519–521; f) W.-J. Chang, H.-M. Lin, K.-H. Lii, *J. Solid State Chem.* **2001**, 157, 233–239; g) A. Choudhury, S. Natarajan, *J. Mater. Chem.* **1999**, 9, 3113–3117; h) Y.-C. Jiang, S.-L. Wang, K.-H. Lii, N. Nguyen, A. Ducouret, *Chem. Mater.* **2003**, 15, 1633–1638; i) H. Meng, G.-H. Li, Y. Xing, Y.-L. Yang, Y.-J. Cui, L. Liu, H. Dong, W.-Q. Pang, *Polyhedron* **2004**, 23, 2357–2362; j) W.-M. Chang, S.-L. Wang, *Chem. Mater.* **2005**, 17, 74–80.
- [150] A. Choudhury, S. Natarajan, *Solid State Sci.* **2000**, 2, 365–372.
- [151] a) S. Mandal, S. K. Pati, M. A. Green, S. Natarajan, *Chem. Mater.* **2005**, 17, 2912–2917; b) S. Mandal, S. Natarajan, *Chem. Eur. J.* **2007**, 13, 968–977.
- [152] S. Mandal, M. A. Green, S. K. Pati, S. Natarajan, *J. Mater. Chem.* **2007**, 17, 980–985.
- [153] S. Mandal, S. Natarajan, *J. Solid State Chem.* **2005**, 178, 2376–2382.
- [154] S. Chakrabarti, M. A. Green, S. Natarajan, *Solid State Sci.* **2002**, 4, 405–412.
- [155] V. K. Rao, K. C. Kam, A. K. Cheetham, S. Natarajan, *Solid State Sci.* **2006**, 8, 692–697.
- [156] a) J. B. Goodenough, *Magnetism and the Chemical Bond*, Wiley, New York, **1963**; b) R. L. Carlin, *Magnetochemistry*, Springer, Berlin, **1986**; c) O. Kahn, *Molecular Magnetism*, VCH, New York, **1993**; d) R. L. Dutta, A. Syamal, *Elements of Magnetochemistry*, EWP, New Delhi, **1993**; e) M. E. Fisher, *Am. J. Phys.* **1964**, 32, 343–346.
- [157] a) J. B. Goodenough, *Phys. Chem. Solids* **1958**, 6, 287–297; b) J. Kanamori, *Phys. Chem. Solids* **1959**, 10, 87–98.
- [158] I. Dzyaloshinsky, *J. Phys. Chem. Solids* **1958**, 4, 241–255.
- [159] a) T. Moriya, *Phys. Rev.* **1960**, 120, 91–98; b) T. Moriya in *Magnetism*, Vol. 1 (Eds.: G. T. Rado, H. Suhl), Academic Press, New York, **1963**, p. 86.
- [160] A. Zheludev, T. Sato, T. Masuda, K. Uchinokura, G. Shirane, B. Roessli, *Phys. Rev. B* **2003**, 68, 024428.
- [161] A. P. Ramirez, *Handbook on Magnetic Materials*, Vol. 13 (Ed.: K. J. H. Busch), Elsevier, Amsterdam, **2001**, p. 423.
- [162] A. P. Ramirez, *Annu. Rev. Mater. Sci.* **1994**, 24, 453–480.
- [163] C. N. R. Rao, G. Paul, A. Choudhury, E. V. Sampathkumaran, A. K. Raychaudhury, S. Ramasesha, I. Rudra, *Phys. Rev. B* **2003**, 67, 134425.
- [164] B. M. Bartlett, D. G. Nocera, *J. Am. Chem. Soc.* **2005**, 127, 8985–8993.
- [165] a) D. Grohol, D. Papoutsakis, D. G. Nocera, *Angew. Chem.* **2001**, 113, 1567–1569; *Angew. Chem. Int. Ed.* **2001**, 40, 1519–1521; b) D. Papoutsakis, D. Grohol, D. G. Nocera, *J. Am. Chem. Soc.* **2002**, 124, 2647–2656; c) D. G. Nocera, B. M. Bartlett, D. Grohol, D. Papoutsakis, M. P. Shores, *Chem. Eur. J.* **2004**, 10, 3850–3859; d) M. P. Shores, E. A. Nytko, B. M. Bartlett, D. G. Nocera, *J. Am. Chem. Soc.* **2005**, 127, 13462–13463.
- [166] S. K. Pati, C. N. R. Rao, *J. Chem. Phys.* **2005**, 123, 234703.
- [167] J. N. Behera, A. Sunderesan, S. K. Pati, C. N. R. Rao, *Chem-PhysChem* **2007**, 8, 217–219.
- [168] a) G. Férey, C. Mellot-Draznieks, C. Serre, F. Millange, J. Dutour, S. Surble, I. Margiolaki, *Science* **2005**, 309, 2040–2042; b) M. Latroche, S. Surble, C. Serre, C. Mellot-Draznieks, P. L. Llewellyn, J.-H. Lee, J.-S. Chang, S. H. Jung, G. Férey, *Angew. Chem.* **2006**, 118, 8407–8411; *Angew. Chem. Int. Ed.* **2006**, 45, 8227–8231; c) J. L. C. Rowsell, O. M. Yaghi, *J. Am. Chem. Soc.* **2006**, 128, 1304–1315, and references therein; d) J. L. C. Rowsell, O. M. Yaghi, *Angew. Chem.* **2005**, 117, 4748–4758; *Angew. Chem. Int. Ed.* **2005**, 44, 4670–4679, and references therein.
- [169] C. N. R. Rao, B. Raveau, *Transition Metal Oxides*, VCH, New York, **1995**.
- [170] a) D.-T. Nguyen, E. Chew, Q. Zheng, A. Choi, X. Bu, *Inorg. Chem.* **2006**, 45, 10722–10727; b) D.-T. Nguyen, X. Bu, *Inorg. Chem.* **2006**, 45, 10410–10412.
- [171] J. N. Behera, A. A. Ayi, C. N. R. Rao, *Chem. Commun.* **2004**, 968–969.
- [172] P. M. Forster, A. K. Cheetham, *Angew. Chem.* **2002**, 114, 475–477; *Angew. Chem. Int. Ed.* **2002**, 41, 457–459.
- [173] a) C. Mellot-Draznieks, J. Dutour, G. Férey, *Angew. Chem.* **2004**, 116, 6450–6456; *Angew. Chem. Int. Ed.* **2004**, 43, 6290–6296; b) G. Férey, C. Serre, C. Mellot-Draznieks, F. Millange, S. Surble, J. Dutour, I. Margiolaki, *Angew. Chem.* **2004**, 116, 6456–6461; *Angew. Chem. Int. Ed.* **2004**, 43, 6296–6301.